

TEXTE

134/2022

Development of a bioaccumulation test using *Hyalella azteca*

Final report

TEXTE 134/2022

Ressortforschungsplan des Bundesministerium für
Umwelt, Naturschutz und nukleare Sicherheit

Forschungskennzahl 3718 67 401 0

FB000548/ENG

Development of a bioaccumulation test using *Hyalella azteca*

Final report

by

Prof. Dr. Christian Schlechtriem

Sebastian Kühr

Dr. Carolin Müller

Fraunhofer Institute for Molecular Biology and Applied
Ecology (Fraunhofer IME),

Division Applied Ecology, 57392 Schmallenberg, Germany

On behalf of the German Environment Agency

Impressum

Herausgeber

Umweltbundesamt
Wörlitzer Platz 1
06844 Dessau-Roßlau
Tel: +49 340-2103-0
Fax: +49 340-2103-2285
buergerservice@uba.de
Internet: www.umweltbundesamt.de

[f/umweltbundesamt.de](https://www.facebook.com/umweltbundesamt.de)

[t/umweltbundesamt](https://twitter.com/umweltbundesamt)

Durchführung der Studie:

Fraunhofer Institut für Molekularbiologie und Angewandte Ökologie, IME
Auf dem Aberg 1
57392 Schmallenberg

Abschlussdatum:

März 2021

Redaktion:

Caren Rauert (IV 1.1 Internationales Chemikalienmanagement);
Ulrich Jöhncke (IV 2.3 Chemikalien)

Publikationen als pdf:

<http://www.umweltbundesamt.de/publikationen>

ISSN 1862-4804

Dessau-Roßlau, Dezember 2022

Die Verantwortung für den Inhalt dieser Veröffentlichung liegt bei den Autorinnen und Autoren.

Kurzbeschreibung: Development of a bioaccumulation test using *Hyalella azteca*

Kürzlich wurde ein Testkonzept für Biokonzentrations-tests mit dem Süßwasserflohkrebs *H. azteca* (HYBIT) beschrieben. Dabei wurde gezeigt, dass Biokonzentrationsfaktoren (BCFs), die für Verbindungen mit unterschiedlichen hydrophoben Eigenschaften ermittelt wurden ($\log K_{ow}$ 2,4 – 7,8), eine starke Korrelation zu denen aus Fischtests aufweisen. Das diesem Bericht zu Grunde liegende Projekt wurde durchgeführt, um die Eignung des HYBIT-Tests zur Prüfung eines erweiterten Kreises von Substanzklassen einschließlich solcher, die schwer zu testen sind, zu untersuchen und erforderlichenfalls das Testkonzept entsprechend zu erweitern. Das Bioakkumulationspotential von hoch lipophilen UV-Stabilisatoren und ionischen organischen PFAS-Verbindungen sowie Silber-, Titandioxid- und Goldnanomaterialien wurde getestet. Die zwei möglichen Ansätze zur Durchführung von Biokonzentrationsstudien mit *H. azteca* unter Verwendung eines semistatischen Testaufbaus oder eines Durchflussansatzes wurden angewendet. Der Einsatz von Lösungsvermittlern und die lösungsmittelfreie Applikation der hydrophoben Testverbindungen wurden verglichen. Wegen der Schwierigkeiten bei der wässrigen Exposition von Nanomaterialien wurden im Rahmen dieses Projekts auch Biomagnifikationsstudien durchgeführt. Wir konnten zeigen, dass der HYBIT-Ansatz die Testung schwer zu applizierender Substanzen ermöglicht und die Ermittlung regulatorischer Endpunkte für die Bioakkumulationsbewertung zulässt. Aufgrund der kürzeren Expositionszeiten und der kleineren verwendeten Versuchseinheiten bietet der HYBIT-Ansatz mehrere Vorteile gegenüber dem Durchfluss-Fischtest. Als Nicht-Wirbeltier-Test kann der *Hyalella*-Biokonzentrations-test (bzw. Biomagnifikationstest) dazu beitragen, die für die behördlichen Tests von Chemikalien erforderliche Fischmenge weiter zu reduzieren.

Abstract: Development of a bioaccumulation test using *Hyalella azteca*

A test concept for bioconcentration tests with the freshwater amphipod *Hyalella azteca* (HYBIT) was recently described. It was shown that the *Hyalella* bioconcentration factors (BCFs) derived for compounds with different hydrophobic characteristics ($\log K_{ow}$ 2.4 – 7.8) show a strong correlation to those from fish tests. This project was carried out to elucidate the suitability of the HYBIT test for testing an extended range of substance classes including difficult to test compounds and, if required, to further enhance the test concept. The bioaccumulation potential of highly lipophilic UV stabilisers and ionic organic PFAS as well as silver, titanium dioxide and gold nanomaterials were tested. The two possible set-ups to conduct bioconcentration studies with *H. azteca* using a semi-static test set-up or a flow-through approach were applied. The solvent-facilitated and solvent-free application of the hydrophobic test compounds were compared. Due to the difficulties regarding the aqueous exposure of nanomaterials, biomagnification studies were also carried out as part of this project. We could show that the HYBIT approach permits the application of difficult to test compounds and enables to derive bioaccumulation endpoints for regulatory assessment. Due to the shorter exposure periods required, and the smaller experimental units used, the HYBIT approach provides several advantages in comparison to the flow-through fish test. As a non-vertebrate test, the *Hyalella* bioconcentration (or biomagnification) test may help to further reduce the amount of fish required for the regulatory testing of chemicals.

Inhaltsverzeichnis

Abbildungsverzeichnis.....	10
Tabellenverzeichnis.....	13
Abkürzungsverzeichnis.....	16
Summary.....	17
Zusammenfassung.....	22
1 Introduction.....	27
2 The <i>Hyalella azteca</i> bioconcentration Test (HYBIT).....	29
2.1 Husbandry of <i>H. azteca</i>	29
2.2 Sexing of <i>H. azteca</i>	29
2.3 Test set-ups.....	31
2.3.1 Semi-static set-up.....	31
2.3.2 Flow-through set-up.....	32
2.3.2.1 Solvent-facilitated application.....	32
2.3.2.2 Solvent-free application.....	33
2.4 BCF calculation.....	34
3 Workpackage 1: Lipophilic and ionic organic compounds.....	37
3.1 Bioconcentration tests with IOCs PFOS and GenX.....	37
3.1.1 Methods.....	37
3.1.1.1 Analyses of water and <i>Hyalella azteca</i> samples.....	37
3.1.2 Results of PFOS and GenX experiments.....	38
3.1.2.1 Determination of extraction efficiency.....	38
3.1.2.2 Results of bioconcentration tests with PFOS.....	39
3.1.2.3 Results of bioconcentration studies with GenX.....	43
3.1.3 Evaluation.....	44
3.2 Bioconcentration tests with highly hydrophobic compounds UV-234 and UV-329.....	46
3.2.1 Methods.....	46
3.2.1.1 Solvent-facilitated test set-up.....	46
3.2.1.2 Solvent-free application: Production of column-generated medium concentrations.....	46
3.2.1.3 Analyses of water and <i>Hyalella azteca</i> samples.....	47
3.2.2 Determination of lipid content.....	47
3.2.3 Results of bioconcentration tests with UV-234 and UV-329.....	47
3.2.3.1 Biological observations.....	47

3.2.3.2	Determination of extraction efficiency.....	47
3.2.3.3	Results of medium and tissue analyses	48
3.2.4	Evaluation	52
3.3	Conclusions	55
4	Workpackage 2: Nanomaterials	56
4.1	Selection and characterization of test substance	56
4.1.1	Characterization using transmissing electron microscopy (TEM).....	56
4.1.2	Examinations using dynamic light scattering.....	57
4.1.3	Results of the characterizations.....	57
4.2	Test concepts for testing nanomaterials	59
4.2.1	Bioconcentration test	59
4.2.2	Biomagnification test.....	61
4.3	Analytics	61
4.3.1	Inductively coupled plasma mass spectrometry (ICP-MS).....	61
4.3.2	Single particle inductively coupled plasma mass spectrometry (sp-ICP-MS)	62
4.4	Bioconcentration tests with NMs and AgNO ₃	63
4.4.1	Bioconcentration test with AgNO ₃	63
4.4.1.1	Test design of the bioconcentration test with AgNO ₃	63
4.4.1.2	Analytics of the bioconcentration tests with AgNO ₃	63
4.4.1.3	Results of the bioconcentration tests with AgNO ₃	63
4.4.1.4	Evaluation of the bioconcentration tests with AgNO ₃	67
4.4.2	Preliminary bioconcentration test with NM 300K	68
4.4.2.1	Preliminary bioconcentration test with NM 300K: Test design and analytics.....	68
4.4.2.2	Results of the preliminary bioconcentration test with NM 300K.....	68
4.4.2.3	Evaluation of the preliminary bioconcentration test with NM 300K.	69
4.4.3	Bioconcentration test with NM 300K	69
4.4.3.1	Bioconcentration tests with NM 300K: Test design and analytics	70
4.4.3.2	Results of the bioconcentration tests with NM 300K.....	70
4.4.3.3	Evaluation of the bioconcentration tests with NM 300K	73
4.4.4	Bioconcentration test with NM 105	75
4.4.4.1	Test design and analytics of the bioconcentration tests with NM 105	75
4.4.4.2	Results of the bioconcentration tests with NM 105.....	75
4.4.4.3	Evaluation of the bioconcentration tests with NM 105	77
4.4.5	Bioconcentration test with AuNMs	79

4.4.5.1	Test design and analytics of the bioconcentration tests with AuNMs	79
4.4.5.2	Results of the bioconcentration tests with AuNMs.....	79
4.4.5.3	Evaluation of the bioconcentration tests with AuNMs	81
4.5	Biomagnification tests with NMs	82
4.5.1	Experimental feed for biomagnification tests and leaching test with NM 300K.....	82
4.5.1.1	Production	82
4.5.1.2	Leaching test with NM 300K.....	82
4.5.2	Biomagnification test with NM 300K.....	83
4.5.2.1	Test design and analytics of the biomagnification test with NM 300K	83
4.5.2.2	Results of the biomagnification test with NM 300K.....	83
4.5.2.3	Evaluation of the biomagnification test with NM 300K	86
4.5.3	Biomagnification test with NM 105	88
4.5.3.1	Test design of the biomagnification test with NM105	88
4.5.3.2	Results of the biomagnification test with NM 105	88
4.5.3.3	Evaluation of the biomagnification test with NM 105.....	90
4.5.4	Biomagnification test with AuNMs	91
4.5.4.1	Test design of the biomagnification test with AuNMs	91
4.5.4.2	Results of the biomagnification test with AuNMs.....	91
4.5.4.3	Evaluation of the biomagnification test with AuNMs.....	92
4.6	Conclusions	93
5	Workpackage 3: Development of an OECD Guideline	94
5.1	Critical evaluation of the HYBIT protocol for testing highly hydrophobic and ionic substances and nanomaterials	94
5.1.1	UV-compounds	94
5.1.2	Ionizable organic compounds	94
5.1.3	Nanomaterials.....	96
6	References.....	98
A	Annex.....	107
A.1	Lipophilic and ionic organic compounds.....	107
A.1.1	Instrumental parameters for analysis of IOCs	107
A.1.2	Instrumental parameters for highly hydrophobic compounds	109
A.1.3	Bioconcentration tests with PFOS and GenX.....	111
A.1.4	Bioconcentration tests with UV-234 and UV-329 – solvent-facilitated application.....	114
A.1.5	Bioconcentration test with UV-329 – solvent-free application	116

A.1.6	Exemplary calibration curves and chromatograms	117
A.2	Nanomaterials.....	123
A.2.1	Bioconcentration tests.....	123
A.2.2	Biomagnification tests	133

Abbildungsverzeichnis

Figure 1:	Picture of a male <i>Hyalella azteca</i> .	30
Figure 2:	Sexual dimorphism in <i>H. azteca</i> .	30
Figure 3:	Schematic overview of the experimental set-up of the semi-static test.	31
Figure 4:	Schematic overview of the flow-through test set-up of the solvent-facilitated application.	33
Figure 5:	Schematic overview of the flow-through test set-up of the solvent-free application.	34
Figure 6:	A typical kinetic time course of a test substance in <i>H. azteca</i> . Uptake and the depuration phase are presented.	35
Figure 7:	In-transformed concentration data of the depuration phase. The linear regression reveals k_2 as the slope of the regression.	36
Figure 8:	PFOS test medium concentration during uptake phase (7 days, PFOS-IME)*.	39
Figure 9:	PFOS concentration in male <i>H. azteca</i> tissue during uptake and depuration phase (PFOS-IME).*	40
Figure 10:	Course of PFOS medium concentration during uptake phase (7 days, PFOS-UBA).*	41
Figure 11:	PFOS concentration in male <i>H. azteca</i> tissue during uptake and depuration phase (PFOS-UBA).*	41
Figure 12:	Course of PFOS medium concentration during uptake phase (PFOS-ext.-IME).*	42
Figure 13:	PFOS concentrations in female <i>H. azteca</i> tissue during uptake and depuration phase (PFOS-ext.-IME).*	42
Figure 14:	Course of GenX medium concentration during uptake phase.*	43
Figure 15:	GenX concentrations in male <i>H. azteca</i> tissue during uptake and depuration phase.*	43
Figure 16:	Bioconcentration study with UV-234: medium concentration during uptake phase (solvent-facilitated application).*	48
Figure 17:	Bioconcentration study with UV-329: medium concentration during uptake phase (solvent-facilitated application).*	49
Figure 18:	Bioconcentration study with UV-329: medium concentration during uptake phase (solvent-free application).*	49
Figure 19:	Bioconcentration study with UV-234: tissue concentrations in <i>H. azteca</i> during uptake and depuration phase (solvent-facilitated application).*	50
Figure 20:	Bioconcentration test with UV-329: tissue concentrations in <i>H. azteca</i> during uptake and depuration phase (solvent-facilitated application).*	51

Figure 21:	Bioconcentration of UV-329: tissue concentration in <i>H. azteca</i> during uptake and depuration phase (solvent-free application).*	51
Figure 22:	TEM image of NM 300K AgNMs (magnification 35kx) and histogram of the size distribution (based on 143 particles).	58
Figure 23:	TEM image of AuNMs (magnification 30kx) and histogram of the size distribution (based on 172 particles).	58
Figure 24:	TEM image of NM 105 (magnification 80kx).	59
Figure 25:	Schematic overview of the flow-through test system for testing nanomaterials.	60
Figure 26:	Total Ag medium concentration in bioconcentration test AgNO _{3-ML} using males.*	64
Figure 27:	Total Ag medium concentration in bioconcentration test AgNO _{3-FL} using females.*	65
Figure 28:	Total Ag medium concentration in bioconcentration test AgNO _{3-FH} using females.*	65
Figure 29:	Total Ag tissue concentrations in bioconcentration tests with AgNO ₃ (uptake phase).	66
Figure 30:	Total Ag tissue concentrations in females during bioconcentration test AgNO _{3-FL} .	66
Figure 31:	Total Ag medium concentration in NM 300K preliminary bioconcentration test.*	68
Figure 32:	Preliminary bioconcentration test with NM 300K: Total Ag tissue concentrations.	69
Figure 33:	Total Ag medium concentration in NM 300K _{Cm} bioconcentration test (Test medium based on culture medium).*	71
Figure 34:	Total Ag tissue concentrations in NM 300K _{Cm} bioconcentration test (Test medium based on culture medium).	72
Figure 35:	Total Ag medium concentration in bioconcentration tests with NM 300K _{Aq} and NM 300K _{Zg} .*	72
Figure 36:	Total Ag tissue concentrations in NM 300K bioconcentration test using Aquarium (NM 300K _{Aq}) and Zuger glass system (NM 300K _{Zg}).	73
Figure 37:	Total TiO ₂ medium concentration in bioconcentration test NM 105 _L .*	76
Figure 38:	Total TiO ₂ medium concentration in bioconcentration test NM 105 _H .*	76
Figure 39:	Exemplary total TiO ₂ tissue concentrations in NM 105 _H bioconcentration test (all data below LOQ).	77
Figure 40:	Total Au medium concentration in the bioconcentration test AuNM _L .*	80

Figure 41:	Total Au tissue concentrations in the bioconcentration test AuNM _L	80
Figure 42:	Total Au medium concentration in the bioconcentration test AuNM _H .*	81
Figure 43:	Total Au tissue concentrations in the bioconcentration test AuNM _H	81
Figure 44:	Feces at the ground of the Zuger glass test system 24 h after the start of the biomagnification test with NM 300K.	84
Figure 45:	TEM HAADF images and the corresponding EDX signals of NPs enriched in the experimental feed.	84
Figure 46:	Total Ag tissue concentrations in NM 300K _L biomagnification test.*	85
Figure 47:	Total Ag tissue concentrations in NM 300K _H biomagnification test.*	85
Figure 48:	Total TiO ₂ tissue concentrations in NM 105 _L biomagnification test.*	89
Figure 49:	Total TiO ₂ tissue concentrations in NM 105 _H biomagnification test.*	89
Figure 50:	Total Au tissue concentrations in AuNM _H biomagnification test.*	91
Figure 51:	Exemplary calibration curve of PFOS used for quantification of medium and tissue samples.	117
Figure 52:	Exemplary chromatogram of PFOS standard (5 µg/L).....	117
Figure 53:	Exemplary calibration curve of GenX used for quantification of medium and tissue samples.	118
Figure 54:	Exemplary chromatogram of GenX standard (5 µg/L).	118
Figure 55:	Exemplary calibration curve of UV-234 used for quantification of medium samples.	119
Figure 56:	Exemplary chromatogram of UV-234 standard (5 µg/L).	119
Figure 57:	Exemplary matrix-matched calibration curve of UV-234 used for quantification of <i>H. azteca</i> samples.....	120
Figure 58:	Exemplary chromatogram of matrix-matched UV-234 standard (5 µg/L).	120
Figure 59:	Exemplary calibration curve of UV-329 used for quantification of medium samples.	121
Figure 60:	Exemplary chromatogram of matrix-matched UV-329 standard (medium) (5 µg/L).....	121
Figure 61:	Exemplary matrix-matched calibration curve of UV-329 used for quantification of <i>H. azteca</i> samples.....	122
Figure 62:	Exemplary chromatogram of matrix-matched UV-329 standard (<i>H. azteca</i>) (5 µg/L).	122

Tabellenverzeichnis

Table 1:	Composition of the reconstituted water (culture medium).....	29
Table 2:	Overview of performed studies with PFOS and GenX.....	37
Table 3:	Recovery rates of PFOS and GenX after extraction and concentration.	38
Table 4:	Results of the bioconcentration tests with PFOS and GenX.....	44
Table 5:	Results of the bioconcentration tests with solvent-facilitated and solvent-free application of UV-234 and UV-329.	52
Table 6:	Hypothetical comparison of BCF studies with UV-329 with different medium concentrations.	53
Table 7:	Comparison of Hyalella and fish BCF values of UV-234 and UV-329.	54
Table 8:	Characteristics of the bioconcentration tests with AgNO ₃ and calculated BCF values.	64
Table 9:	Specifications of the bioconcentration studies with NM 300K and calculated BCF values.	70
Table 10:	Specifications of the bioconcentration studies with NM 105 and calculated BCF values.	75
Table 11:	Specifications of the bioconcentration studies with AuNMs and calculated BCF values.	79
Table 12:	Characteristics of the biomagnification studies with NM 300K and calculated BMF values.	87
Table 13:	Characteristics of the biomagnification studies with NM 105 and calculated BMF values.	88
Table 14:	Characteristics of the biomagnification studies with AuNM and calculated BMF values.	92
Table 15:	Overview of chromatographical conditions for analysis of PFOS and GenX in medium and <i>H. azteca</i> samples.	107
Table 16:	MS parameter for PFOS and GenX.	108
Table 17:	Mass transitions.	108
Table 18:	Overview of chromatographical conditions for analysis of UV-234 and UV-329 in medium and <i>H. azteca</i> samples.....	109
Table 19:	MS parameter.....	110
Table 20:	Mass transitions.	110
Table 21:	Bioconcentration test PFOS, TWA 49.4 µg PFOS/L, males: total PFOS concentration in <i>H. azteca</i> tissue and standard deviation.	111
Table 22:	Bioconcentration test PFOS, TWA 49.98 µg PFOS/L, males: total PFOS concentration in <i>H. azteca</i> tissue and standard deviation (performed at UBA).	111
Table 23:	Bioconcentration test PFOS, TWA 39.22 µg PFOS/L, females: total PFOS concentration in <i>H. azteca</i> tissue and standard deviation.....	112

Table 24:	Bioconcentration test GenX, TWA 49.4 µg GenX/L, total GenX concentration in <i>H. azteca</i> tissue and standard deviation.....	113
Table 25:	Bioconcentration test UV-234, TWA 0.997 µg UV-234/L, total UV-234 concentration in <i>H. azteca</i> tissue and standard deviation.....	114
Table 26:	Bioconcentration test UV-329, TWA 0.078 µg UV-329/L, total UV-329 concentration in <i>H. azteca</i> tissue and standard deviation.....	115
Table 27:	Solvent-free bioconcentration test UV-329, TWA 0.208 µg UV-329/L, total UV-329 concentration in <i>H. azteca</i> tissue and standard deviation.....	116
Table 28:	Bioconcentration test AgNO _{3-ML} , TWA 0.67 µg Ag/L, males: total Ag concentration in <i>H. azteca</i> tissue and standard deviation.	123
Table 29:	Bioconcentration test AgNO _{3-FL} , TWA 0.64 µg Ag/L, females: total Ag concentration in <i>H. azteca</i> tissue and standard deviation, * end of uptake.....	124
Table 30:	Bioconcentration test AgNO _{3-FH} , TWA 1.64 µg Ag/L, females: total Ag concentration in <i>H. azteca</i> tissue and standard deviation.....	125
Table 31:	Preliminary bioconcentration test NM 300K, TWA 3.734 µg Ag/L: total Ag concentration in <i>H. azteca</i> tissue and standard deviation.....	126
Table 32:	Bioconcentration test NM 300K, TWA 3.00 µg Ag/L, conducted by UBA with classic aquarium set-up: total Ag concentration in <i>H. azteca</i> tissue and standard deviation.	127
Table 33:	Bioconcentration test NM 300K, TWA 6.729 µg Ag/L, aquarium: total Ag concentration in <i>H. azteca</i> tissue and standard deviation.....	128
Table 34:	Bioconcentration test NM 300K, TWA 6.827 µg Ag/L, Zuger glass: total Ag concentration in <i>H. azteca</i> tissue and standard deviation.....	129
Table 35:	Bioconcentration test NM 105, TWA 3.30 µg TiO ₂ /L: total TiO ₂ concentration in <i>H. azteca</i> tissue and standard deviation.....	130
Table 36:	Bioconcentration test AuNPs, TWA 0.085 µg Au/L: total Au concentration in <i>H. azteca</i> tissue and standard deviation.....	131
Table 37:	Bioconcentration test AuNPs, TWA 0.704 µg Au/L: total Au concentration in <i>H. azteca</i> tissue and standard deviation.....	132
Table 38:	Biomagnification test NM 300K, food conc. 0.07 mg Ag/kg: total Ag concentration in <i>H. azteca</i> tissue and standard deviation.....	133

Table 39:	Biomagnification test NM 300K, food conc. 0.751 mg Ag/kg: total Ag concentration in <i>H. azteca</i> tissue and standard deviation.....	133
Table 40:	Biomagnification test NM 105, food conc. 3.667 mg TiO ₂ /kg: total TiO ₂ concentration in <i>H. azteca</i> tissue and standard deviation.....	134
Table 41:	Biomagnification test NM 105, food conc. 19.4 mg TiO ₂ /kg: total TiO ₂ concentration in <i>H. azteca</i> tissue and standard deviation.....	134
Table 42:	Biomagnification test AuNM, food conc. 0.889 mg Au/kg: total Au concentration in <i>H. azteca</i> tissue and standard deviation.	135

Abkürzungsverzeichnis

BAF	Bioaccumulation factor
Ag+	Ag ⁺ ions
BCF	Bioconcentration factor
BCF_{SS}	Bioconcentration factor estimated during the steady state
BMF	Biomagnification factor
BMF_k	Kinetic Biomagnification factor
BMF_{SS}	Biomagnification factor estimated during the steady state
DLS	Dynamic light scattering
EDX	Energy Dispersive X-ray Spectroscopy
HDW	Holding and dilution water
HYBIT	<i>Hyalella azteca</i> Bioconcentration Test
IOCs	Ionic organic compounds
LC	Liquid chromatography
LC-MS/MS	Liquid Chromatography with tandem mass spectrometry
LOD	Limit of detection
LOQ	Limit of quantification
MNMs	Manufactured nanomaterials
MRM	Multiple reaction monitoring mode
MS	Coupled mass spectrometry
MTs	Metallothioneins
NMs	Nanomaterials
NPs	Nanoparticles
OECD	Organisation for Economic Co-operation and Development
PFOA	Perfluorooctanic acid
PFOS	Perfluorooctane sulfonic acid
PLL	Poly-L-Lysine
REACH	Registration, Evaluation, Authorisation and Restriction of Chemicals (regulation of the European Union)
SE	Secondary electron
sp-ICP-MS	Single particle inductively coupled plasma mass spectrometry
TEM	Transmission electron microscopy
TG	Test guideline
TRR	Total radioactive residues
TWA	Time weighted average
UHQ	Ultra high quality water
UBA	Umweltbundesamt (German Environment Agency)
UVs	Phenole benzotriazoles

Summary

Bioconcentration, defined as the enrichment of a xenobiotic substance in an organism from the surrounding medium, is a central process in ecotoxicology. The Bioconcentration factor (BCF) expressing the potential of a test substance to be accumulated from the surrounding medium is the ultimate decisive bioaccumulation criterion as part of the regulatory chemical safety assessment of pesticides, pharmaceuticals and other chemicals. The BCF determination is part of the bioaccumulation assessment under the European Chemicals Registration REACH (European Parliament Council, 2006) or others like Kashinho in Japan (Naiki, 2010), TCFA in Korea (Korea Ministry of Government Legislation, 2008), KKDIK in Turkey (Ministry of Environment and Urbanization (MoEU) of Turkey, 2017) or HPV in the USA (US EPA, 2004).

The BCF is commonly determined by fish flow-through tests according to OECD test guideline 305 (Organisation for Economic Co-operation and Development (OECD), 2012). The suitability of this established test is limited due to the fact, that it was developed for water-soluble and primary lipophilic test substance. Furthermore, fish flow-through tests usually require more than 100 animals per test, are costly and may last several weeks.

From the ethical point of view, especially in view of the 3R principles, defined as Replacement, Reduction and Refinement, alternative test methods would be of value (de Wolf et al., 2007; Russell et al., 1959). From the regulatory point of view new test methods are also needed due to the challenges involved in the testing of certain groups of substances that are difficult to test like e.g. highly hydrophobic, water-insoluble as well micro or nanoparticulate compounds.

The REACH Guidance on Information Requirements and Chemical Safety Assessment allows taxonomic groups other than fish, e.g. amphipods, to be used for the bioaccumulation assessment of chemical compounds which may help to waive further studies using fish as test organisms (European Parliament Council, 2006).

The freshwater amphipod *Hyalella azteca* is a well established test organism for ecotoxicological studies (Borgmann, 2002; Environment Canada, 2013; US EPA, 2000). The epibenthic amphipod can easily be cultured in the laboratory, is available during the complete year and shows a high reproduction rate and fast growth. Experimental animals can be raised within a few weeks to adult size suitable for the usage in bioaccumulation tests (Schlechtriem et al., 2019).

In 2019, Schlechtriem et al. (2019) described a test concept for bioconcentration tests with the freshwater amphipod *H. azteca* (HYBIT) and tested about 20 organic compounds with different hydrophobic characteristics ($\log K_{ow}$ 2.4 – 7.8). The results obtained were compared with fish BCF values described in the literature. It was shown that the results from HYBIT tests show a strong correlation to those from fish tests. An international ring test was carried out in 2020 to test the transferability of the test protocol and to compare the results obtained by different labs using HYBIT in order to support the development of a new OECD Test guideline (TG).

This project was carried out to supplement the HYBIT ring test by elucidating the limitations of the method with regard to the testing of difficult to test compounds and, if required, to further improve the approach to allow testing of an extended range of substance classes. The project was divided in two parts: i) Workpackage 1 involved bioconcentration tests with lipophilic and ionic organic compounds (IOCs) and ii) Workpackage 2 covered bioconcentration and biomagnification tests with metal ions and nanomaterials (NMs).

The first pair of test compounds tested in Workpackage 1 were the IOCs perfluorooctane sulfonic acid (PFOS) and the ammonium salt of hexafluoropropylene oxide dimer acid (HFPO-DA) fluoride (GenX). PFOS was chosen as a global pollutant and a representative of fluorochemicals that can be found in biota samples from nearly all places around the world. It can even be found in secluded locations like the Arctic (e.g., Bossi et al., 2005; Kannan et al., 2001; Martin et al., 2004; Taniyasu et al., 2003). PFOS is a stable end product of the degradation of a wide variety of sulfonated fluorochemicals that have been produced for over 40 years to be used as surfactants, fire-fighting foams or polymers for textiles (Kannan et al., 2002). The production of PFOS in 2000 was around 3,000 tons per year (US EPA, 2001). The high-energy carbon-fluorine bonds in the molecule cause high stability against photolysis, hydrolysis and biodegradation causing a high persistence in the environment (Kissa, 2001).

There is still limited knowledge on the toxicity of PFOS, but there are some indications that PFOS is responsible for hepatic toxicity and alterations in the metabolism and intercellular communication (Berthiaume and Wallace, 2002; Hoff et al., 2003; Hu et al., 2002).

The bioaccumulation potential of PFOS was investigated in different studies. According to de Vos et al. (2008) the bioaccumulation behavior of PFOS is comparable to that of short and medium chained fatty acids. Bossi et al. (2005) described the biomagnification of PFOS along the marine food chain with resulting concentrations of 1,285 ng/g in the liver of polar bears. A bioaccumulation factor (BAF) value of around 180 for PFOS in *Daphnia magna* was determined by Dai et al. (2013). Goeritz et al. (2013) estimated a BMF of 0.42 for PFOS in market size rainbow trouts. Martin et al. (2003) estimated compartment specific BCF values of 1,100, 4,300 and 5,400 for carcass, blood and liver of rainbow trout. These values allow a comparison with the results of the tests carried out as part of this project using *H. azteca*.

PFOS has been listed as a persistent organic pollutant (POP) since 2009 and has been implemented in the POP regulation under European law since 2010 allowing manufacture only for certain uses. Thus, alternatives such as GenX (replacement for perfluorooctanoic acid, PFOA) were developed and have been produced within a range of 10 to 100 tons per year in Europe (ECHA, 2021). Concentrations of GenX ranging from 107.6 to 68,500 ng/L were measured in the water of rivers near to industrial parks (Heydebreck et al., 2015; Liu et al., 2017; Pan et al., 2017). Pan et al. (2017) measured concentrations of GenX in the blood (1,500 ng/mL), the liver (587 ng/g) and the filet (118 ng/g) of wild *Cyprinus carpio* living in the Xiaoqing River (China) with water concentrations of 5,200 - 68,500 ng GenX/L. Even in humans living near this river a blood serum concentration of 2.93 ng GenX/mL was measured.

The second pair of organic compounds tested in Workpackage 1 consisted of UV-234 and UV-329. These substances are two representatives of phenole benzotriazoles (UVs) which have been used as ultraviolet filters (sun protection) e.g. in polymer based products to extend their lifespan. UVs are highly lipophilic and thus are suspected of being highly bioaccumulative and they have been shown to accumulate e.g. along the marine food chain (Nakata et al., 2009). Due to their usage in products as cosmetics and sun protections these compounds can enter the aquatic and terrestrial environment via waste water and sewage sludge, respectively. UVs were found in sewage sludges (Casado et al., 2013; Liu et al., 2012; Ruan et al., 2012; Zhang et al., 2011), in sediments (Carpinteiro et al., 2012; Kameda et al., 2011; Nakata et al., 2009; Zhang et al., 2011), and marine ecosystems and were also found in organisms like fishes and mussels (Bachelot et al., 2012; Kim et al., 2011; Nakata et al., 2012, 2009).

In this project, for all tested organic compounds BCF_{ss} and BCF_k were determined following the protocol of the HYBIT method (Schlechtriem et al., 2019; Kosfeld et al., 2020). We were able to show that GenX has a lower bioaccumulation potential (BCF_{ss} of 2.85 and BCF_k of 7.25) than

PFOS with BCF_{ss} values between 111 and 259 and BCF_k values between 185 and 405, depending on the duration of the uptake phase. Thus, both compounds seem not to be highly bioaccumulative for aquatic organisms. For the UV compounds BCF values above 5,000 were determined (considering the low analytical recovery of UV-234).

The applied methods were suitable to generate stable exposure concentrations in the test system and allowed the determination of clear uptake and elimination kinetics of the test compounds. However, it should be mentioned that the use of solvent (used to facilitate the application of the UV compounds) caused a strong growth of biofilm in the test system, even under flow-through conditions. It can only be speculated how the results obtained were influenced by the potential ingestion of biofilm by the grazing organisms. The formation of biofilm could be avoided by using column generated concentrations requiring no use of solvent.

In Workpackage 2 a source of metal ions and three nanomaterials were applied which were selected based on their physico-chemical properties.

a) Silver nitrate ($AgNO_3$)

$AgNO_3$ was tested as a source of Ag^+ ions (Ag^+), which is known to be bioavailable for *H. azteca* (Kuehr et al., 2018). Ag^+ can be released from AgNPs. The following testing of AgNMs allowed the comparison of the obtained BCFs for a dissolved and a nanoparticulate form of the same element.

b) The silver nanomaterial NM 300K

NM 300K was chosen as an example of AgNMs, one of the most examined and commercialized groups of nanomaterials, e.g. due its antibacterial properties (Bone et al., 2012; Fabrega et al., 2011; McGillicuddy et al., 2017; Vale et al., 2016; Zhang et al., 2016) that are based on the release of Ag^+ (Bragg and Rainnie, 1974; Feng et al., 2000; Schreurs and Rosenberg, 1982). The used NM 300K is one of the representative test and reference materials of the *European Commission's Joint Research Centre* and has been in the scope of the *OECD Working party on Manufactured Nanomaterials Sponsorship Program* (Klein et al., 2011). NM 300K represents a well dispersible and ion releasing nanomaterial.

c) The titanium dioxide nanomaterial NM 105

TiO_2 NMs do not release ions and are chemically inert under environmental conditions, but are one of the most commercially used nanomaterials (Piccinno et al., 2012). NM 105 is a representative test and reference material from the *European Commission's Joint Research Centre* and has been also in the scope of the *OECD Working party on Manufactured Nanomaterials Sponsorship Program*. NM 105 represents the group of non-ion releasing and highly sedimenting NMs (depending on the conditions) (Rasmussen et al., 2014). TiO_2 NMs are able to alter the bioavailability and extend of the effects of co-contaminants like organic compounds or metals for aquatic organisms (Balbi et al., 2014; Fan et al., 2016; Farkas et al., 2015; Zhang et al., 2007; Zhu et al., 2011).

d) Gold nanomaterials from BBI Solutions

The AuNPs from BBI Solutions represent nanomaterials that are chemically inert and well dispersible. AuNPs are used e.g. in the field of medicine e.g. for drug delivery, as x-ray contrast agent or for cancer therapy and in chemical, photonic and catalytic applications (Dreaden et al., 2012; Ghosh et al., 2008; Hainfeld et al., 2006; Huang et al., 2008; Wang and Schaaf, 2012; Yang et al., 2003).

To determine the BCFs of the test substances, each test substance was tested in two bioconcentration and biomagnification tests at two concentrations except for AgNO₃ that was only tested in bioconcentration tests.

Testing NMs requires the establishment of stable exposure conditions. The tests were conducted using a slightly modified Zuger glass test system as described by Kuehr et al. (2020c). This system was used as an alternative for the commonly used aquaria, due to experiences of very instable NMs including exposure media leading to very inhomogeneous exposure concentrations caused by e.g. fast sedimentation (pers. communication R. Zeumer). In the case of NM 300K an additional test using aquaria as described by Schlechtriem et al. (2019) was carried out to compare the results obtained in different test vessels. In contrast to previous studies with fish both test systems, aquaria and Zuger glass test system showed to be suitable for testing the bioaccumulation of AgNMs in *H. azteca*.

With the exception of NM 105, we were able to estimate BCF values for the test substances under steady state conditions and gained clear kinetics for the uptake of the metals and NMs. The highest BCF_{SS} values between 4,965 and 5,094 were estimated for Ag⁺ (AgNO₃ exposure). By testing AgNO₃ we were also able to show that the sex of animals does not alter the BCF_{SS} if the exposure occurred under similar conditions. The elimination of Ag from the animals' tissue occurred slowly and incompletely. It is unclear whether the binding of Ag⁺ was the result of metal-binding proteins or of metal sequestration as phosphorus or sulfur granules (Ahearn et al., 2004). Silver is known to induce the expression of metallothioneins, metal binding proteins (Lansdown et al., 1999). Metallothioneins are known to be present in a wide range of species as protective detoxifying mechanism (Borgmann, 2002; Heerden et al., 2004; Legeay et al., 2005; Norey et al., 1990; Ringwood et al., 2010; Žnidaršič et al., 2005). Silver is further known to be stored in sinks even after a long elimination phase after a preceding exposure and thus may be relevant for secondary poisoning and transfer along the food chain (Kampe et al., 2018; Kuehr et al., 2020c). Similar observations were made in the depuration phase of the tests with NM 300K. This finding underlines the hypothesis that the bioaccumulation of Ag (from AgNMs) is mainly driven by the released ions. Tests with NM 300K showed, that the usage of a test medium with a higher ionic strength and higher concentrations of halogens or sulfates (Borgmann Medium), does not prevent the uptake and accumulation of Ag from AgNMs, e.g. by the precipitation as insoluble AgCl, Ag₂S or AgCO₃. BCF_{SS} values of NM 300K ranging from 453 to 604 were nearly ten times lower than those from the tests with AgNO₃.

BCF_{SS} values of 166 and 424 were estimated for the higher and lower exposure concentration of Au in the bioconcentration tests with the AuNMs, respectively. A rapid elimination was observed, that reduced the body burden of the animals to the initial level from the test start within 48 h.

Even if there occurred no bioaccumulation of TiO₂ in the bioconcentration tests with NM 105, we were still able to detect ingested NPs in the animal samples using single particle coupled plasma mass spectrometry (sp-ICP-MS).

Due to the difficulties involved in the aqueous exposure of NMs, biomagnification studies were also carried out as part of this project. For the biomagnification tests an experimental diet was prepared for each test following the protocol of Kampfraath et al. (2012) with adjustments to enrich the alginate based DECOTABs with the nanomaterials. The enriched DECOTABs were examined using transmission electron microscopy (TEM) which revealed that the materials were still present in the diet in a (nano)-particulate form after the feed preparation process.

BMF_{SS} values were estimated for all tested NMs. The lowest BMF_{SS} were obtained for the AuNMs (0.017), followed by NM 105 (0.024 and 0.12 for the high and low TiO₂ diet concentration).

Higher BMF_{ss} values of 0.245 and 0.93 were calculated for NM 300K with high and low Ag diet concentration, respectively. A slow and incomplete elimination of Ag was observed during the depuration phase of the NM 300K biomagnification test which might be again explained by the binding of Ag⁺ released from dietary AgNMs during the digestion process.

The different bioaccumulation studies with the freshwater amphipod *H. azteca* principally demonstrated the suitability of the HYBIT protocol (Schlechtriem et al., 2019). However, depending on the physico-chemical properties of the test compound modifications of the test system (e.g. use of Zuger glass system) might be required for establishing constant exposure conditions of metals and NMs. Even if the fate and localization of the NMs measured in the animal samples (sp-ICP-MS and total metal content) remained unclear, the applied approaches still allow to draw conclusions on the bioaccumulation potential of NMs. Methods like correlative microscopy including TEM are required for the absolute evidence of the real incorporation of NMs in the animals' tissue or penetration into cells.

The *Hyalella* bioconcentration and biomagnification approach can provide valuable endpoints for the bioaccumulation assessment of NMs and should be taken in consideration within a tiered assessment approach as presented by (Handy et al., 2018). A bioaccumulation assessment scheme for the testing of NMs integrating the modified HYBIT protocol was suggested by Kühr et al. (2021).

Zusammenfassung

Biokonzentration ist definiert als die Anreicherung einer xenobiotischen Substanz aus dem umgebenden Medium im Organismus von Tieren und stellt einen zentralen Aspekt der Ökotoxikologie dar. Der Biokonzentrationsfaktor (BCF), welcher das Potenzial einer Verbindung ausdrückt sich aus dem Umgebungsmedium im Organismus anzureichern, stellt den maßgeblichen Endpunkt der Bewertung des Bioakkumulationspotenzials im Rahmen der Regulation von Pestiziden, Pharmazeutika und anderer Chemikalien dar. Die Bestimmung des BCF-Werts ist somit auch Teil der Bioakkumulationsbeurteilung im Rahmen der Europäischen Chemikalienverordnung REACH (European Parliament Council, 2006) oder auch anderer Gesetze oder Verordnungen wie Kashinho in Japan (Naiki, 2010), TCFA in Korea (Korea Ministry of Government Legislation, 2008), KKDIK in der Türkei (Ministry of Environment and Urbanization(MoEU) of Turkey, 2017) oder HPV in den USA (US EPA, 2004).

Der BCF wird meist in Durchflussstudien mit Fischen gemäß der OECD Test Richtlinie 305 (Organisation for Economic Co-operation and Development (OECD), 2012) ermittelt. Die Eignung dieses etablierten Tests wird häufig dadurch gemindert, dass er für wasserlösliche und lipophile Verbindungen entwickelt wurde. Zudem erfordern diese Tests jeweils über 100 Versuchstiere, sind kostenaufwendig und dauern mehrere Wochen.

Aus ethischer Sicht, speziell unter Beachtung des 3R Prinzips, welches mit *Replace*, *Reduce* und *Refine* als Grundlage für den verantwortungsvollen Umgang mit Tierversuchen gilt, wären alternative Tests sehr wertvoll (de Wolf et al., 2007; Russell et al., 1959). Aus regulatorischer Sicht werden ebenfalls neue Ansätze benötigt, welche den Herausforderungen des Testens anderer Stoffgruppen gerecht werden, die z.B. aufgrund ihrer geringen Wasserlöslichkeit oder ihrer partikulären Eigenschaften schwer zu testen sind.

Gemäß der *REACH Guidance on Information Requirements and Chemical Safety Assessment* können auch andere taxonomische Gruppen als die der Fische (z. B. Amphipoden) verwendet werden, um Daten zur Beurteilung des Bioakkumulationspotenzials zu generieren und so weitere Fischstudien zu vermeiden (European Parliament Council, 2006).

Die Süßwasseramphipode *Hyalella azteca* ist ein gut etablierter Testorganismus für den Einsatz im Rahmen ökotoxikologischer Studien (US EPA, 2000; Borgmann, 2002, Environment Canada., 2013). Die epibenthisch lebende Amphipode kann unter Laborbedingungen gehalten werden und zeigt dabei eine hohe Reproduktionsfähigkeit und ein zügiges Wachstum. Über das gesamte Jahr hinweg können die Kleinkrebse für den Einsatz im Rahmen von Bioakkumulationstest kultiviert werden. Diese Eigenschaften machen *H. azteca* zu einem geeigneten Kandidaten für einen alternativen Testansatz zur Bestimmung des Bioakkumulationspotenzials von Chemikalien.

In 2019 beschrieben Schleichtriem et al. (2019) ein Testkonzept zur Durchführung von Biokonzentrationstest mit *H. azteca* (HYBIT) und ermittelten *Hyalella* BCF Werte für über 20 verschiedene organische Verbindungen unterschiedlicher Hydrophobizität mit log K_{ow} Werten von 2,4 – 7,8. Die ermittelten BCF-Werte wurden mit Fisch BCF Werten aus der Literatur verglichen. Dabei konnte eine starke Korrelation der Werte aus den beiden verschiedenen Ansätzen aufgezeigt werden. Um die Anwendbarkeit des neuen Testprotokolls und die Variabilität der damit gewonnene BCF-Werte aus verschiedenen Laboren genauer zu überprüfen, wurde im Jahr 2020 ein internationaler Ringtest durchgeführt, um die Entwicklung einer neuen OECD Richtlinie zum HYBIT zu unterstützen.

Dieses Projekt sollte die im Rahmen des Projekts CEFIC LRI ECO 40 und des Ringtests durchgeführten Studien ergänzen. Durch den Einsatz schwer zu testender Substanzen sollten die

potentiellen Grenzen der Testmethode untersucht und ggf. notwendige Veränderungen des Testprotokolls aufgezeigt werden. Auf diese Weise soll zukünftig das Testen einer möglichst breiten Masse an Stoffen auf Basis des HYBIT Protokolls ermöglicht werden.

Hierzu wurde das Projekt in zwei Arbeitspakete unterteilt: i) Arbeitspaket 1, befasste sich mit der Testung lipophiler und ionischer organischer Verbindungen ii) Arbeitspaket 2, legte den Fokus auf die Testung von Metallionen und Nanomaterialien im Rahmen von *Hyalella* BCF-Studien. Das übergreifende Ziel des Projekts war die Unterstützung der Entwicklung einer OECD Richtlinie zum Testen neutraler und ionischer Verbindungen sowie, wenn geeignet, einer Anleitung zur Anpassung der Methode zum Testen von Nanomaterialien.

Im Arbeitspaket 1 wurden vier Verbindungen in Biokonzentrationstests mit *H. azteca* getestet. Dabei kamen zuerst die beiden ionischen organischen Verbindungen (engl. *ionic organic compounds*, IOCs) PFOS und GenX zum Einsatz.

PFOS wurde als Schadstoff und Repräsentant der Fluorochemikalien ausgewählt, die sich weltweit in Biotaprobenn, selbst an abgelegenen Orten wie der Arktis, finden lassen (z.B. Bossi et al., 2005; Kannan et al., 2001; Martin et al., 2004; Taniyasu et al., 2003). PFOS ist ein stabiles Endprodukt des Abbaus einer großen Spanne an sulfonierten Fluorochemikalien, die seit mehr als 40 Jahren z.B. als Tenside, Feuerlöschschaum oder Polymere der Textilbranche eingesetzt werden (Kannan et al., 2002). Die Produktion von PFOS lag im Jahr 2000 bei etwa 3 000 Tonnen (US EPA, 2001). Die stabilen Kohlenstoff-Fluor-Verbindungen begründen die hohe Stabilität gegenüber Photolyse, Hydrolyse und biologischem Abbau, welche die hohe Persistenz bedingt (Kissa, 2001).

Die Toxizität von PFOS ist bisher noch nicht sehr gut beschrieben, es gibt jedoch einige Hinweise, dass PFOS für hepatische Toxizität und für Veränderungen im Metabolismus und auch in der interzellulären Kommunikation verantwortlich ist (Berthiaume and Wallace, 2002; Hoff et al., 2003; Hu et al., 2002).

Das Bioakkumulationspotenzial von PFOS wurde in mehreren Studien untersucht. Nach de Vos et al. (2008) ist das Bioakkumulationspotenzial von PFOS vergleichbar mit dem von kurz- und mittelkettigen Fettsäuren. Bossi et al. (2005) beschreiben die Biomagnifikation von PFOS entlang der marinen Nahrungskette, welche zu einer Konzentration von 1 285 ng/g in der Leber von Eisbären führte. Ein BAF Wert von rund 180 wurde für *Daphnia magna* bestimmt (Dai et al., 2013). Goeritz et al. (2013) ermittelten einen BMF Wert von 0,42 für PFOS in adulten Regenbogenforellen. Martin et al. (2003) bestimmten Kompartiment-spezifische BCF Werte von 1 100, 4 300 und 5 400 für die Karkasse, das Blut und die Leber der Regenbogenforelle. Diese Werte ermöglichen somit einen groben Vergleich mit den Werten, welche in den Tests mit *H. azteca* gewonnen wurden.

PFOS ist seit 2009 als persistenter organischer Schadstoff (engl. *persistent organic pollutant* – POP) gelistet und ist in der POP-Verordnung nach europäischem Recht implementiert. Dies hat zur Folge, dass Herstellung und Verwendung der Substanz nur für bestimmte Verwendungszwecke zulässig sind. Als Alternative wurden Stoffe wie das Ammoniumsalz der Hexafluoropropylen Oxid Trimer Säure (GenX), eingesetzt, das alleine in Europa als Ersatzstoff für PFOA in einer Größenordnung von 10 bis 100 t pro Jahr produziert wird (ECHA, 2021).

GenX Konzentrationen von 107,6 bis 68 500 ng/L wurden im Wasser von Flüssen in der Nähe von Industrieparks gemessen (Heydebreck et al., 2015; Liu et al., 2017; Pan et al., 2017). (Pan et al., 2017) haben GenX Konzentrationen im Blut (1 500 ng/mL), der Leber (587 ng/g) und dem Filet (118 ng/g) Karpfen ermittelt, welche im Xiaoqing River (China) leben. Die GenX

Konzentrationen in diesem Fluss betragen 5 200 - 68 500 ng GenX/L. Im Blutserum der dort lebenden Menschen wurde GenX mit einer Konzentration von 2,93 ng GenX/mL gefunden.

Neben den beiden ionischen organischen Verbindungen, kamen in Arbeitspaket 1 die beiden hoch hydrophoben Stoffe UV-234 und UV-329 zum Einsatz. Beide organischen Verbindungen sind Repräsentanten der Phenol-Benzotriazole (UVs), welche als Filter für ultraviolette Strahlung z. B. in polymerbasierten Produkten eingesetzt werden, um deren Lebensspanne zu erhöhen. UVs weisen aufgrund ihrer meist hohen Lipophilie ein hohes Bioakkumulationspotenzial auf und werden verdächtig, sich im marinen Nahrungsnetz stark anreichern zu können (Nakata et al., 2009).

Aufgrund ihrer Verwendung in Kosmetikprodukten und Sonnenschutzmitteln gelangen diese Verbindungen durch das Abwasser in die aquatische Umwelt und durch Klärschlämme in die terrestrischen Systeme. UVs konnten in Klärschlamm (Casado et al., 2013; Liu et al., 2012; Ruan et al., 2012; Zhang et al., 2011), in Sediment (Carpinteiro et al., 2012; Kameda et al., 2011; Nakata et al., 2009; Zhang et al., 2011) und in marinen Ökosystemen (z.B. in Fischen und Muscheln) gefunden werden (Bachelot et al., 2012; Kim et al., 2011; Nakata et al., 2012, 2009).

Dem Protokoll der HYBIT Methode (Schlechtriem et al., 2019; Kosfeld et al., 2020) folgend, konnten für alle getesteten organischen Verbindungen BCF_{ss} und BCF_k bestimmt werden. Wir konnten aufzeigen, dass GenX (BCF_{ss} von 2,85 und BCF_k von 7,25) ein geringeres Bioakkumulationspotenzial aufweist als PFOS mit BCF_{ss} Werten zwischen 111 und 259 und BCF_k Werten zwischen 185 und 405, abhängig von der Dauer der Expositionsphase. Beide Verbindungen scheinen aus regulatorischer Sicht nicht bioakkumulierend zu sein, wenn man von den ermittelten BCF Werten ausgeht. Für die UV-Verbindungen wurden hingegen BCF Werte von über 5 000 ermittelt unter Berücksichtigung der geringen analytischen Wiederfindung von UV-234.

Die im Rahmen der Testung der UV-Verbindungen eingesetzten Methoden (mit und ohne Lösungsvermittler) können als geeignet für die Generierung stabiler Expositionskonzentrationen angesehen werden und erlaubten im Rahmen der Studie die Erfassung klarer Kinetiken für die Aufnahme und die Elimination der Verbindungen. Es sollte jedoch erwähnt werden, dass lösungsmittelbasierte Applikation der UV Verbindungen zu einem starken Biofilmbewuchs im Testsystem führte. Inwieweit die in diesem Fall erzielten Ergebnisse durch die Aufnahme des Biofilms durch die Organismen beeinflusst wurden, kann nur spekuliert werden. Durch die Verwendung der Säulenelutionsmethode und Testung von „Column generated concentrations“, konnte die Bildung von Biofilm unterbunden werden.

Im Rahmen von Arbeitspaket 2 wurden $AgNO_3$ als Quelle von Ag^+ Ionen und drei Nanomaterialien (NMs) getestet, welche hinsichtlich ihrer unterschiedlichen physikalisch-chemischen Eigenschaften ausgewählt wurden:

e) Silbernitrat ($AgNO_3$)

$AgNO_3$ wurde zur Ergänzung der Studien mit AgNMs als Quelle von Ag^+ Ionen (Ag^+) getestet, da die Bioverfügbarkeit und Akkumulation von Ag^+ Ionen in *H. azteca* bereits bekannt ist (Kuehr et al., 2018). Der Einsatz von $AgNO_3$ ermöglichte den Vergleich von BCF Werten der gelösten Form (Ag^+ Ionen) mit BCF Werten für Ag aus Tests mit AgNMs als nanopartikuläre Form desselben Elements.

f) Silbernanomaterial NM 300K

NM 300K wurde als Repräsentant der Gruppe der AgNMs gewählt, eines der am meisten untersuchten kommerziell verwendeten NMs überhaupt, bedingt u. a. durch seine antibakterielle Wirkung, welche auf der Freisetzung von Ag^+ basiert (Bone et al., 2012; Fabrega

et al., 2011; McGillicuddy et al., 2017; Vale et al., 2016; Zhang et al., 2016). Das getestete NM 300K ist ein repräsentatives Test- und Referenzmaterial des *European Commission's Joint Research Centre* sowie der *OECD Working party on Manufactured Nanomaterials Sponsorship Program* (Klein et al., 2011) und repräsentiert hier die Gruppe der gut dispergierbaren und ionenfreisetzenden Nanomaterialien.

g) Titandioxidnanopartikel NM 105

TiO₂NMs sind die mit am meisten verwendeten Nanomaterialien, sie sind chemisch nahezu inert und setzen keine Ionen frei (Piccinno et al., 2012). NM 105 ist ebenfalls ein repräsentatives Test- und Referenzmaterial des *European Commission's Joint Research Centre* und der *OECD Working party on Manufactured Nanomaterials Sponsorship Program* (Rasmussen et al., 2014). TiO₂NMs können die Bioverfügbarkeit und das Ausmaß der Effekte von Co-Kontaminaten wie organischer Verbindungen oder Metalle für aquatische Organismen beeinflussen (Zhang et al., 2007; Zhu et al., 2011; Balbi et al., 2014; Farkas et al., 2015; Fan et al., 2016).

h) Goldnanopartikel von BBI Solutions

Die ausgewählten AuNPs von BBI Solutions repräsentieren die Nanomaterialien, welche chemisch inert und gut dispergierbar sind. AuNPs werden u. a. in der Medizin eingesetzt, z. B. als *Drug-Delivery-System*, als Röntgenkontrastmittel oder in der Krebstherapie. Aber auch in der Chemie, Photonik sowie für katalytischen Prozesse in vielen weiteren Bereichen (Dreaden et al., 2012; Ghosh et al., 2008; Hainfeld et al., 2006; Huang et al., 2008; Wang and Schaaf, 2012; Yang et al., 2003).

Um das Bioakkumulationspotenzial der ausgewählten Testsubstanzen zu ermitteln, wurde jedes Testmaterial in mindestens zwei Konzentrationen in Biokonzentrations- und Biomagnifikationstest getestet. AgNO₃ wurde als einzige Substanz nicht im Biomagnifikationstest verwendet.

Die Durchführung von BCF-Studien mit NMs setzt eine kontinuierliche stabile Exposition der Versuchstiere voraus. Durch die Sedimentationsneigung einzelner NMs kann ggf. der Einsatz modifizierter Testsysteme erforderlich sein. Die Tests wurden in dem von Kuehr et al. (2020c) beschriebenen Zugerglas System getestet, welches für die Studien mit *H. azteca* leicht modifiziert wurde. Dieses System wurde als eine Alternative zum klassischen Aquarium als Testbecken entwickelt, da es Erfahrungen mit instabilen NM-Expositionsmedien gibt, die zu inhomogenen Expositionskonzentrationen aufgrund starker Sedimentation etc. führten (Persönliche Kommunikation mit Richard Zeumer). Im Fall von NM 300K wurde ein zusätzlicher Test durchgeführt, um die mit dem Zugerglas-System gewonnenen Ergebnisse mit jenen zu vergleichen, die in Aquarien, wie durch Schlechtriem et al. (2019) beschrieben, gewonnen wurden.

Mit Ausnahme von NM 105 konnten für jede Testsubstanz BCF Werte unter steady state Bedingungen ermittelt und klare Kinetiken für die Aufnahme und Elimination von Metallen oder NMs aufgezeigt werden. Der höchste BCF_{SS} Wert zwischen 4 965 und 5 094, wurde für Ag aus AgNO₃ bestimmt. Durch die Tests mit AgNO₃ konnten wir zudem zeigen, dass das Geschlecht der Tiere den BCF_{SS} nicht beeinflusst, solange die Exposition unter möglichst vergleichbaren Bedingungen abläuft. Die Elimination von Ag aus dem tierischen Organismus erfolgte langsam und nicht vollständig. Es ist unklar, ob diese für Ag beobachtete Senke das Ergebnis der Bindung der Ionen an metallbindende Proteine oder einer Sequestrierung des Metalls durch Phosphor oder Schwefel war (Ahearn et al., 2004). Ag ist dafür bekannt, die Expression von Metallothioneinen (metallbindende Schutzproteine) zu induzieren (Lansdown et al., 1999). Metallothioneine sind in vielen Spezies als Schutz- und Entgiftungsmechanismus vertreten

(Borgmann, 2002; Heerden et al., 2004; Norey et al., 1990; Ringwood et al., 2010; Žnidaršič et al., 2005). Dies kann dazu führen, dass Ag nach vorheriger Exposition während einer folgenden Depurationsphase im Organismus verbleibt (Senke) und der Elimination somit weitreichend entgehen kann (Kampe et al., 2018; Kuehr et al., 2020c). Diese Mechanismen könnten von hoher Relevanz für die Weiterreichung und Anreicherung von Ag entlang der Nahrungskette sein. Die Bildung einer entsprechenden Senke wurde auch in der Eliminationsphase eines Tests mit NM 300K beobachtet, wodurch die Hypothese, dass die Bioakkumulation von Ag primär auf der Aufnahme von Ag⁺ basiert unterstützt werden konnte. Durch die Verwendung eines Mediums mit höherer ionischer Stärke und höheren Konzentrationen an Halogenen und Sulfat (Borgmann Medium), konnte gezeigt werden, dass die Aufnahme und Akkumulation von Ag aus AgNMs nicht durch das Medium unterbunden wird, etwa durch Präzipitation von unlöslichem AgCl, Ag₂S oder AgCO₃. Die ermittelten BCF_{SS} Werte für Ag aus AgNMs (453 bis 604) waren jedoch 10-mal niedriger als die für Ag aus AgNO₃.

BCF Werte von 166 und 424 wurden für die höhere und niedrigere Au Konzentration in den Biokonzentrationsstests mit AuNMs ermittelt. Eine schnelle Elimination des Au aus den Organismen führte dazu, dass die zum Teststart gemessene Gewebekonzentration nach 48 h Depuration wieder erreicht wurde. Auch wenn im Vergleich keine Bioakkumulation von TiO₂ in den Biokonzentrationsstudien mit NM 105 festgestellt wurde, konnte dennoch nach Exposition die NMs mittels Einzelpartikel-Massenspektrometrie mit induktiv gekoppeltem Plasma (sp-ICP-MS) in den Tierproben detektiert werden.

Um den besonderen Eigenschaften der NMs Rechnung zu tragen, wurde neben den Biokonzentrationsstudien auch die Exposition über das Futter getestet. Für die Biomagnifikationstests wurde ein experimentelles Futter hergestellt, indem das Protokoll von Kampfraath et al. (2012) zur Herstellung von DECOTABs nach leichter Modifikation verwendet wurde, um mit NMs angereicherte die DECOTABs herzustellen. Die angereicherten DECOTABs wurden mittels Transmissionselektronenmikroskopie (TEM) untersucht, wobei sich zeigte, dass die NMs während der Futtermittelherstellung ihre (nano)partikuläre Form beibehalten. Für alle in diesem Projekt getesteten NMs wurden BMF_{SS} Werte ermittelt. Der niedrigste BMF_{SS} wurde für die AuNMs (0,017) ermittelt, gefolgt von NM 105 (0,024 und 0,12 für die hohe und niedrige Konzentration). Höhere BMF_{SS} Werte von 0,245 und 0,93 wurden für NM 300K (hohe und niedrige Konzentration) berechnet. Während der Eliminationsphase des Biomagnifikationstests mit NM 300K wurde eine langsame und unvollständige Eliminierung des Ag aus dem Organismus der Tiere beobachtet, was auf die Freisetzung und Anreicherung gelösten Silbers hindeutet.

Die verschiedenen Bioakkumulationsstudien mit der Süßwasseramphipode *H. azteca* demonstrieren die Eignung des HYBIT (Schlechtriem et al., 2019) zur Einstellung konstanter und homogener Expositionsbedingungen von Metallen und Nanomaterialien und somit zur Testung von NMs. Für die Testung sedimentierender NMs stehen modifizierte Expositionssysteme (Kühr et al., 2020a, c) zur Verfügung. Auch wenn die Mechanismen der Anreicherung von NMs und deren Lokalisierung im Gewebe unklar bleiben, erlaubt der im Projekt durchgeführte Testansatz dennoch eine Bewertung des Bioakkumulationspotentials von Ionen/NMs. Für eine weiterführende Untersuchung der Aufnahme/Akkumulation von NMs in das tierische Gewebe wären Methoden wie die korrelative Mikroskopie, inklusive TEM, erforderlich. Die vorgestellte Testmethode sowie die durch sie gewonnenen Bioakkumulationsfaktoren können in einer gestuften Bewertung, etwa wie von Handy et al. (2018) für NMs vorgestellt, einfließen. Ein Bewertungsschema der Bioakkumulation von NMs unter Berücksichtigung der im Rahmen von BCF/BMF-Studien mit *H. azteca* ermittelten Endpunkte, wurde kürzlich von Kühr et al. (2021) beschrieben.

1 Introduction

Bioaccumulation is one of the central processes in ecotoxicology and describes the enrichment of xenobiotics in organisms. The scientific assessment of compounds that bioaccumulate in organisms or biomagnify in food webs play a key role within the PBT-assessment. The potential of compounds to bioaccumulate from the surrounding media is commonly expressed as bioconcentration factor (BCF) and represents a decisive bioaccumulation criterion as part of the regulatory chemical safety assessment of chemicals (REACH), biocides (Regulation (EG) Nr. 528/2012), pesticides (Regulation (EG) Nr. 1107/2009) and pharmaceuticals (Guidelines 2001/83/EG and 2001/82/EG). The BCF reflects the proportion of the internal concentration of a test organism under steady state conditions compared to the concentration in the test medium (REACH Regulation (EC), Annex XIII). Threshold values of $> 2,000$ and $> 5,000$ are used for the classification as PBT or vPvB compound within the framework of the bioaccumulation assessment (European Parliament Council, 2006).

BCF determination is commonly based on fish flow-through tests carried out according to OECD TG 305 (Organisation for Economic Co-operation and Development (OECD), 2012). Even though such tests are well established, they need 100 - 200 fishes per study, are expensive and long running. In addition, ethics of animal testing are intensively discussed especially with regard to the 3R-principles (de Wolf et al., 2007; Russell et al., 1959). Thus, alternative test methods would be of value.

The usage of invertebrates is in accordance with the REACH Guidance on Information Requirements and Chemical Safety Assessment (ECHA, 2017). Here it is described that apart from fish other taxonomic groups may be used to determine the bioaccumulation potential of substances.

H. azteca is present in nearly all freshwaters of North and Middle America (Bousfield, 1958; de March, 1978) and is considered as highly suitable for bioaccumulation testing due to its short life cycle and sensitivity for environmental chemicals and metals (Blaser et al., 2008; Othman and Pascoe, 2001; Wood et al., 2002). Thus, *H. azteca* is an established organism used in ecotoxicity studies with and without sediment (American Society for Testing and Materials, 2003; Environment Canada, 2013; US EPA, 2000).

About 20 organic compounds with different hydrophobic character ($\log K_{ow}$ 2.4-7.8) have been tested (Schlechtriem et al., 2019). Results were compared with BCFs for the same compounds which were determined using fish studies to show the relationship between the values from both test systems. Strong correlations were revealed. Within the CEFIC-LRI-Project ECO 40 (Investigations on the bioconcentrations of xenobiotics in the freshwater amphipod *Hyaella azteca* and inter-laboratory comparison of a new BCF test protocol) a test protocol for testing the bioaccumulation potential of chemicals using the epibenthic amphipod *H. azteca* was developed (Kosfeld et al., 2020). An international ring test with three lipophilic substances was carried out in 2020 to confirm the transferability of the test protocol.

The *H. azteca* Bioconcentration Test (HYBIT) was developed for neutral (lipophilic) organic compounds. However, under environmental conditions many compounds are present in an ionized form (Franco et al., 2010). The electric charge of molecules has a strong impact on the physico-chemical characteristics leading to a different environmental behaviour compared to the neutral form. The REACH guidelines (R.1, R.7b; (European Parliament Council, 2006))

explain, that ionic organic compounds (IOCs) should be assessed independently (pH dependence of the log K_{ow} or log D_{ow} on the pH).

Recently, the bioconcentration and metabolism of laurate, the anion of lauric acid (dodecanoic acid), was tested in *H. azteca* (Raths et al., 2020). Lauric acid (pK_a of 5.0) is completely dissociated at $pH > 7$. The results proved that the HYBIT was suitable to test the ionic organic compound. Nevertheless, more IOCs need to be tested using the HYBIT to elucidate the suitability of the system and the comparability of the results with those determined using fish.

Another challenge in the bioaccumulation assessment is the use of a suitable testing procedure for manufactured nanomaterials (MNMs). During bioconcentration studies the increase of a substance concentration in the animals' organism is measured and compared to the concentration of the surrounding medium. The exposure concentration of the substance should not vary more than 20 % from the average concentration measured during the exposure phase. However, the established test system (fish flow-through test according to OECD TG 305) was developed for water-soluble test substances. However, most NMs tend to sediment in aquatic environments causing problems with respect to the perpetuation of stable and continuous exposure conditions during fish flow-through tests with MNMs. Thus, the establishment of suitable experimental conditions for determining the bioaccumulation potential of NMs is difficult and the development of test methods adapted to the specific needs for testing nanomaterials are required (Aschberger et al., 2011; Hankin et al., 2011).

Kuehr et al. (2020c) developed a test system allowing stable and continuous exposure conditions for testing NMs in bioaccumulation studies with the fresh water bivalve *Corbicula fluminea*. However, due to the filtering process of the mussels the test system only allows to determine bioaccumulation factors (BAF) that are less specific with respect to the exposure or uptake pathway.

Using *H. azteca* as test organism may allow to elucidate both, BCF and biomagnification factors (BMF), when NMs are tested by aqueous or dietary exposure, respectively. *H. azteca* has been used in a wide range of ecotoxicological and bioaccumulation tests with metals (Alves et al., 2009; Ball et al., 2006; Borgmann et al., 2004; Norwood et al., 2007, 2006). Kuehr et al. (2018, 2020a) and Poynton et al. (2019) examined the uptake, toxicity and accumulation of metals from NMs present in the medium or sediment. The usage of the HYBIT seems to be a promising strategy for bioaccumulation testing. If required, modified test systems with an adjusted exposure scenario as described by Kuehr et al. (2020c) could be applied to ensure constant exposure conditions.

The aim of this project was to test the bioaccumulation potential of lipophilic and ionic organic compounds (IOCs) as well as nanomaterials (NMs) to confirm the suitability of the HYBIT for testing an extended range of compounds including substances with difficult physico-chemical characteristics and to determine potential limitations of the test concept. The results obtained from this project will help to develop an OECD TG for neutral and ionic organic compounds and if suitable, to develop a guidance to adjust the TG for testing MNMs.

2 The *Hyalella azteca* bioconcentration Test (HYBIT)

In 2020 an international ring test to validate the bioconcentration test with freshwater amphipods *Hyalella azteca* (HYBIT) was carried out. A description of the test protocol and a summary of the results obtained are described by Schlechtriem et al. (in prep.).

Bioconcentration studies carried out as part of this project were performed in accordance with the HYBIT protocol with modifications where required. A brief presentation of the animal husbandry and sexing procedure as well as of the different test set-ups applied in this project is provided in this chapter.

2.1 Husbandry of *H. azteca*

The used amphipods were taken from the stock culture of Fraunhofer IME, Schmallenberg. The culturing procedure was carried out according to Kuehr et al. (2018). The strain originates from “Fred’s Haustierzoo” (Cologne, Germany). The stock culture was kept in 2 L-flasks stocked with 30 adult animals each at 25 °C ± 2 °C and 500 – 1000 Lux with a light : dark cycle of 16 : 8 h. The amphipods were kept in reconstituted water as culture medium. The composition of the culture medium is presented in Table 1 (Borgmann, 1996). The animals were fed 5 mg of ground fish feed (Tetramin®, Tetra) three times a week. Once a week, juveniles were separated from the parents and cultured in separate flasks until they reached a sufficient size for the usage in bioconcentration tests (approximately 8 weeks). Only healthy animals free from observable diseases and abnormalities were used for the studies.

Table 1: Composition of the reconstituted water (culture medium) (Borgmann, 1996)

Nutrient solution	Compound	Molecular formula	Concentration [mmol/L]
1	Calcium chloride dihydrate	CaCl ₂ * 2 H ₂ O	0.004
	Sodium bromide	NaBr	0.00004
	Potassium chloride	KCl	0.0002
2	Potassium hydrogen carbonate	NaHCO ₃	0.004
3	Magnesium sulfate	MgSO ₄	0.001

2.2 Sexing of *H. azteca*

Male and female individuals are separated before usage in bioconcentration studies to avoid breeding during the test. Therefore, males (Figure 1) are distinguished by the presence of a large gnathopod and females by the absence of a gnathopod and presence of eggs in the marsupial plate as described by Schlechtriem et al. (2019) (Figure 2). To collect male or female amphipods, adult *H. azteca* (animals older than 2 months) are transferred into a petri dish and examined under a stereomicroscope (magnification factor: 6 - 10 x).

Figure 1: Picture of a male *Hyalella azteca*.



Source: Fraunhofer IME.

During the mating process, the male amphipod is attached to the dorsal side of the female amphipod. Female and male amphipods can be separated by using spring steel tweezers. Generally, only healthy amphipods, which show a normal behavior, are selected. Test organisms which are used in bioconcentration studies should be older than 2 months. An Artemia sieve of wider mesh size (appr. 900 μm) is used to separate larger amphipods and to obtain test organisms of similar size. The male amphipods are collected, counted, and transferred into beakers (2 L, polypropylene) filled with a mix of culture medium (50 %) and dilution water (50 %) to allow gradual adaptation of the animals to the test medium. Instead of the cotton gauze used during husbandry, steel mesh shelters are used during the study and are placed in the beakers to provide a sufficiently dimensioned place of refuge for the dense group of animals. However, each beaker should not contain more than 130 to 150 amphipods to avoid competitive behavior and cannibalism. The selected test organisms remain in the collection beakers until the start of the test. The holding conditions (feeding, light, temperature) during this phase are the same as the husbandry conditions described above. The sexing should take place 1-2 days before test start. If the time period between separating and test start is longer than 2 days, the amount of selected male amphipods should be recounted. If necessary, animal losses should be replaced by additional male amphipods.

Figure 2: Sexual dimorphism in *H. azteca*.



Arrows indicate sex-specific characteristics. A: female *H. azteca* with eggs, B: male *H. azteca* with gnathopods.

Source: Schlechtriem et al., in prep.

2.3 Test set-ups

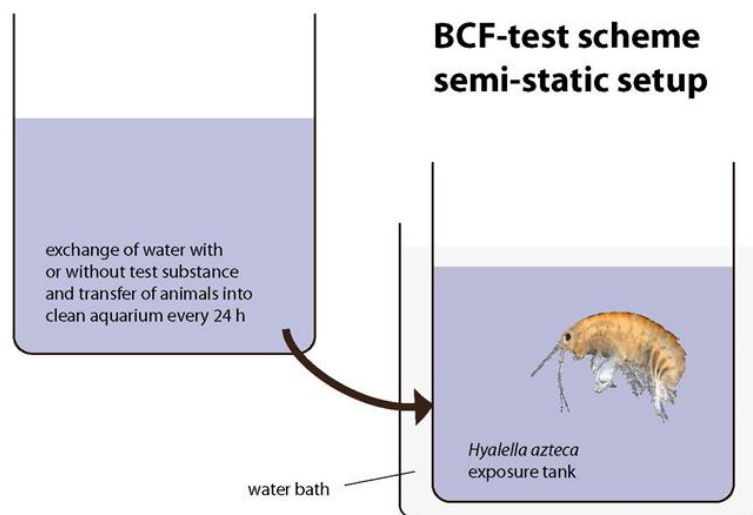
There are two possible set-ups to conduct bioconcentration studies with *H. azteca*: Using a semi-static test set-up with a full daily water exchange and a flow-through approach with an exchange rate of e.g. 5 times the total volume per day. The flow-through approach is usually required when the concentration of the test substance cannot be kept stable over 24 h in the exposure tanks ($\pm 20\%$ of the mean concentration). In this case a solvent-facilitated and a solvent-free application can be performed.

For both concepts holding and dilution water (HDW) fulfilling the requirements defined by OECD TG 305 is used (Organisation for Economic Co-operation and Development (OECD), 2012).

2.3.1 Semi-static set-up

A stock solution of the test substance is prepared using an appropriate solvent. The solvent stock solution is used to prepare a basic solution of the test substance in HDW at a defined concentration. Therefore, typically around 1000 μL of the solvent stock solution are pipetted into a substance reservoir with a screw cap (e.g. 10 L-brown glass bottle). After carefully evaporating the solvent to complete dryness (maybe facilitated using nitrogen air flow), the bottle is filled with HDW. The solution is then stirred overnight (at least 14 h) using a magnetic stirrer resulting in the basic solution. Care must be taken to ensure that the water solubility of the test substance is not reached at this point. Freshly prepared basic solutions need prepared on a daily basis. A sufficient amount of stock solution was prepared at the beginning of the study, stored appropriately, and used throughout the study for the preparation of basic solutions.

Figure 3: Schematic overview of the experimental set-up of the semi-static test.



Source: Schlechtriem et al., in prep.

A suitable volume of the basic solution is added to the exposure tank, which is then mixed with the respective volume of HDW to provide the exposure concentration. The exposure tank is thermo-regulated by an outer water bath. After addition of the HDW, the test medium (test

solution) should be stirred thoroughly to guarantee homogeneous exposure conditions. The experimental tank (aquarium) needs to be covered in order to avoid evaporation and thus changes in the concentration of the test substance. A continuous aeration of the test media using a glass capillary is needed if a proper oxygen saturation (> 60 %) cannot be maintained. Sampling procedures (water and animals) during the test were carried out in the morning before the daily feeding routine, where possible. Water exchanges were carried out by preparing a (clean) tank filled with fresh test media (uptake phase) or HDW (depuration phase) and transferring all remaining animals into the new vessel using a small net. Water temperature in the exposure tank should be adjusted before filling with *H. azteca*. The used tank is cleaned and can be used for the next media exchange. A schematic overview of the experimental set-up of the semi-static test is presented in Figure 3. The exposure tank is placed in a water bath to maintain a constant temperature. Animals are transferred every 24 h into a new tank with freshly prepared test medium (uptake period) or HDW (depuration period).

2.3.2 Flow-through set-up

For flow-through tests, a system which continuously dispenses and dilutes a stock solution of the test substance is required to deliver the test concentrations to the test chambers. At least five volume replacements through each test chamber per day should be achieved. The total flow rate through the test chamber (flow rate of test media leaving the mixing chamber which includes both, the flow of stock solution and dilution water) should be checked 48 hours prior to test start and then at least daily during the test. It needs to be ensured that this flow rate does not vary by more than 20 % (Organisation for Economic Co-operation and Development (OECD), 2012).

The flow-through system requires additional technical equipment e. g. metering pump, proportional diluter, saturator system and a greater amount of test substance compared to the semi-static set-up.

Using a solvent-facilitated application, generally, care must be taken that the final solvent concentration in the test media is below 0.1 mL/L (= 0.01 %, the maximum solvent level for fish as stated by the guideline OECD 305 (Organisation for Economic Co-operation and Development (OECD), 2012)). A brief description of the procedure is provided in Chapter 2.3.2.1. Depending on the concentrations measured in the test system, the flow rates (dose and/or HDW) may be adjusted to achieve the intended test concentration. However, care must be taken that the dose applied within 24 h does not exceed the total volume of the substance reservoir. Alternatively, the concentration of basic solution or solvent stock solution used for dosing may be adapted to achieve the intended test concentration.

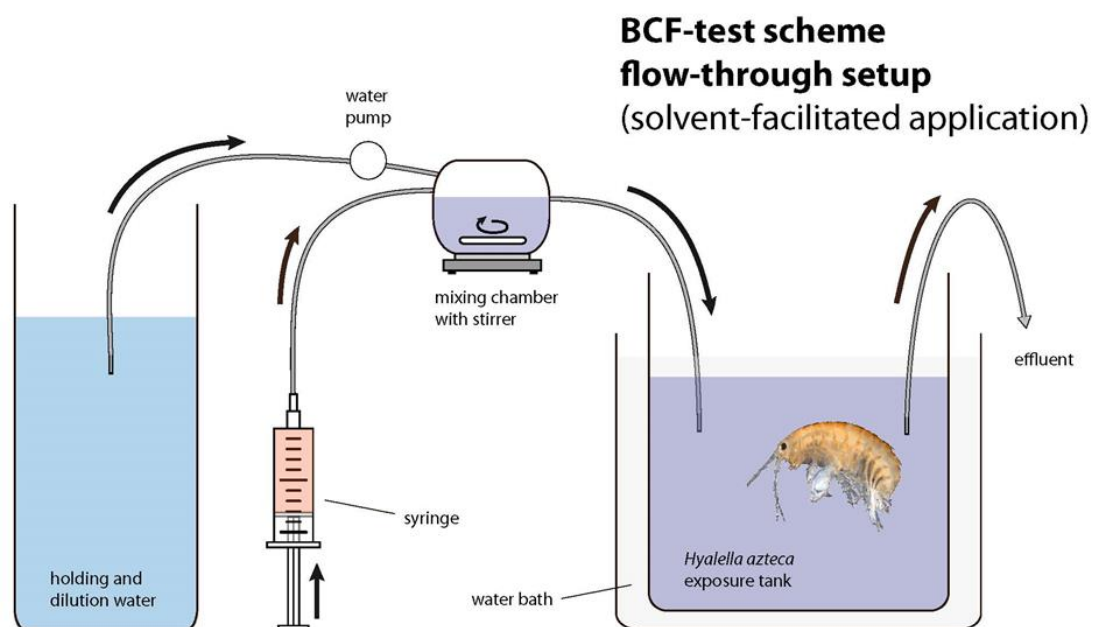
At the end of the uptake phase and after completion of all uptake phase samplings, the remaining amphipods are transferred for intermediate storage into a clean glass vessel filled with HDW. The pumps connected to the test system are stopped and all materials, which were previously exposed to the test substance, are replaced. The test chamber is emptied and replaced by a new clean aquarium of the same size as used during the uptake phase. The clean aquarium is filled with HDW and the pump system (water pump only) is re-started. The amphipods are transferred into a sieve, rinsed with HDW and placed into the uncontaminated water for depuration.

2.3.2.1 Solvent-facilitated application

A schematic overview of the flow-through test set-up for solvent-facilitated application is presented in Figure 4. An adequately concentrated stock solution of the test substance in solvent is prepared and filled into a 50 mL infusion pump syringe as substance reservoir. After

connecting the syringe to the infusion pump system, the stock solution from the reservoir is pumped at a defined flow rate (e.g. appr. 10 $\mu\text{L}/\text{min}$) into a mixing chamber with magnetic stirring. Through a second inlet of the mixing chamber HDW is added to reach a defined total flow rate (e.g. appr. 100 mL/min) and to provide the exposure concentration. The test medium flows continuously into the test vessel, which is thermo-regulated by an outer water bath. The substance reservoir (syringe) has to be refilled on a regular basis (appr. every three days at a flow rate of appr. 10 $\mu\text{L}/\text{min}$). For this, both pumps, substance pump (syringe infusion pump) and HDW pump, need to be stopped and the syringe refilled with stock solution in solvent. The flow rate of HDW and syringe infusion pump has to be adjusted and monitored before and during the uptake phase. The exposure tank is placed in a water bath to maintain a constant experimental temperature of 25 ± 2 °C. No cleaning of the test system is required during the uptake phase, however, the exposure tank and the connected equipment need to be replaced before the start of the depuration phase.

Figure 4: Schematic overview of the flow-through test set-up of the solvent-facilitated application.



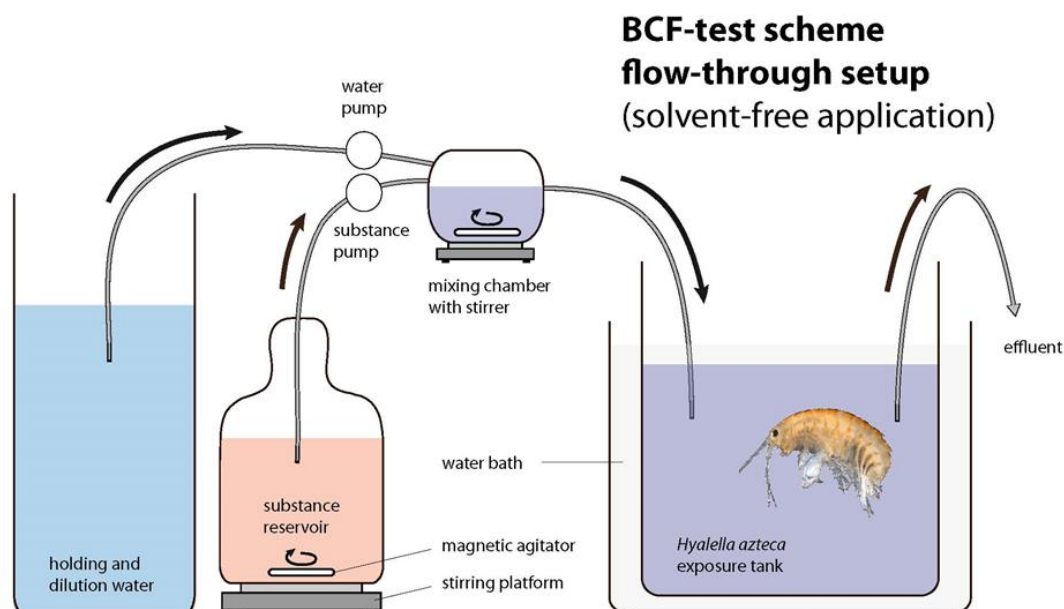
Source: Schlechtriem et al., in prep.

2.3.2.2 Solvent-free application

As an alternative to the above described solvent-facilitated application, the test substance may be delivered to the test chambers by dosing a basic solution of the test substance in HDW (Figure 5). A concentrated basic solution is prepared as described above for the semi-static test set-up. The basic solution of the test substance is prepared daily. It is stirred constantly and serves as substance reservoir. The reservoir is connected to a membrane pump with a glass capillary tube. The aqueous solution from the reservoir is pumped at a defined flow rate (5 mL/min) into a mixing chamber with magnetic stirring. HDW is added by a second inlet of the mixing chamber to reach a defined total flow rate (e.g. approximately 100 mL/min). The test medium flows continuously into the experimental tank, which is thermo-regulated by an outer water bath. The flow rate of HDW and substance reservoir (basic solution in HDW) needs to be

adjusted and monitored before and during the uptake phase. The exposure tank is placed in a water bath to maintain a constant experimental temperature of 25 ± 2 °C. The substance reservoir is renewed on a daily basis. No cleaning of the exposure tank is required during the uptake phase, however, the exposure tank and the connected equipment needs to be replaced before the start of the depuration phase.

Figure 5: Schematic overview of the flow-through test set-up of the solvent-free application.



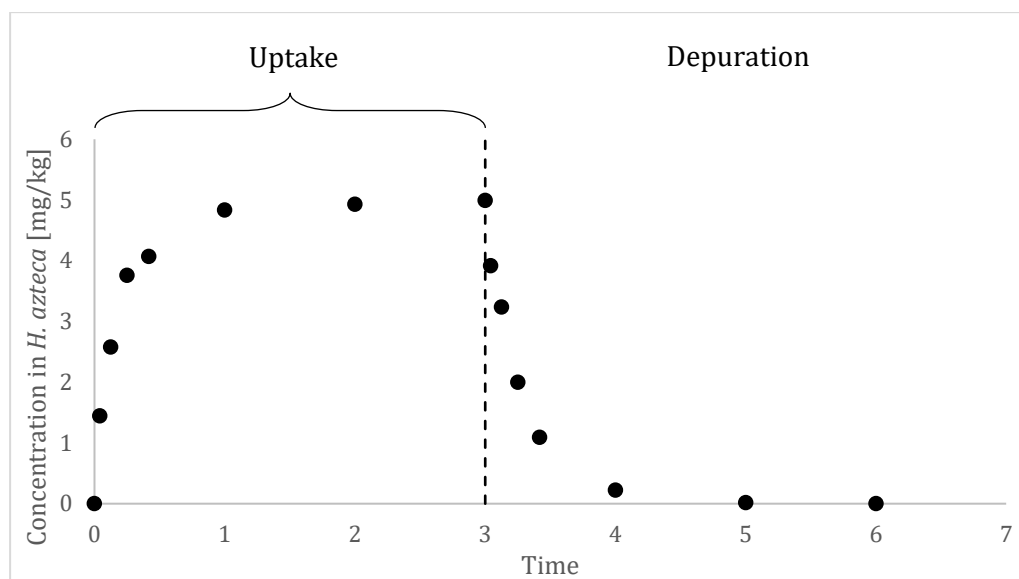
Source: Schlechtriem et al. in prep.

A second solvent-free alternative is the usage of a solid-phase desorption dosing system (Schlechtriem et al., 2017). Here, column generated concentrations are delivered to the test chambers by dosing a basic solution of the test substance in HDW. For that application method the test substance is coated onto a carrier material (e.g. Florisil® or sea sand) which is filled into a glass column. Afterwards a continuous flow of HDW (e.g. 5 mL/min) produced by a pump is led through the column dissolving a defined amount of test substance. The column outlet is led into the mixing chamber with magnetic stirring. HDW is added by a second inlet of the mixing chamber to reach a defined total flow rate (e.g. approximately 100 mL/min). The produced test medium flows continuously into the experimental tank. The flow rate of the column outlet and diluting HDW needs to be adjusted and monitored before and during the uptake phase. As mentioned, the exposure tank is placed in a water bath to maintain a constant experimental temperature of 25 ± 2 °C. Cleaning of the exposure tank is not required during the uptake phase, but the exposure tank and the connected equipment needs to be replaced before the start of the depuration phase.

2.4 BCF calculation

The bioconcentration factor (BCF) is determined based on the test item concentrations measured in *H. azteca* and water samples collected during the uptake phase as well as during the depuration phase of the study (Figure 6).

Figure 6: A typical kinetic time course of a test substance in *H. azteca*. Uptake and the depuration phase are presented.



The method used for BCF determination in *H. azteca* is largely based on the method described for fish in Annex 5 of the OECD Test Guideline 305 (Organisation for Economic Co-operation and Development (OECD), 2012). Detailed assumptions for the applied bioconcentration model can be found there. In contrast to the BCF determination in fish according to OECD TG 305, growth can be neglected in *H. azteca* BCF calculations due to the short duration of the studies.

In short:

H. azteca as 1-compartment model

1st order kinetics

Change of concentration in *H. azteca* is described by (Equation 1):

$$\frac{dC_h}{dt} = k_1 * C_w - k_2 * C_h \quad (\text{Equation 1})$$

k_1 overall uptake rate constant; L kg⁻¹day⁻¹

k_2 overall depuration rate constant; day⁻¹

C_h chemical concentration in *H. azteca* at steady-state; mg kg⁻¹

C_w chemical concentration in the water (TWA); mg L⁻¹

In general, two BCF types can be distinguished and are calculated: the steady-state BCF (BCF_{SS}) and the kinetic BCF (BCF_k). The BCF_{SS} is the ratio of test substance concentration in *H. azteca* during steady state and the test substance concentration in water (Equation 2). For the latter, the time-weighted average concentration is calculated from the chemical concentrations measured in the water during the uptake phase (Organisation for Economic Co-operation and Development (OECD), 2012). The kinetic BCF is the ratio of the uptake and depuration constant, which are determined by fitting the obtained data to the bioconcentration model (Equation 3).

$$BCF_{SS} = \frac{C_h \text{ (at steady-state)}}{C_w} \quad (\text{Equation 2})$$

$$BCF_k = \frac{k_1}{k_2} \quad (\text{Equation 3})$$

Calculation details

There are two ways to determine the uptake and depuration rates in a bioconcentration study: Both parameters are determined either simultaneously, or sequentially. So far, in *H. azteca* studies the sequential method is applied, meaning that in a first step the loss rate k_2 is calculated from the depuration data.

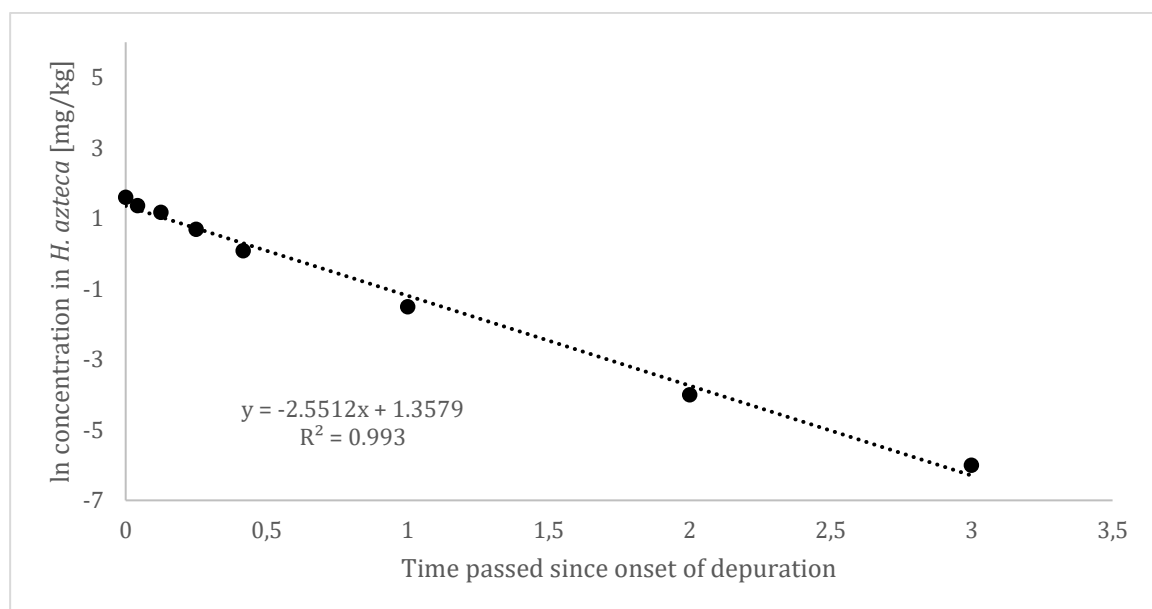
This is performed as follows:

First, the depuration data is ln-transformed. A linear regression onto the model (Equation 4):

$$y = m * x + b \quad (\text{Equation 4})$$

is performed on the data set (using e.g. Microsoft Office Excel). The concentration data is regressed against the time passed since the onset of depuration.

Figure 7: In-transformed concentration data of the depuration phase. The linear regression reveals k_2 as the slope of the regression.



The linear regression reveals two parameters: 'm', as the slope of the regression and 'b' as intercept of the y-axis. The slope of the regression in the example given in Figure 7 is -2.5512.

By inserting the loss rate constant k_2 in the corresponding model for the uptake kinetic a non-linear fit (performed by a suitable computational program, e.g. SigmaStat) is applied, determining the uptake constant k_1 . A simultaneous determination of k_1 and k_2 and consecutive BCF determination can be performed by a computer program. The guidance document for the OECD TG 305 proposes a package for the programming software R that enables such an estimation. Application of the R package and interpretation of results can be obtained from the OECD TG 305 guidance document.

3 Workpackage 1: Lipophilic and ionic organic compounds

3.1 Bioconcentration tests with IOCs PFOS and GenX

3.1.1 Methods

The bioconcentration tests with PFOS and GenX were performed using the semi-static set-up as described in Chapter 2.3.1. The test media were produced with a nominal test substance concentration of 50 µg/L and were exchanged every 24 h. Medium samples were taken from the fresh and aged medium every 24 h and stored at -20 °C until analysis. Animal samples were taken every 24 h and stored, after being blotted dry and weighed, at -20 °C until analysis. One test with GenX and three tests with PFOS were performed. The tests lasted 14 days with 7 days for the uptake and the depuration phase, each. One of the tests with PFOS was conducted at the Umweltbundesamt (UBA) where the same conditions were applied as by Fh IME except for the composition of the exposure medium. UBA used culture medium as described above (see Table 1) whereas Fh IME used HDW as test medium. The third experiment with PFOS was performed with HDW at Fh IME but the uptake phase was extended to 10 days to make sure that steady state was definitely reached. The following depuration phase lasted 14 days instead of 7 days as applied within the three shorter studies. In contrast to the other studies, female animals were used. Table 2 summarizes the differences between the performed tests. During the tests the animals were fed DECOTABs. The agar-agar based cubes were produced as described by Kuehr et al. (2020a). In brief, 500 mg agar-agar were dissolved in 23 mL boiling UHQ under constant stirring using a magnet stirrer and 1,500 mg ground TetraMin® flakes were added to the dissolved matrix. The suspension was stirred for 2 min and transferred into silicon ice trays with a well size of 1 mL. The trays were stored at 4 °C until DECOTABs were completely hardened. The feeding occurred ad libitum at Fh IME and with 5 DECOTABs every 24 h at UBA.

Table 2: Overview of performed studies with PFOS and GenX.

study code	test substance	duration of uptake phase	duration of depuration phase	test medium	sex	performing institution
PFOS-IME	PFOS	7 days	7 days	HDW	m	Fh IME
PFOS-UBA	PFOS	7 days	7 days	culture medium*	m	UBA
PFOS-ext.-IME	PFOS	10 days	14 days	HDW	f	Fh IME
GenX	GenX	7 days	7 days	HDW	m	Fh IME

with HDW = holding and dilution water, m = male, f = female and * = Borgmann medium (Borgmann, 1996).

3.1.1.1 Analyses of water and *Hyalella azteca* samples

The chemical analysis of the test substances was performed by liquid chromatography (LC) with coupled mass spectrometry (MS). The analyses of medium and *H. azteca* samples were carried out in the multiple reaction monitoring (MRM) mode and quantification of the analytes was performed internally with deuterated standards. Quality control samples with one low ($C_{low} = 1 \mu\text{g/L}$) and one high ($C_{high} = 10 \mu\text{g/L}$) concentration were run alongside each measurement. For specific conditions see Annex. Note, GenX was quantitated via the mass of a formed bicarbonate adduct. Therefore, ammonium bicarbonate was added to all solutions

(diluting solution and LC eluents). Calibrations for medium and tissue analysis of GenX samples and the medium samples collected during the bioconcentration tests with PFOS consisted of at least 6 points ranging from 0.25 – 50 µg/L. The calibration of PFOS extracted from *H. azteca* samples ranged from 0.025 – 50 µg/L. All medium samples were measured after 1:10 dilution with UHQ-water. *H. azteca* samples were processed by solid-liquid extraction. Therefore, 4 mL methanol (or acetonitrile for PFOS-ext.-IME) were added to the biological sample, homogenized for 30 seconds and then treated in an ultrasonic bath for 10 min. The samples were centrifuged for 5 min at 5,000 rpm and supernatants were transferred into a volumetric flask. After this, the dispersing tool was washed with 3 mL of the respective solvent. This washing solvent was then used for the second extraction step, which was similar to the first one. A third extraction step, using the solvent for washing the dispersing tool, was performed and the combined supernatants were filled up to a total volume of 10 mL. The extracts obtained were subsequently analyzed by liquid chromatography with tandem mass spectrometry (LC-MS/MS). PFOS samples were diluted by a factor of 10. GenX samples were first concentrated and then measured after 1:1 dilution. The volume of the samples was reduced by evaporating the solvent by means of a nitrogen stream.

The efficiency rates for this protocol were tested beforehand. Blank *H. azteca* samples were spiked with a specific amount of the test substance in five replicates. After extraction of the samples, the recovery rates were calculated based on the amount of the spiked compound. In addition to the investigation of extraction efficiency, the stability during evaporation of the solvent was tested and evaluated with regard to the spiked amount of the test substance.

3.1.2 Results of PFOS and GenX experiments

3.1.2.1 Determination of extraction efficiency

The *H. azteca* samples spiked with specific amounts of the test substances were extracted with methanol and acetonitrile in five replicates each. Subsequently extracts were concentrated by evaporation of the solvents by the means of a nitrogen stream. Table 3 summarizes the efficiency rates with regard to the spiked amount.

Table 3: Recovery rates of PFOS and GenX after extraction and concentration.

substance	extraction solvent	recovery extraction [%]	recovery concentration [%]
PFOS	acetonitrile	97.8	93.9
PFOS	methanol	99.4	*
GenX	acetonitrile	83.4	33.5
GenX	methanol	103.3	93.5

* = experiment not performed.

For both analytes, the extraction protocol was efficient. The recovery rates were determined to be 83.4 – 103.3 % with methanol and acetonitrile. The recovery of the concentration of extracts with acetonitrile was 93.9 % and 33.5 % for PFOS and GenX, respectively. Thus, this method was assessed to be suitable for PFOS but not for GenX analysis. The concentration of GenX samples

extracted with methanol showed a recovery rate of 93.5 % confirming the suitability of the method for analysis of *H. azteca* samples.

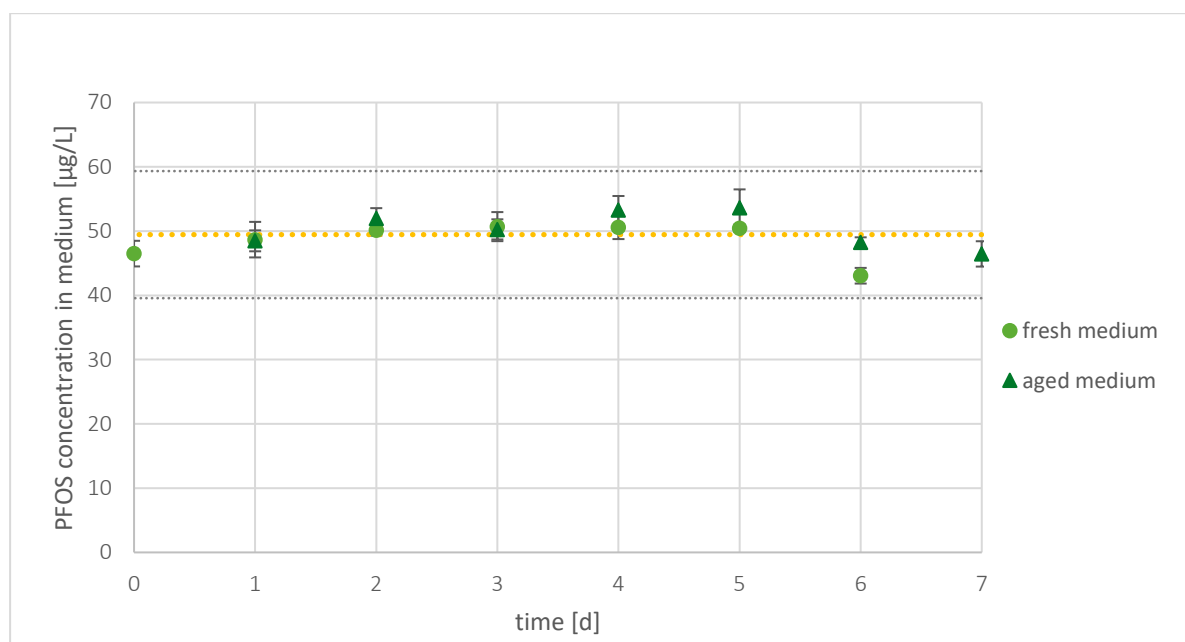
3.1.2.2 Results of bioconcentration tests with PFOS

During all measurements, two quality controls ($C_{low} = 1 \mu\text{g/L}$ (low) and $C_{high} = 10 \mu\text{g/L}$ (high)) were measured to check the quality of each measurement. For being acceptable, analytical standards containing the respective amount of matrix had to be measured with a recovery of 80 - 120 %. In the course of the PFOS-IME bioconcentration test with male *H. azteca* a time weighted average (TWA) concentration in the test medium of $C_W = 49.4 \mu\text{g PFOS /L}$ was measured (Figure 8). The maximum tissue concentration was 9.51 mg/kg at the end of the uptake phase (168 h / 7 d; Figure 9). The steady state tissue concentration is defined as follows (Organisation for Economic Co-operation and Development (OECD), 2012):

- ▶ concentration of test substance in tissue should not vary by more than $\pm 20 \%$ during the last days of exposure and
- ▶ during the latest analyses of the tissue concentration ($< 20 \%$) no further significant increase should be detected

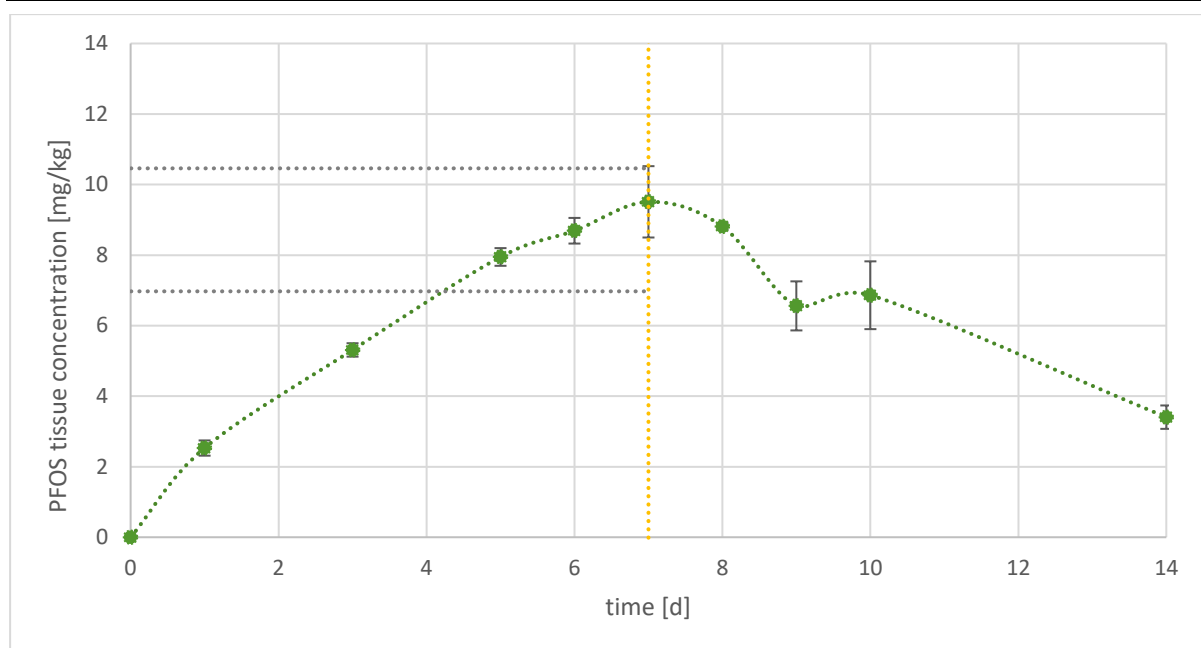
During this study a steady state concentration in the test medium was reached at the end of the uptake phase. The steady state concentration of 8.72 mg/kg between days 5 – 7. To calculate the steady state BCF (BCF_{ss}) the steady state tissue concentration is divided by the TWA. For this study a BCF_{ss} of 176 was calculated. The determination of the kinetic BCF (BCF_k) is based on the two rate constants k_1 and k_2 for uptake and depuration, respectively. The depuration rate constant was determined by linear regression following first order kinetics of the tissue concentrations during depuration with $k_2 = 0.148$. The uptake rate constant was calculated with the software SigmaStat also following first order kinetics and was determined to be $k_1 = 44.6$.

Figure 8: PFOS test medium concentration during uptake phase (7 days, PFOS-IME)*.



*Yellow dotted line marks average PFOS concentration in test medium (TWA = 49.4 $\mu\text{g/L}$); black dotted lines mark the $\pm 20 \%$ concentration range considering the calculated TWA concentration. Source: Fh IME, own diagram.

Figure 9: PFOS concentration in male *H. azteca* tissue during uptake and depuration phase (PFOS-IME).*



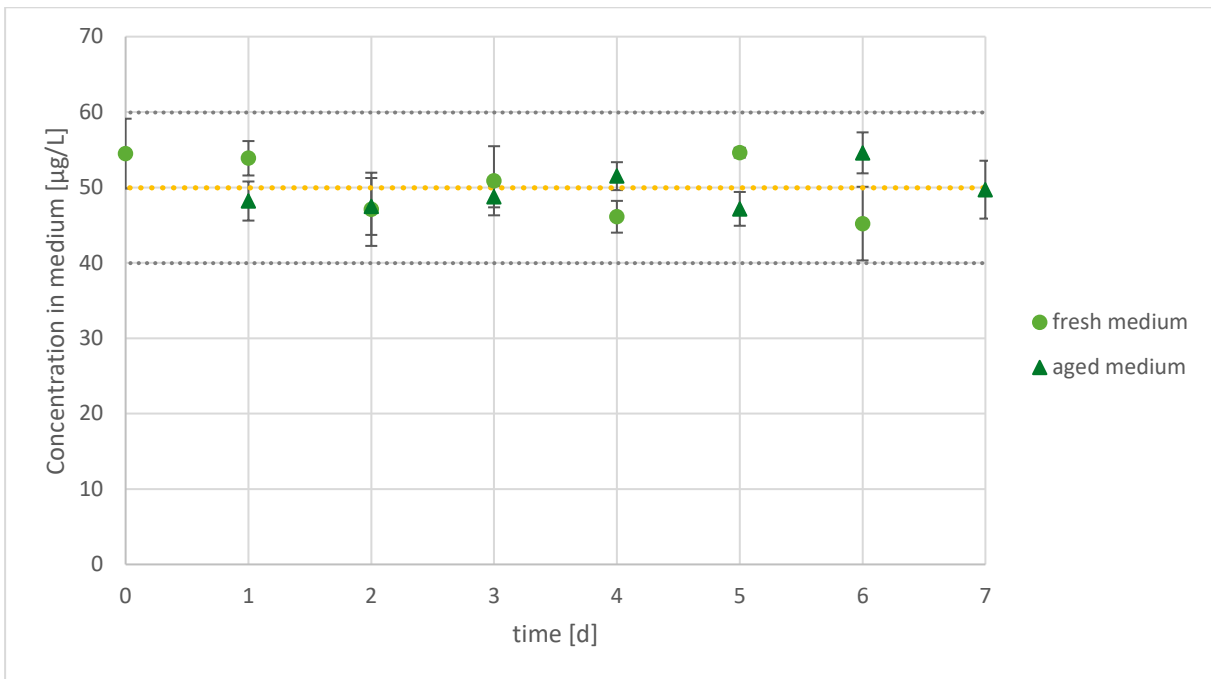
*Yellow vertical line marks the end of the uptake phase. Black dotted lines mark the $\pm 20\%$ range of the average tissue concentration measured between days 5-7. Source: Fh IME, own diagram.

A second bioconcentration test with the same set-up and the same duration of uptake and depuration phase was performed at UBA. The only difference was the medium for the application of the test substance. Instead of HDW culture medium, Borgmann medium (see Table 1) was used (Borgmann, 1996). All samples collected during this study were shipped to Fh IME for subsequent analysis. A TWA medium concentration of $49.98 \mu\text{g PFOS/L}$ was determined after measurement of fresh and aged samples (Figure 10). The maximum tissue concentration was measured towards the end of the uptake phase with 5.89 mg/kg (144 h / 6 d). A steady state tissue concentration of 5.56 mg/kg was calculated for days 5 – 7 of the uptake phase (Figure 11). Based on these data, a BCF_{ss} of 111 was calculated. After determination of $k_2 = 0.149$ by fitting a 1-compartment model to the measured concentrations in *Hyaella* during the depuration phase, an uptake rate constant ($k_1 = 27.6$) was calculated by nonlinear regression analysis. Based on the uptake rate and elimination rate a kinetic BCF_k of 185 was calculated (Table 4).

To investigate whether a real steady state was reached, a third bioconcentration test with an extended uptake and an extended depuration phase was performed (PFOS-ext.-IME). This test was performed with female amphipods.

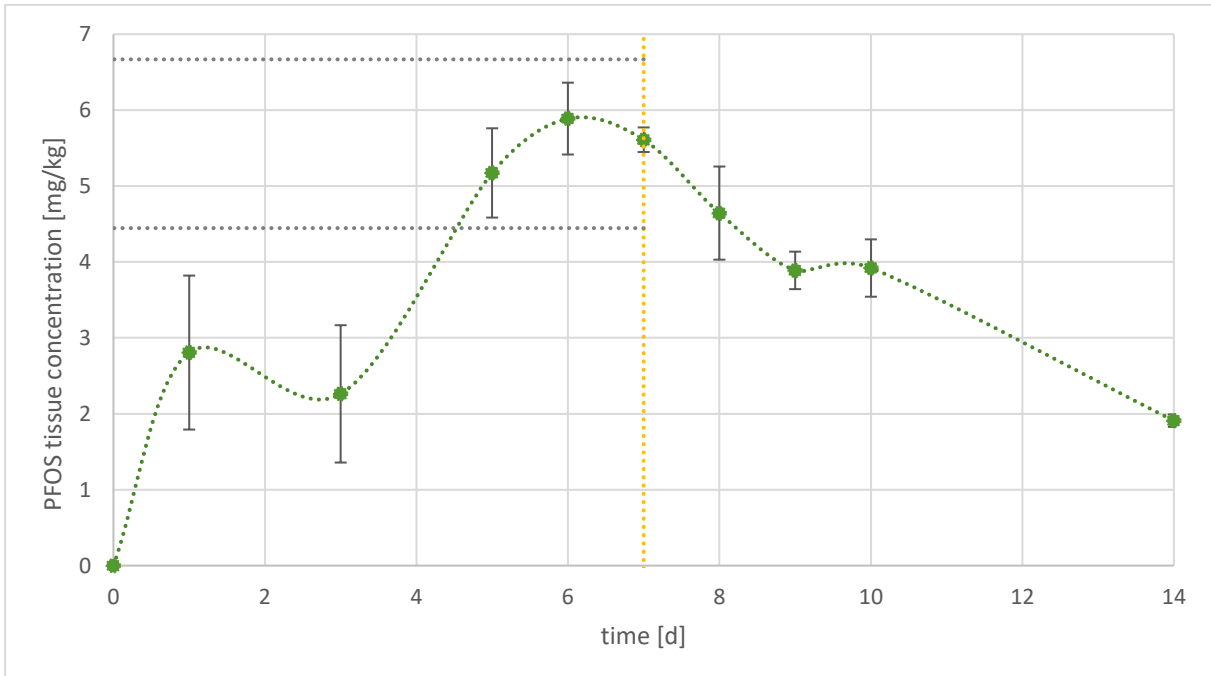
Over the 10 days of exposure (uptake phase) a TWA of $39.2 \mu\text{g PFOS/L}$ was determined (Figure 12). A steady state tissue concentration of 10.2 mg/kg between the days 6 – 10 of uptake was measured resulting a BCF_{ss} of 245. Based on the measured uptake ($k_1 = 55.8$) and elimination kinetics ($k_2 = 0.137$) a BCF_k of 406 could be calculated (Figure 13).

Figure 10: Course of PFOS medium concentration during uptake phase (7 days, PFOS-UBA).*



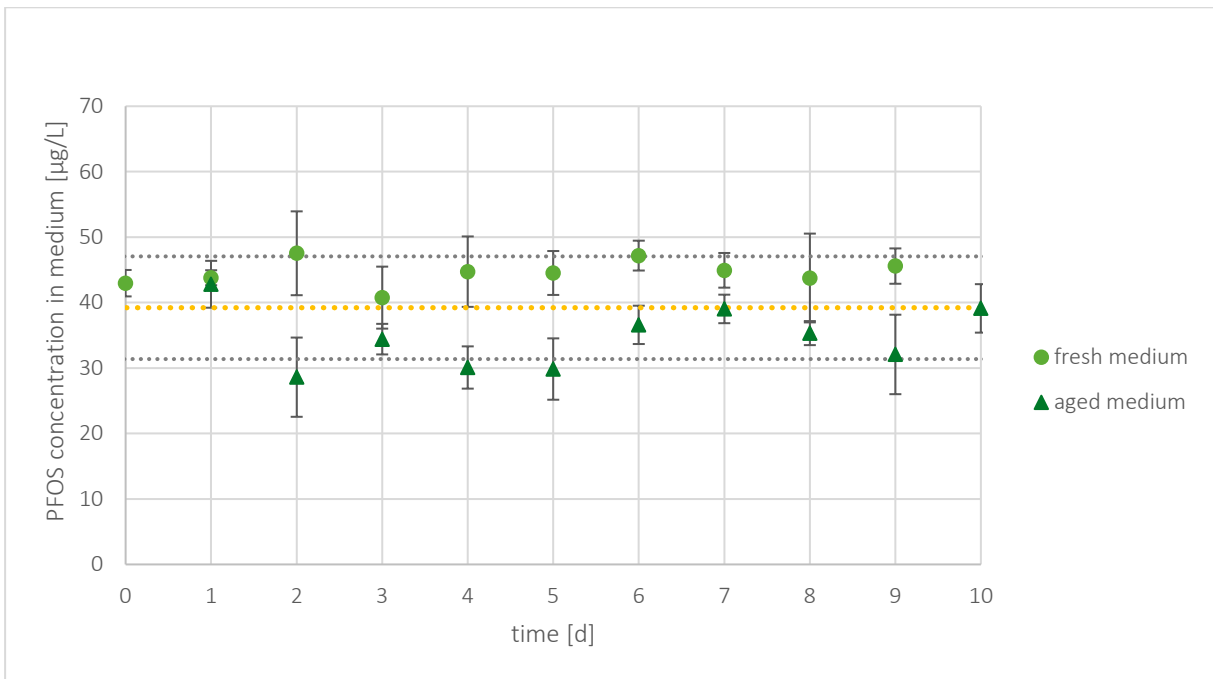
*Yellow dotted line marks average PFOS concentration in test medium (TWA = 49.98 µg/L); black dotted lines mark the ± 20 % concentration range considering the calculated TWA concentration. Source: Fh IME, own diagram.

Figure 11: PFOS concentration in male *H. azteca* tissue during uptake and depuration phase (PFOS-UBA).*



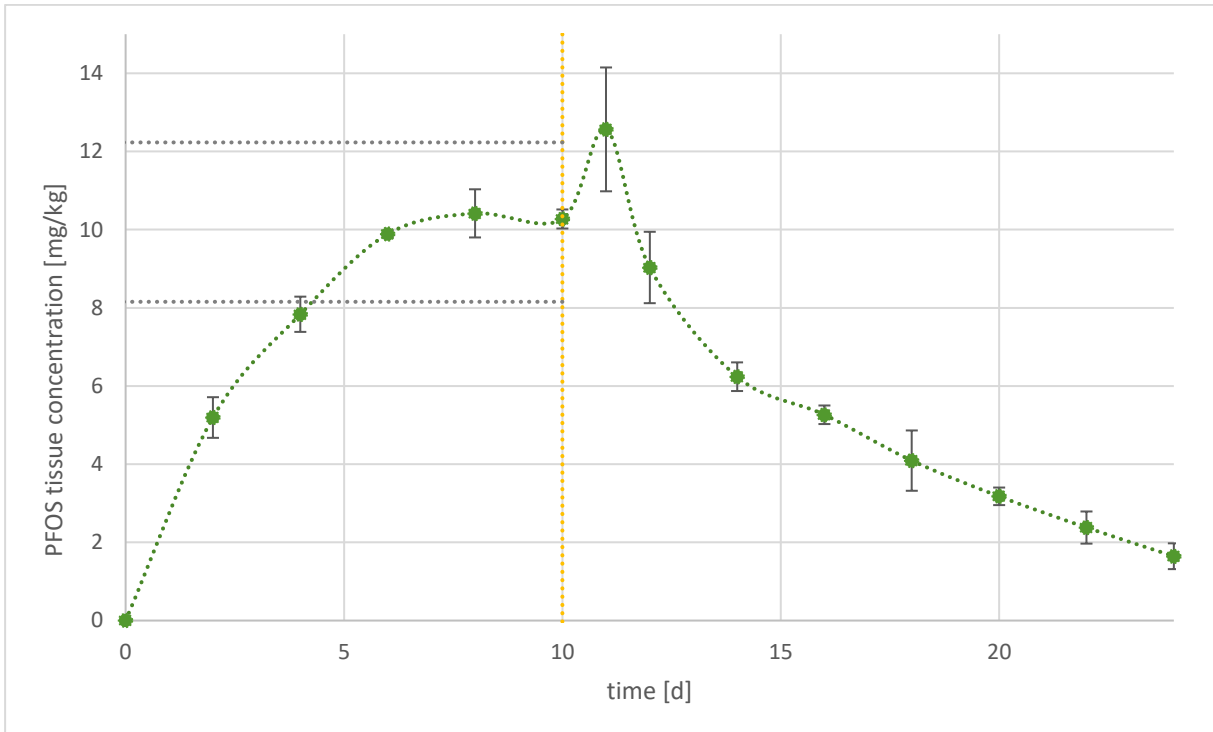
*Yellow vertical line marks the end of the uptake phase. Black dotted lines mark the ± 20 % range of the average tissue concentration measured between days 5-7. Source: Fh IME, own diagram.

Figure 12: Course of PFOS medium concentration during uptake phase (PFOS-ext.-IME).*



*Yellow dotted line marks average PFOS concentration in test medium (TWA = 39.22 µg/L); black dotted lines mark the ± 20 % concentration range considering the calculated TWA concentration. Source: Fh IME, own diagram.

Figure 13: PFOS concentrations in female *H. azteca* tissue during uptake and depuration phase (PFOS-ext.-IME).*

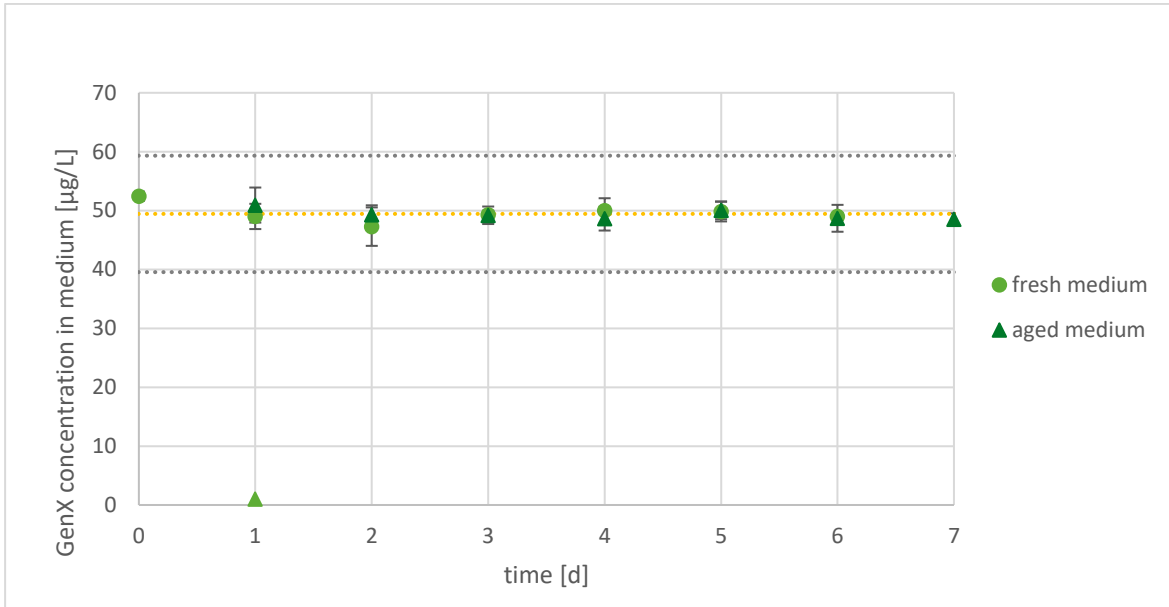


*Yellow vertical line marks the end of the uptake phase. Black dotted lines mark the ± 20 % range of the average tissue concentration measured between days 6-10. Source: Fh IME, own diagram.

3.1.2.3 Results of bioconcentration studies with GenX

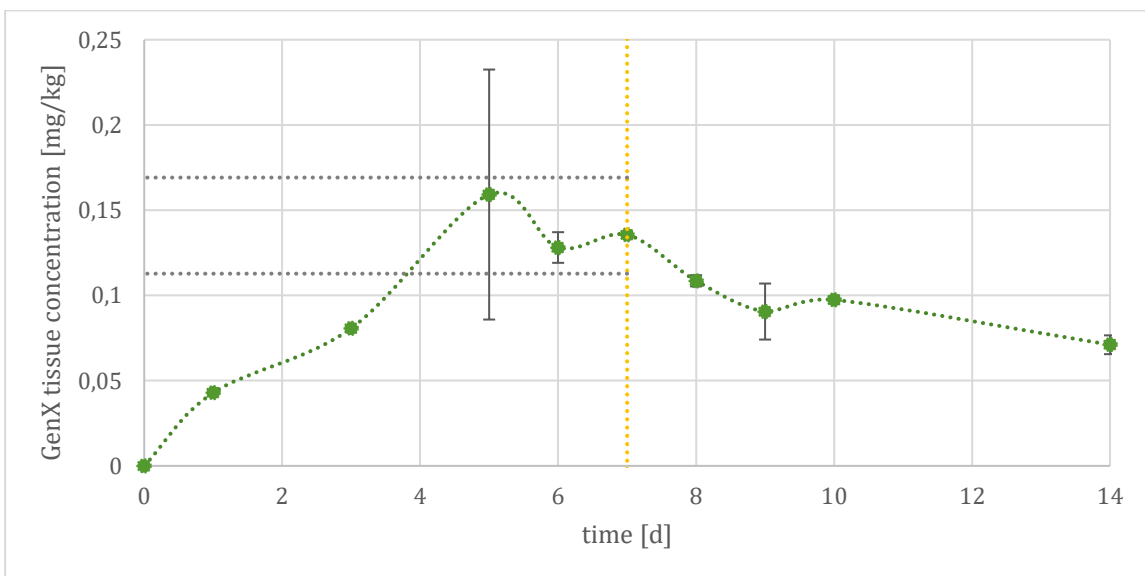
The maximum tissue concentration (Figure 15) achieved in this study was 0.136 mg/kg at the end of the uptake phase (168 h / 7 d) after exposure to a TWA GenX concentration of 49.4 µg/L (Figure 14). With the calculated mean steady state tissue concentration between days 5, 6 and 7 of 0.141 mg/kg during the uptake phase a BCF_{ss} of 2.85 could be determined (Table 4). With the calculation of k_1 (=0.598) and k_2 (=0.0815) the BCF_k of 7.34 was computed.

Figure 14: Course of GenX medium concentration during uptake phase.*



*Yellow dotted line marks average GenX concentration in test medium (TWA = 49.4 µg/L); black dotted lines mark the ± 20 % concentration range considering the calculated TWA concentration. Source: Fh IME, own diagram.

Figure 15: GenX concentrations in male *H. azteca* tissue during uptake and depuration phase.*



*Yellow vertical line marks the end of the uptake phase. Black dotted lines mark the ± 20 % range of the average tissue concentration measured between days 5-7. Source: Fh IME, own diagram.

Table 4: Results of the bioconcentration tests with PFOS and GenX.

study code	$c_{w, TWA}$ [$\mu\text{g/L}$]	$c_{H,ss}$ [mg/kg]	k_1 [L/(kg*day)]	k_2 [day ⁻¹]	BCF _{ss} [L/kg]	BCF _k [L/kg]
PFOS-IME	49.4	8.72	44.6	0.148	176	302
PFOS-UBA	50.0	5.56	27.6	0.149	111	185
PFOS-ext.-IME	39.2	10.2	55.8	0.137	245	406
GenX	49.4	0.141	0.598	0.0815	2.85	7.34

3.1.3 Evaluation

PFOS and GenX seem to be bioavailable for *H. azteca* if exposed via the water. The semi-static set-up showed to be suitable for the continuous exposure of stable concentrations of the permanent ionic compounds. Although the calculated BCF_{ss} and BCF_k values differ approximately by a factor of 1.5 to 2, steady state conditions were obviously reached in all studies after 7 days of exposure. Steady state conditions were confirmed in the third study with PFOS with an extended exposure phase lasting 10 days. In general, the extended test with PFOS led to higher tissue concentrations and also slightly higher BCF values, but steady state was reached after days 6 – 8 following the definition given by the OECD 305 (Organisation for Economic Co-operation and Development (OECD), 2012). It can be only speculated whether the increased BCF values were induced by the lower exposure concentration of $c_{w, TWA} = 39.2 \mu\text{g/L}$ compared to the other studies pointing to a concentration dependence of the BCF values. In this context also the selection of female animals might be discussed which were only used in this study. However, former tests with accumulating neutral organic compounds showed that there does not seem to be a difference between male and female organisms (Schlechtriem et al., 2019) and as the test item (PFOS) consists of permanent organic ions, it is expected that the difference in fat content between male and female should not have an effect on the results obtained. The lowest tissue content was found during the second test with PFOS conducted with Borgmann medium. The use of this medium with a higher ionic strength might result in altered bioavailability of PFOS. Here the uptake rate constant was lower than in the two other studies strengthening the argument of altered bioavailability of the ionic compound. Importantly, the depuration rate constants of all three studies with PFOS were comparable with $k_{2, \text{mean}} = 0.145 \pm 0.007$ (RSD of 4.60 %).

Generally, the three studies uniformly confirmed the low bioaccumulation potential of PFOS with BCF values varying from 111 – 245 for BCF_{ss} and 185 – 406 for BCF_k. Further studies are required to elucidate the bioaccumulation mechanisms of ionic organic compounds such as PFOS and to explain the potential concentration dependence observed in this study.

In the bioconcentration study with the PFOA substitute GenX a very low tissue concentration of 0.141 mg/kg was observed leading to BCF_{ss} and BCF_k values of 2.85 and 7.34, respectively, and confirming the low bioaccumulation potential of the test item. BCF studies were performed with carp using two different test concentrations: 0.02 and 0.2 mg/L (Hoke et al., 2016; Kobayashi, 2009). BCF_{ss} estimates of 30 and < 3, were obtained respectively, pointing to a concentration dependence of GenX bioconcentration as described above for PFOS.

Schlechtriem et al. (2019) described that BCF values resulting from fish studies show a strong correlation with *Hyalella* BCF values. In this project it was aimed to test an extended range of

organic compounds with the HYBIT approach including ionic organic compounds. The results obtained were compared with fish BCF data of the same compounds described in the literature. For PFOS, relatively high and compartment specific BCFs of 1,100, 4,300 and 5,400 were reported for carcass, blood and liver of market size rainbow trout, respectively (Martin et al., 2003). The reported BCF values for PFOS in fish are at least one order of magnitude higher than those gained with the HYBIT. Differences in fish and *Hyalella* BCF values are often explained by the different lipid content of the test species. However, due to the low storage lipid accumulation of PFOS, normalization of BCF values to an average total lipid content, as commonly applied for hydrophobic substances, is of limited value. Data on tissue distribution of PFOS (PFAS) are scarce, display substantial inconsistencies between different studies and species (Shi et al., 2018) and are completely missing for aquatic invertebrate species such as freshwater amphipods. However, as long as the bioaccumulation mechanisms and exposure routes of PFAS are unknown, the transfer of *Hyalella* bioconcentration test results to other species should be avoided. The simple prediction of B or non-B classification of ionizable organic compounds in the standard fish test based on *Hyalella* BCF values as suggested for hydrophobic substances (Schlechtriem et al., 2019) is currently not possible.

3.2 Bioconcentration tests with highly hydrophobic compounds UV-234 and UV-329

Ultraviolet (UV) filters are commonly used in cosmetic formulation such as sunscreens and skin care products in order to reduce the risk of skin cancer. However, research has demonstrated potential bioaccumulation of these compounds in aquatic organisms and birds (Nakata et al., 2009; Nakata et al., 2012). The identification and scientific assessment of compounds that bioaccumulate in organisms and biomagnify in food webs play a key role within the regulatory chemical safety assessment. The bioaccumulation potential of compounds is commonly expressed as bioconcentration factor (BCF), determined in flow-through studies with fish according to OECD TG 305. However, fish bioconcentration studies with highly hydrophobic compounds are extremely challenging with regard to the establishment of constant exposure concentrations of highly hydrophobic compounds (Schlechtriem et al., 2017). UVs are difficult to apply due to their very low solubility in water. In this study we tested the suitability of the new test system for testing the bioaccumulation potential of UV compounds.

3.2.1 Methods

3.2.1.1 Solvent-facilitated test set-up

The bioconcentration tests with UV-234 and UV-329 were performed using the solvent-facilitated flow-through set-up as described in Chapter 2.3.2.1. The test media were produced with a nominal concentration of 1 µg/L and applied at a flow rate of 6 L/h. Medium samples were taken every 24 h (Figures 16 - 18) and stored at -20 °C until analysis. *Hyaella azteca* samples were taken frequently (Figures 19 - 21), blotted dry, weighted, and stored at -20 °C until analysis. The uptake and depuration phases lasted 7 days in both studies. During the tests the animals were fed DECOTABS as uncontaminated diet.

3.2.1.2 Solvent-free application: Production of column-generated medium concentrations

In addition to the solvent-facilitated application of UV-234 and UV-329 a solvent free column-generated application of UV-329 was performed (Chapter 2.3.2.2). The solvent-free application was performed with an uptake and depuration phase lasting 5 days and 6 days, respectively.

In two 250 mL flasks 1.25 g UV-329 were solved in tert-butyl-methyl-ether (tBME) and filled up with tBME to the 250 mL mark. In two 2 L round flasks 250 g Florisil® (60 – 100 mesh) were weighted and the tBME solutions were combined with the Florisil®. The 250 mL flasks were rinsed with additional 250 mL tBME and the solution was added to the Florisil® leading to a ratio of 2:1 of tBME:Florisil® (v:w). The suspension was mixed thoroughly and the solvent was gradually removed with a rotary evaporator (40 °C water bath and 150 mbar) to obtain a powder. The spiked powder was transferred into a metal tray and incubated at 60 °C in a drying cabinet overnight.

On the next day, an empty glass column was rinsed with the aid of a peristaltic pump at a water flow of 5 mL/min. The dried Florisil® powder was bloated with HDW and transferred into the wetted column. With the aid of a metal pin all remaining air bubbles within the solid phase were removed and the solid phase became compacted during this process.

In total, the column was loaded with 5 mg test substance/g Florisil® powder and constantly rinsed with HDW at a flow rate of 5 mL/min constantly dripping into the mixing chamber. Within the mixing chamber the column eluate got further diluted and the resulting test medium was directed into the test vessel with a total flow rate of 6 L/h. Media samples were frequently taken for analysis.

3.2.1.3 Analyses of water and *Hyalella azteca* samples

Chemical analysis of the UV substances in the test media and *Hyalella* samples collected during the studies was performed by liquid chromatography with coupled mass spectrometry (LC-MS). MS analyses of all samples were carried out in the MRM mode on two different instruments (see Annex A1.1 for further information). Quantification of analytes was performed externally using matrix-matched (UV-329) or solvent (UV-234) calibrations, as no isotope-labelled analytical standards were available. Quality control samples were run alongside each measurement ($c = 1 \mu\text{g/L}$ (low) and $10 \mu\text{g/L}$ (high) for solvent-facilitated setup and $c = 0.5 \mu\text{g/L}$ (low) and $5 \mu\text{g/L}$ (high) for solvent-free set-up).

Medium samples were measured without further dilution. *H. azteca* samples were processed by means of solid-liquid extraction with acetonitrile. The low tissue concentrations required a concentration of the sample content in case of the experiments with solvent-facilitated application. The reduction of the sample volume was carried out by evaporating the solvent with the aid of a nitrogen stream. Efficiency rates of this protocol were tested beforehand. The experimental set-up of the extraction and concentration procedure is described in Chapter 3.1.1.1.

The extracts obtained were analyzed by LC-MS/MS. UV-234 extracts were diluted 1:1. The concentrated samples collected during the UV-329 tests with and without solvent-facilitated application were diluted 1:10 and 1:5, respectively.

3.2.2 Determination of lipid content

The lipid content in the amphipods was determined for animals sampled at test start, end of the uptake phase and end of the depuration phase. For lipid extraction the method of Smedes (1999) adapted by Schlechtriem et al. (2012) was used.

3.2.3 Results of bioconcentration tests with UV-234 and UV-329

3.2.3.1 Biological observations

In the test systems with solvent-facilitated set-up a strong biofilm formation was observed. In both tests, animals used the biofilm as substrate, and it cannot be excluded that the animals ingested the microbial biomass. Despite the strong formation of the biofilm, the tests were not stopped during the uptake phase. During the test with UV-329 a significant mortality of the test animals was observed after 3 days of depuration. In the test with UV-234 no increased mortality was observed.

The test with column-generated concentrations of UV-329 proceeded without any complications. Neither formation of biofilm nor a higher mortality rate could be observed.

3.2.3.2 Determination of extraction efficiency

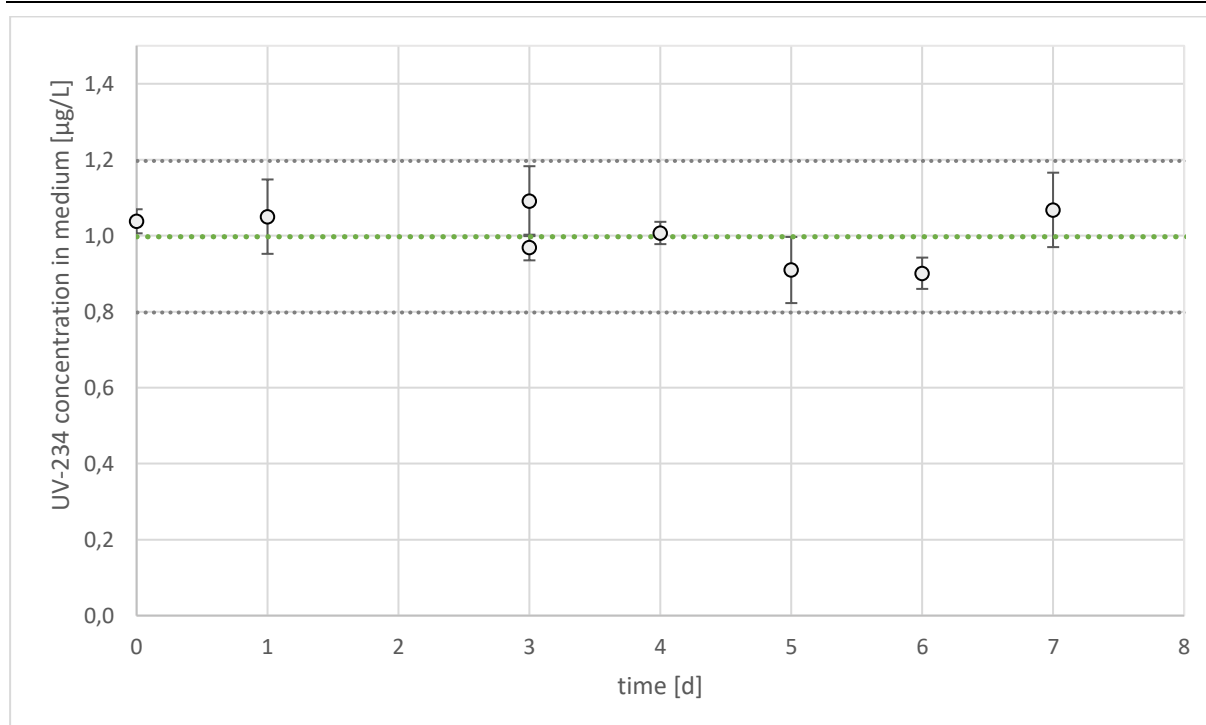
H. azteca samples spiked with specific amounts of the test substances were extracted with acetonitrile in five replicates each. Subsequent extracts were concentrated by evaporation of the solvents by the means of a nitrogen stream. For both analytes, the extraction and the concentration protocol showed to be of appropriate efficiency. Recovery rates of extraction were determined to be 97.8 % ($n = 4$) and 115 % ($n = 5$) and for concentration 98.1 % ($n = 5$) and 89.5 % ($n = 3$) for UV-234 and UV-329, respectively. During those analyses, quality controls ($c = 1 \mu\text{g/L}$ (low) and $10 \mu\text{g/L}$ (high)) showed a recovery of 80 – 120 %, except for the low concentration of UV-234 which only showed a recovery of 68.8 %. Still methods were assessed to be suitable for UV-234 and UV-329 analysis in *H. azteca* samples.

3.2.3.3 Results of medium and tissue analyses

Medium samples collected during the uptake phase of all three tests have been analyzed without further dilution. All samples collected during the test with solvent-facilitated application have been stored until analysis (at -20 °C).

The TWA concentration of UV-234 during the uptake phase was determined to be $0.997 \pm 0.073 \mu\text{g UV-234/L}$. Noteworthy, the quality controls (QCs) ranged from 71.9 – 95.5 % and the calibration ranged between $1 \mu\text{g/L}$ and $25 \mu\text{g/L}$. The measured concentrations of the medium samples were thus in the range of the lowest calibration standards leading to potential deviations of the measured concentrations. But especially the solvent-facilitated application allowed a good adjustment of the test concentrations, which supported the accuracy of the results obtained (Figure 16).

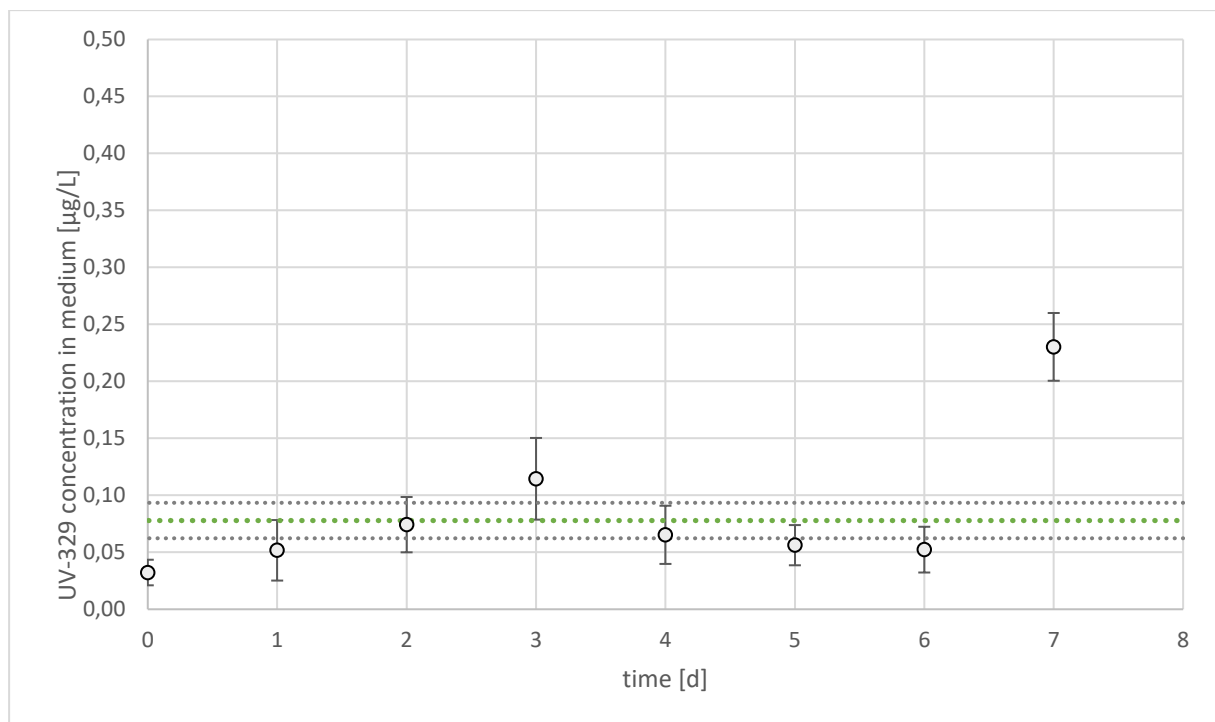
Figure 16: Bioconcentration study with UV-234: medium concentration during uptake phase (solvent-facilitated application).*



*Green dotted line marks average UV-234 concentration in test medium (TWA = $0.997 \mu\text{g/L}$); black dotted lines mark the $\pm 20\%$ concentration range considering the calculated TWA concentration. Source: Fh IME, own diagram.

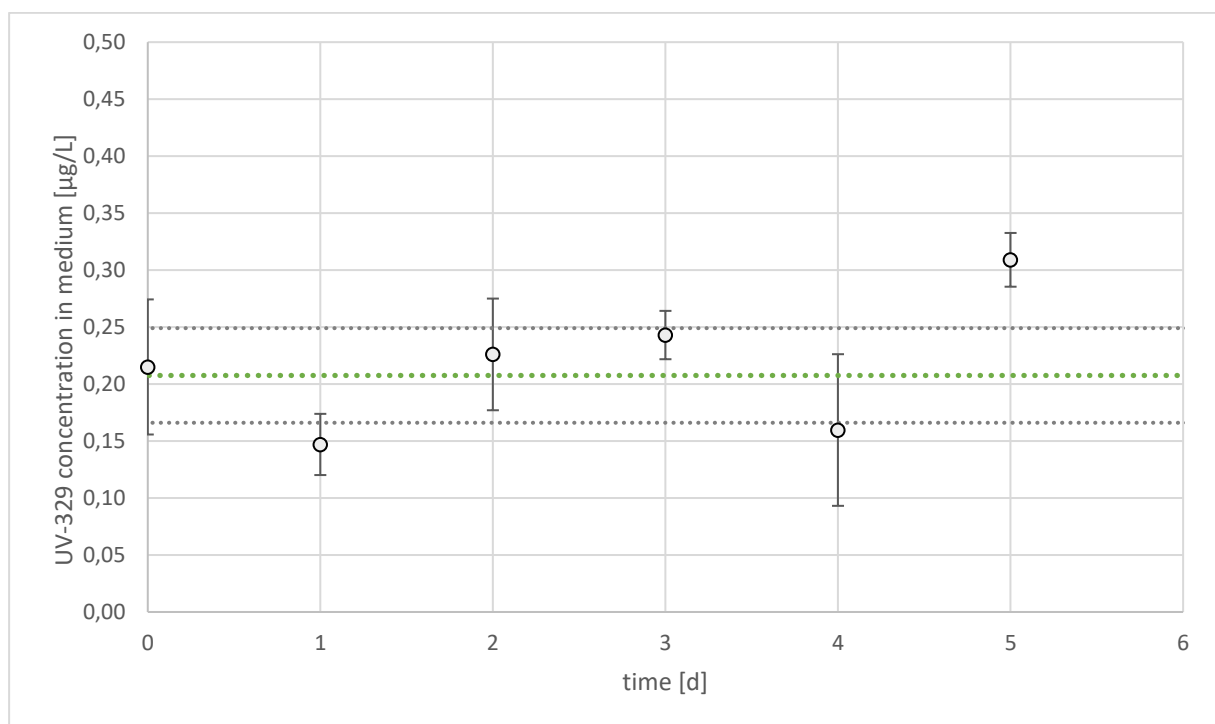
The TWA concentration of UV-329 during the solvent-facilitated experiment was determined to be $0.078 \pm 0.051 \mu\text{g UV-329/L}$. All samples were measured at the end of the uptake phase and analyzed medium samples revealed a test concentration of $0.078 \mu\text{g/L}$. Low and high QCs showed recoveries of 98-112 %. These results must be viewed carefully, as they are below the lowest calibration standard (calibration ranging from $0.1 \mu\text{g/L}$ - $25 \mu\text{g/L}$) (Figure 17). The TWA concentration of the solvent-free application of UV-329 was determined to be $0.208 \pm 0.055 \mu\text{g UV-329/L}$. All results fit into the calibration range of $0.05 \mu\text{g/L}$ - $10.0 \mu\text{g/L}$ and low ($c = 0.5 \mu\text{g/L}$) and high ($c = 5 \mu\text{g/L}$) QCs showed good recoveries with 91.6 – 124.4 % throughout all measurements. All samples have been analyzed daily without being stored beforehand (Figure 18).

Figure 17: Bioconcentration study with UV-329: medium concentration during uptake phase (solvent-facilitated application).*



*Green dotted line marks average UV-329 concentration in test medium (TWA = 0.078 µg/L); black dotted lines mark the ± 20 % concentration range considering the calculated TWA concentration. Source: Fh IME, own diagram.

Figure 18: Bioconcentration study with UV-329: medium concentration during uptake phase (solvent-free application).*



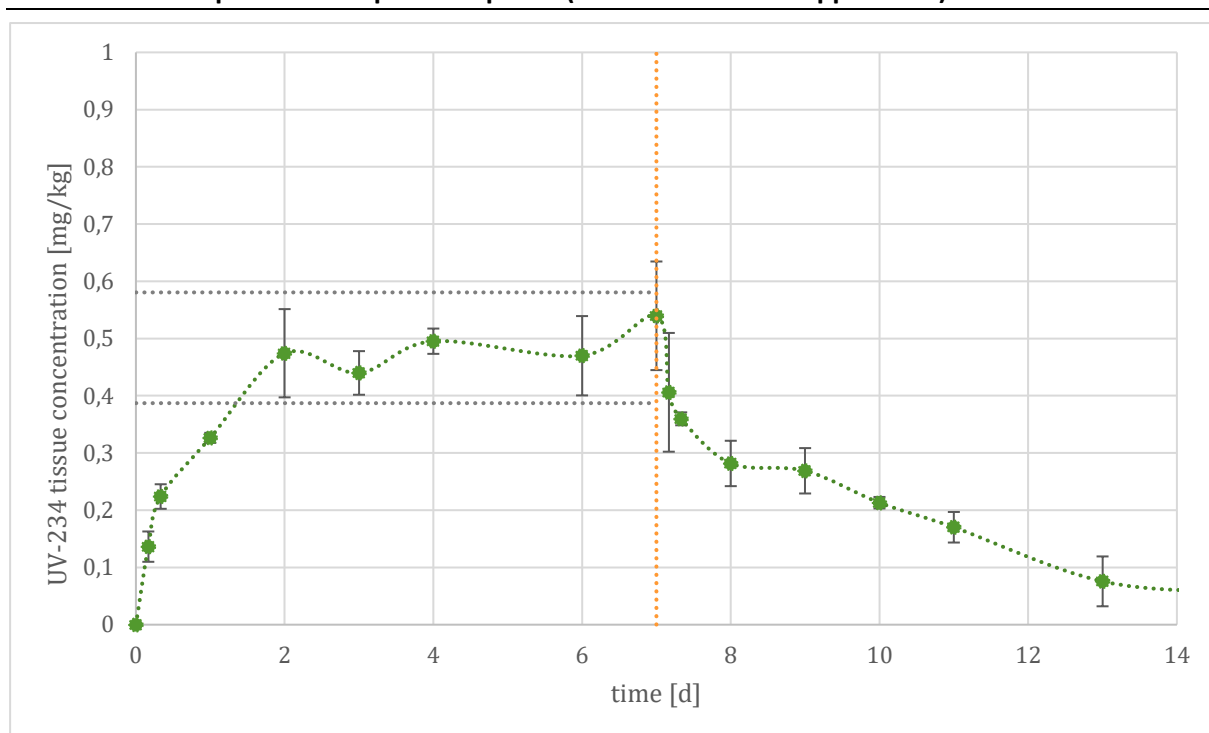
*Green dotted line marks average UV-329 concentration in test medium (TWA = 0.208 µg/L); black dotted lines mark the ± 20 % concentration range considering the calculated TWA concentration. Source: Fh IME, own diagram.

Hyalella tissue concentrations of the hydrophobic compounds UV-234 and UV-329 in the course of the studies were determined with maximum tissue concentrations of 0.540 mg /kg for UV-234 measured at the end of the uptake phase.

For UV-329 two completely different results have been measured depending on the application method: solvent-facilitated or solvent-free. For the solvent-facilitated application a maximum tissue concentration of 6.45 mg/kg for UV-329 was measured at the end of the uptake phase. Whereas a tissue concentration of 1.79 mg/kg was determined for the solvent-free application, which was lower compared to the previous study (factor 3.6).

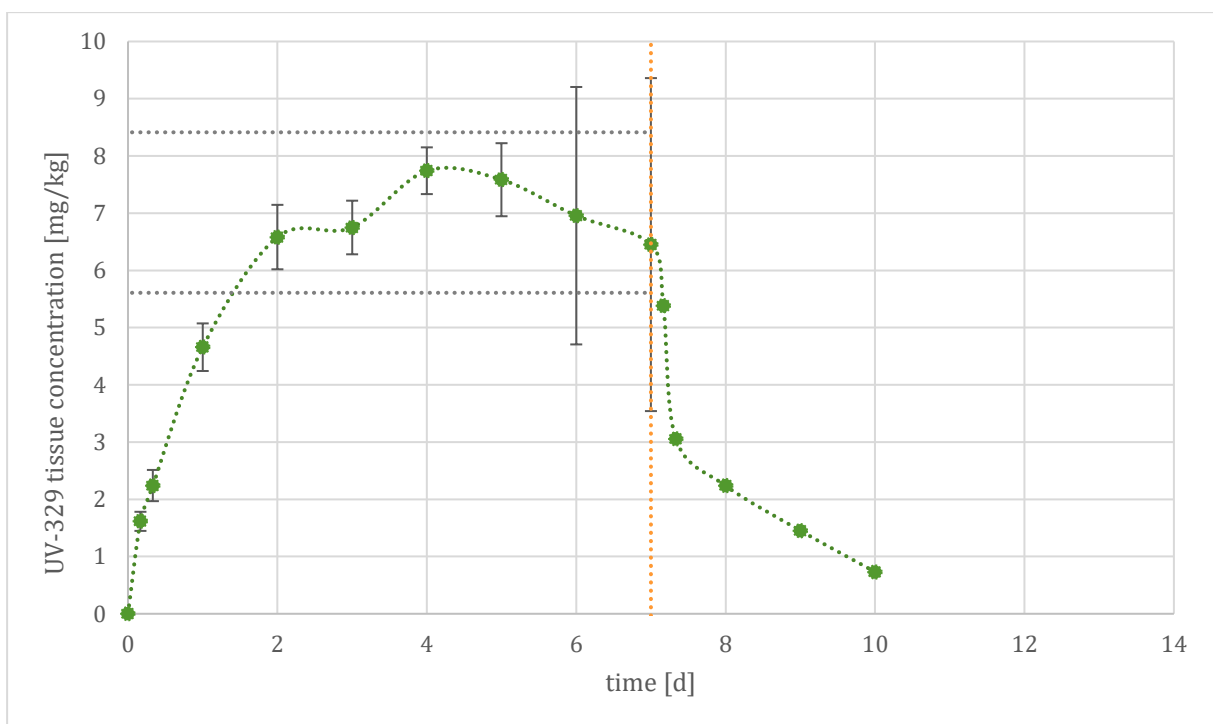
In all experiments steady state tissue concentrations were reached and enabled the calculation of BCF_{ss} values (Figures 19 - 21). BCF_{ss} values of 485 and 90,043 were determined for the solvent-facilitated tests with UV-234 and UV-329, respectively and 7,744 for the test with solvent-free application of UV-329. All values were lipid-normalized, resulting in BCF_{ssL} values of 1,005 (UV-234, with solvent), 186,542 (UV-329, with solvent) and 18,397 (UV-329 without solvent) (Table 5).

Figure 19: Bioconcentration study with UV-234: tissue concentrations in *H. azteca* during uptake and depuration phase (solvent-facilitated application).*



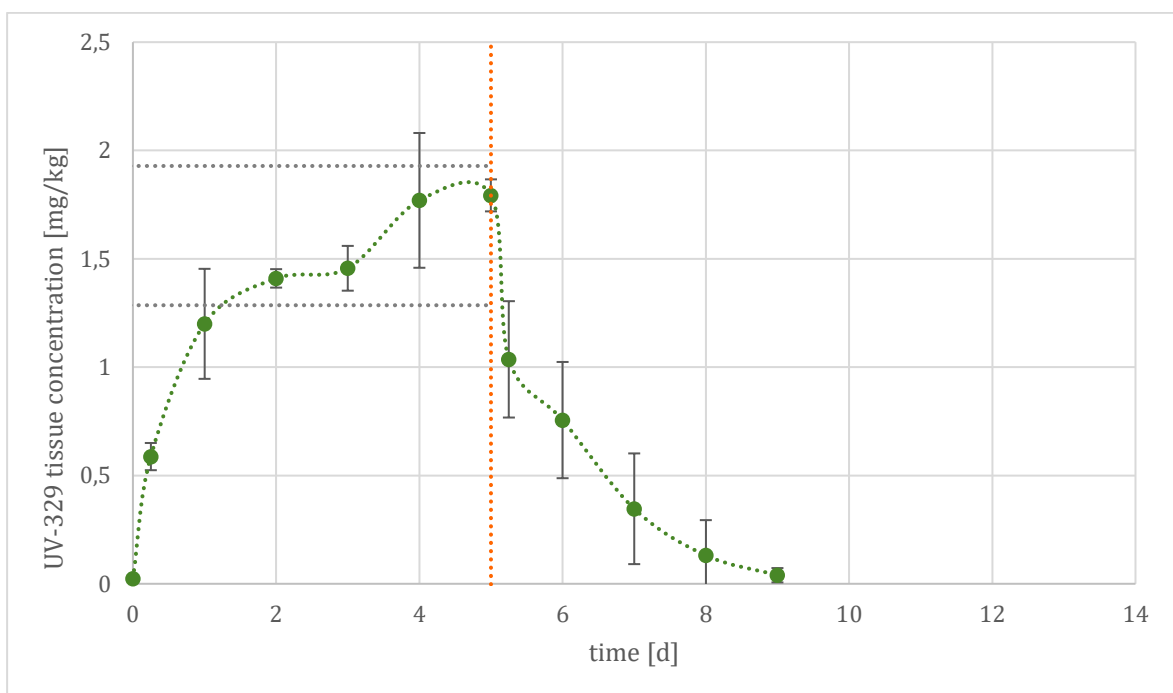
*Yellow vertical line marks the end of the uptake phase. Black dotted lines mark the $\pm 20\%$ range of the average tissue concentration measured between days 2-7. Source: Fh IME, own diagram.

Figure 20: Bioconcentration test with UV-329: tissue concentrations in *H. azteca* during uptake and depuration phase (solvent-facilitated application).*



*Yellow vertical line marks the end of the uptake phase. Black dotted lines mark the $\pm 20\%$ range of the average tissue concentration measured between days 2-7. Source: Fh IME, own diagram.

Figure 21: Bioconcentration of UV-329: tissue concentration in *H. azteca* during uptake and depuration phase (solvent-free application).*



*Yellow vertical line marks the end of the uptake phase. Black dotted lines mark the $\pm 20\%$ range of the average tissue concentration measured between days 2-5. Source: Fh IME, own diagram.

For calculation of BCF_k values the depuration rate constant k_2 was determined by linear regression which was then used to derive the uptake rate constant k_1 by non linear regression. BCF_k values (BCF_{kL}) of 725 L/kg (1,502 L/kg), 100,601 L/kg (208,415 L/kg) and 8,352 L/kg (19,842 L/kg) for UV-234, UV-329 tested with solvent and UV-329 tested without solvent were calculated, respectively (Table 5).

Table 5: Results of the bioconcentration tests with solvent-facilitated and solvent-free application of UV-234 and UV-329.

Substance	Solvent	Target conc. [$\mu\text{g/L}$]	TWA [$\mu\text{g/L}$]	k_1 [L/kg/day]	k_2 [1/d]	BCF_k [L/kg]	BCF_{kL} [L/kg]	BCF_{ss} [L/kg]	BCF_{ssL} [L/kg]
UV-234	x	1 $\mu\text{g/L}$	0.997	198	0.273	725	1,502	485	1,005
UV-329*	x	1 $\mu\text{g/L}$	0.0779	66,085	0.657	100,601	208,415	90,043	186,542
UV-329			0.208	8,288	0.992	8,352	19,842	7,744	18,397

*See detailed discussion of results in Chapter 3.2.4.

During tissue analysis quality controls (QCs) were run alongside each measurement. For UV-234 a solvent calibration was used to quantify the samples. To observe the suitability of the solvent calibration, quality controls containing the same volume of matrix as the samples were used and showed recoveries of 88.0 – 96.2 % for the high concentration ($c = 10 \mu\text{g/L}$) and only 10.2 – 19.3 % for the low concentration ($c = 1 \mu\text{g/L}$). The majority of samples yielded concentrations around the higher QC. Within this measurements QCs with concentrated blank matrix, processed like the samples, were examined. But here only the higher QC showed very low recoveries of 13.4 %. In verifying measurements a solvent calibration was measured together with QCs containing no matrix, immediate matrix and concentrated matrix. In this case, all recoveries were within the range of 88.4 – 140 %.

For the solvent-facilitated application of UV-329, QCs with the immediate matrix and concentrated matrix were measured alongside the samples. Here a recovery of 82 – 100 % (low and high concentration) for the immediate matrix and 29.2 – 37.5 % for the low QC and 72.0 – 80.0 % for the high QC of the concentrated matrix containing QCs were determined. The recoverys of QCs during the solvent-free experiment with UV-329 were in the range of 83.6 – 118 %.

3.2.4 Evaluation

Testing of the highly hydrophobic compounds UV-234 and UV-329 turned out to be highly challenging with regard to the application of the test items as well as the analysis of the water and tissue samples. Prior to extraction of the animal samples collected during the studies to investigate the tissue concentrations recovery experiments for the extraction procedure and the sample concentration steps were performed with acceptable results. During those measurements blank matrix was spiked, extracted, concentrated and analyzed. During this measurement QCs were measured to assess the calibration (with matrix: 68.8 – 115 % (UV-234) and 100 – 107 % (UV-329), without matrix 77.1 – 103.4 (UV-234)). As samples from the validation experiment for the extraction and concentration procedures with UV-234 and UV-329

had a known amount of test substance which constant recoveries between 86.0 – 120 %, this validation could serve as a verification of the recovery of test item extracted from the immediate matrix samples and thus to evaluate tissue concentrations during the solvent-facilitated experiments. Surprisingly the medium concentrations between both solvent-facilitated tests differed by more than one order of magnitude although the set-up was comparable. With 0.997 µg/L, the TWA concentration of UV-234 was in the range of the target concentration (1 µg/L), however, the TWA concentration of UV-329 was only 0.0779 µg/L. Comparing both studies, it was striking that test animals accumulated UV-329 to a far higher degree resulting a BCF values > 100,000.

The low TWA concentrations measured during the test with UV-329 might be explained by a measuring artefact related to the aqueous medium concentration. For instance, it can be only speculated how the strong growth of biofilm in the test system affected the exposure conditions of this treatment. Therefore, the study was repeated using a solvent-free application of UV-329. During this experiment no formation of biofilm was observed and the mortality rate was in a normal range. Apart from the biological observations the analysis of the collected samples was straight forward with QCs showing recoveries in the acceptable range. The medium samples were measured immediately without storage and higher, more stable medium concentrations were measured.

BCF values calculated for the solvent-free test are about one order of magnitude lower than those resulting from the solvent-facilitated test. If the tissue concentrations of animals collected from the test with solvent-facilitated exposure are related to the nominal concentration of 1 µg/L the following endpoints are calculated: $k_1 = 5,145 \text{ L/kg/d}$, $k_2 = 0.657 \text{ 1/d}$, $\text{BCF}_k = 7,833 \text{ L/kg}$, $\text{BCF}_{\text{KL}} = 16,227 \text{ L/kg}$, $\text{BCF}_{\text{SS}} = 7,010 \text{ L/kg}$, $\text{BCF}_{\text{SSL}} = 14,524 \text{ L/kg}$. The recalculated BCF values are very similar to the results obtained from the solvent-free test (Table 6). All these findings strengthen the hypothesis that during the first test with UV-329 an artefact related to the measurement of the aqueous medium concentrations occurred which was supposed to be induced by the high formation of biofilm and/or the storage of the medium samples.

It becomes clear that UV-329 has a very high potential to bioaccumulate in *H. azteca* with BCF_{KL} values at least three times higher than 5,000 L/kg. On the contrary, UV-234 which is even more hydrophobic showed a BCF_{KL} of 1,502 L/kg only. Although no biofilm formation comparable to the study with UV-329 and no significant deviation from the target concentration was observed in the test with UV-234, also in this case it should be investigated how this compound would behave in a solvent-free bioconcentration test with *H. azteca*.

Table 6: Hypothetical comparison of BCF studies with UV-329 with different medium concentrations.

Substance	Solvent	TWA [µg/L]	k_1 [L/kg/day]	k_2 [1/d]	BCF_k [L/kg]	BCF_{KL} [L/kg]	BCF_{SS} [L/kg]	BCF_{SSL} [L/kg]
UV-329*	x	0.0779	66,085	0.657	100,601	208,415	90,043	186,542
UV-329	x	Nominal concentration	5,145	0.657	7,833	16,227	7,010	14,524
UV-329		0.208	8,288	0.992	8,352	19,842	7,744	18,397

*Most possibly erroneous BCF calculations caused by a potential measuring artefact related to the aqueous medium concentrations present in the test system.

As shown by Schlechtriem et al. (2019), bioconcentration studies with the freshwater amphipod *H. azteca* result in BCF estimates which show a strong correlation with fish BCF values. It was concluded that *Hyalella* BCF values can be assessed in accordance with the regulatory B criterion (BCF > 2000, i.e., REACH) and thereby enable the prediction of B or non-B classification in the standard fish test. BCF values calculated for *H. azteca* tend to be higher compared to fish leading to a type I error falsely inferring the existence of a high bioaccumulation potential for a chemical in fish (BCF > 2000) that is not there (Schlechtriem et al. 2019).

The results obtained in the *Hyalella* test with UV-234 confirm the results obtained in a fish test described in the substance related REACH registration dossier (Table 7). However, there is a large difference between the BCF values calculated for UV-329, with *Hyalella* showing a far higher bioaccumulation potential compared to fish.

Table 7: Comparison of *Hyalella* and fish BCF values of UV-234 and UV-329.

Substance	Solvent	Conc. (TWA) [µg/L]	BCF _{KL} [L/kg]	BCF _{SSL} [L/kg]	Solvent	Conc. [µg/L]	BCF _{KL} [L/kg]	BCF _{SSL} [L/kg]
	BCF studies with <i>H. azteca</i>				BCF studies with <i>Oncorhynchus mykiss</i> *, **			
UV-234	X	0.997	1,502	1005	X	nominal: 0.3 µg/L measured: 0.33 ±0.02 µg/L	1,286	1,063
UV-329		0.208	19,842	18,397	X	nominal: 0.2 µg/L measured: 0.19 ±0.01 µg/L	458	461

* UV-234: <https://echa.europa.eu/de/registration-dossier/-/registered-dossier/11135/5/4/2/?documentUUID=617b9e9b-a098-4a72-ad57-5cc5d53deed8>

** UV-329: <https://echa.europa.eu/de/registration-dossier/-/registered-dossier/13220/5/4/2/?documentUUID=e0ac66f4-ba8f-461a-aaeb-0cd0f9f85aa2>

In both fish studies, concentrations of test substance in filtered water samples were measured as total radioactive residues (TRR) and remained within ± 20% of the mean measured concentration. The radioactivity in the test solutions was reported as µg substance equivalent/kg (L) water. For the determination of the radioactivity in the fish collected during the uptake and elimination period the measured radioactivity of each combusted tissue sample was corrected for the background, burning factor and control fish. The radioactivity in the tissue was reported as weight equivalent in µg substance equivalent/kg fish. The BCF was based on the analyses of total radioactive residues in water and fish tissue and thus also includes residues of possible metabolites of the test substance in the water and fish. Differences in the metabolic transformation of UV-compounds may explain divergent results as obtained for UV-329.

3.3 Conclusions

The aim of the first work package was to run the test system with four substances which showed difficulties in the application and/or a conspicuous bioaccumulation behaviour when applied in the fish test. In this way, it was intended to identify the limitations of the *Hyalella* test procedure and to derive potential adjustments if necessary. Two ionizable substances and two substances with a high log K_{ow} , i.e. substances that were expected to be readily adsorbed to the walls of the experimental units, were used.

The BCF studies showed that the *Hyalella* test system is also suitable for the testing of phenolic benzotriazoles and may thus help to identify UV compounds that bioaccumulate in aquatic organisms. The results reveal the high bioaccumulation potential of the two highly lipophilic test compounds UV-234 and UV-329. However, solvents should not be used for the preparation of test media to avoid microbial growth in the test system. The use of column generated concentrations allowing the production of test media without using solvent is recommended instead.

The studies with PFOS and GenX demonstrated that the *Hyalella* test is also suitable for testing ionizable organic compounds, however, the test conditions may have a significant effect on the result of bioconcentration studies as shown for the use of different test media or the performance of the bioconcentration experiments with male or female test animals. As long as the bioaccumulation mechanisms of ionizable organic compounds such as PFOS are mostly unknown, the simple prediction of B or non-B classification in the standard fish test based on *Hyalella* BCF values as suggested for hydrophobic substances is not possible. However, the *Hyalella* test can still help to further elucidate the bioaccumulation potential of emerging compounds in aquatic organisms and provide BCF values for regulatory purposes.

4 Workpackage 2: Nanomaterials

4.1 Selection and characterization of test substance

Within this project three different nanoparticles were tested in the *Hyalella* bioaccumulation test to prove the suitability and to determine the limitations of this test for testing nanomaterials.

The NMs were selected based on their major characteristics that are expected to lead to different behaviour within the tests system. The following characteristics were taken into account for the selection of the NMs:

- i) Ion releasing
- j) Non ion releasing and well dispersible
- k) Non ion releasing and mediocre dispersible

Based on these criteria the following NMs were chosen:

- l) NM 300K, silver NM
- m) BBI Solutions gold NM
- n) NM 105, titanium dioxide NM

In addition, silver nitrate was tested in the bioconcentration tests as dissolved form of Ag to compare the results with the results from the NM 300K (ion releasing) based exposure.

Note, the content of Chapter 4 was published as Kuehr et al. 2020a.

4.1.1 Characterization using transmitting electron microscopy (TEM)

The stock material and processed nanomaterials were characterized using transmitting electron microscopy (TEM) in combination with energy dispersive x-ray (EDX) analyses to assess the elemental composition of the NMs and thus to confirm their identity. The feed stock dispersions of NM 300K were diluted 1:10⁶ in UHQ prior to TEM analysis. NM 105 (20 mg) was suspended in 100 mL of 0.2 % Novachem and sonicated for 10 min before being further diluted (1:20). The diluted suspension (1 mL) was directly centrifuged (1 h, ~14,000 x g) on TEM grids. The AuNM suspension was centrifuged directly without any dilution. Samples of the experimental diet enriched with NMs (Chapter 4.5) were dried by lyophilization at -52 °C and 0.47 mbar (Alpha 1-2 LDplus, Christ) for 24 h and ground to a fine powder using a mortar. The freeze dried material (30 mg) was added to 1 mL of 0.2 % FL-70 (Thermo Fisher Scientific) and sonicated for 1 minute in a Vial Tweeter (Hielscher Ultrasonics GmbH). The resulting dispersion was diluted 1:1 in UHQ and directly centrifuged onto TEM grids. As the NMs carried a negative surface charge, the TEM grids were functionalized with Poly-L-Lysine (PLL, 0.1 % (w/v) in H₂O, Sigma Aldrich) to enhance NM deposition on the TEM grids. The preparation of the TEM grids is described in more detail in (Uusimaeki et al., 2019). A dedicated scanning transmission electron microscope (STEM, HD2700Cs, Hitachi), operated at an acceleration voltage of 200 kV was used to investigate the TEM grid. For image formation the secondary electron (SE) or the high-angle annular dark field (HAADF) signal was used. Elemental analyses were conducted using an EDX system (EDAX) and the spectra were recorded and processed using Digital Micrograph (v.1.85, Gatan Inc.).

4.1.2 Examinations using dynamic light scattering

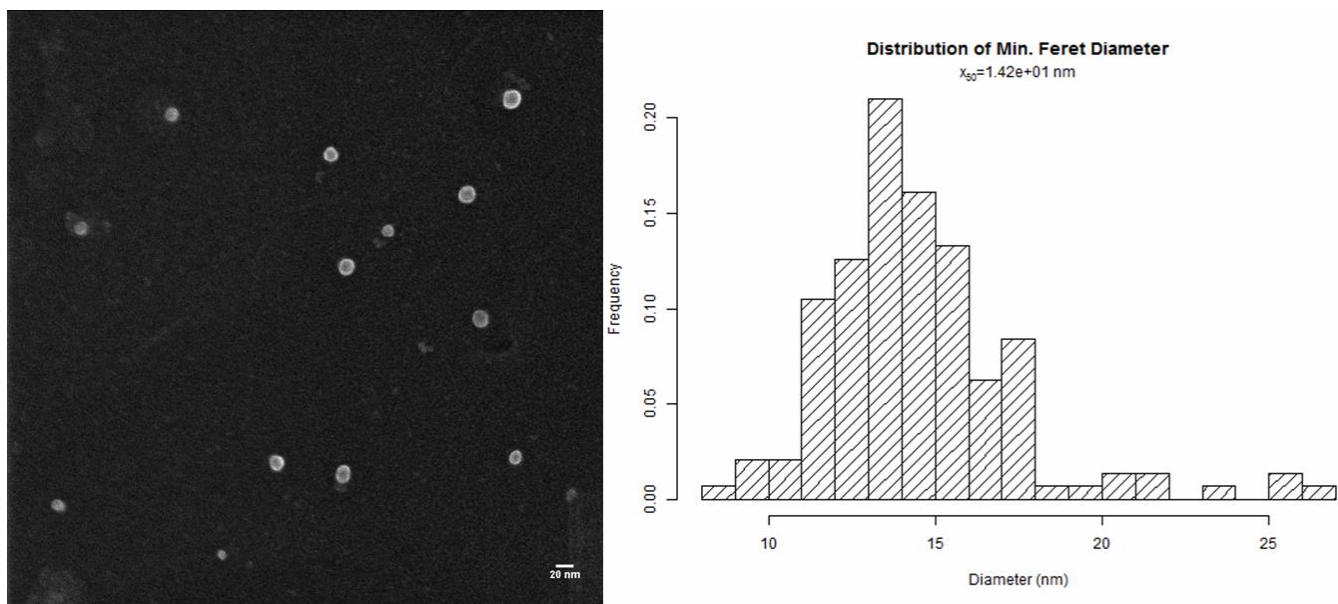
The stock materials were also characterized for their hydrodynamic diameter using dynamic light scattering (DLS) with a zetasizer (Zetasizer Nano Series, Malvern). Each stock material was measured in UHQ and additionally in the reconstituted water (culture medium) prepared according to Borgmann (1996) (Table 1) as dispersion medium to investigate potential effects of the medium. The dispersion medium was filtrated using syringe filters with a 0.2 µm pore-size (Minisart® NML, 0.2 µm) before dispersing the particles. The dispersions were freshly made, hand shaken for 1 min and sonicated for 10 min with a pulsation pause ratio of 0.2 / 0.8 using an ultrasonic homogenizer (Bandeline Sonoplus HD2200 ultrasonic homogenizer, 200 Watt, Bandelin Cup Horn BB6) before analysis. Concentrations were chosen to get count rates of 150 kcps or slightly higher values. The measurements were performed using disposable polystyrene cuvettes with an optical path of 1 cm. Each sample was measured after an equilibration time of 180 s in 3 runs of 10 single measurements for 10 s each at 25 °C. Z-Average and percentage of different peak intensities were calculated by the Zetasizer software.

4.1.3 Results of the characterizations

The diameters of the stock materials (NM 300K and AuNMs) derived from TEM measurements were in agreement with their nominal diameters (14.2 and 62.7 nm for the AgNMs and AuNMs, respectively) (Figures 22 - 23). For the NM 105 no diameters were determined because of particle agglomeration that occurred during the transferring of the NMs on the TEM grids due to the lack of a stabilizing agent (Figure 24). The DLS measurements resulted in values of 26.7 nm (NM 300K), 351.1 nm (NM 105) and 60.7 nm (AuNMs) for the hydrodynamic diameter when measured in UHQ water.

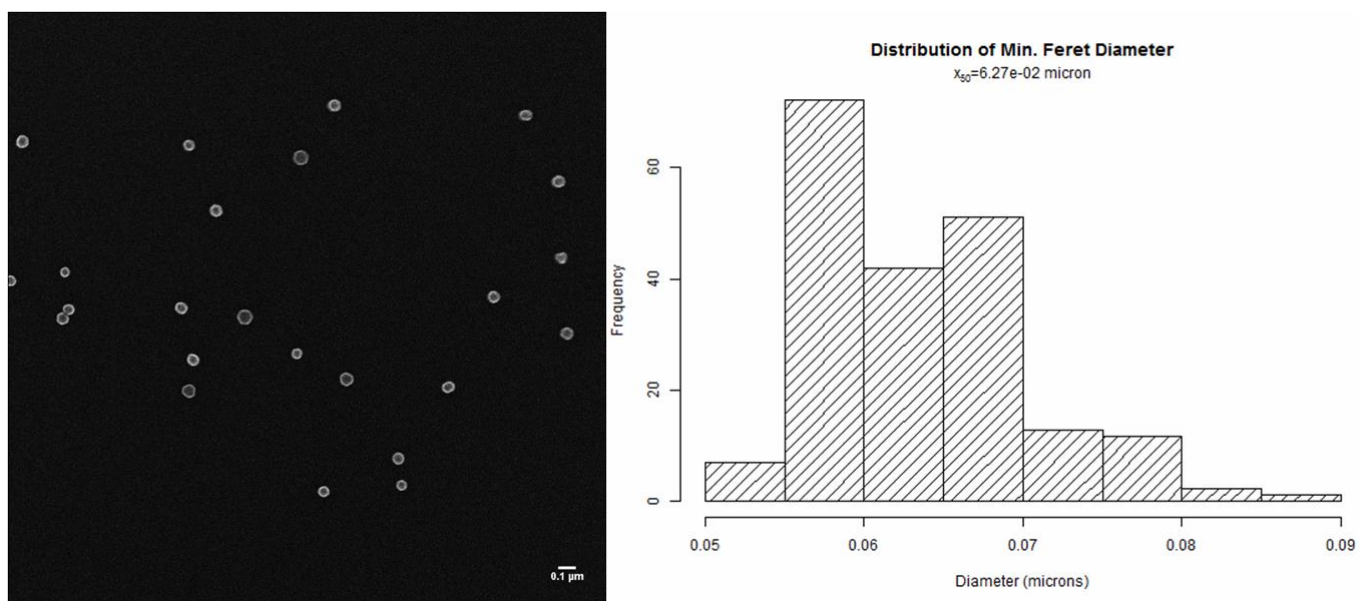
For all NMs higher hydrodynamic diameters were measured when suspended in dilution water that was used in the tests. For the AgNMs and AuNMs the measured values of 51.2 and 143.5 nm were two-times higher, whereas the value measured for the TiO₂NMs was more than 5 times higher in the dilution water (1861 nm). The hydrodynamic diameter of the NM 300K NMs additionally measured in the culture medium used in one of the bioconcentration tests was also around two times higher (50.3 nm) compared to the value measured in UHQ water.

Figure 22: TEM image of NM 300K AgNMs (magnification 35kx) and histogram of the size distribution (based on 143 particles).



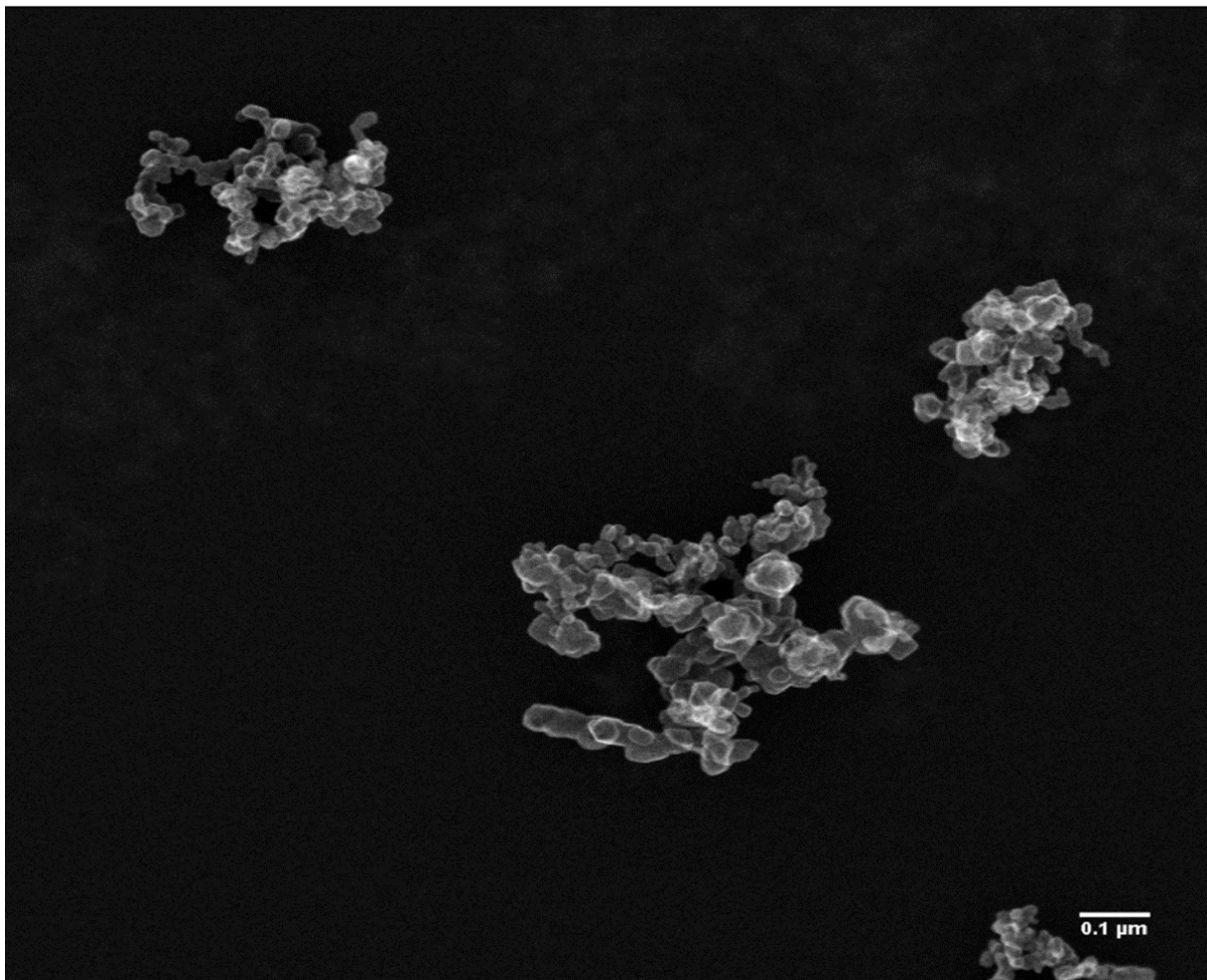
Source: EAWAG, Switzerland, in Kuehr et al. (2020a).

Figure 23: TEM image of AuNMs (magnification 30kx) and histogram of the size distribution (based on 172 particles).



Source: EAWAG, Switzerland, in Kuehr et al. (2020a).

Figure 24: TEM image of NM 105 (magnification 80kx).



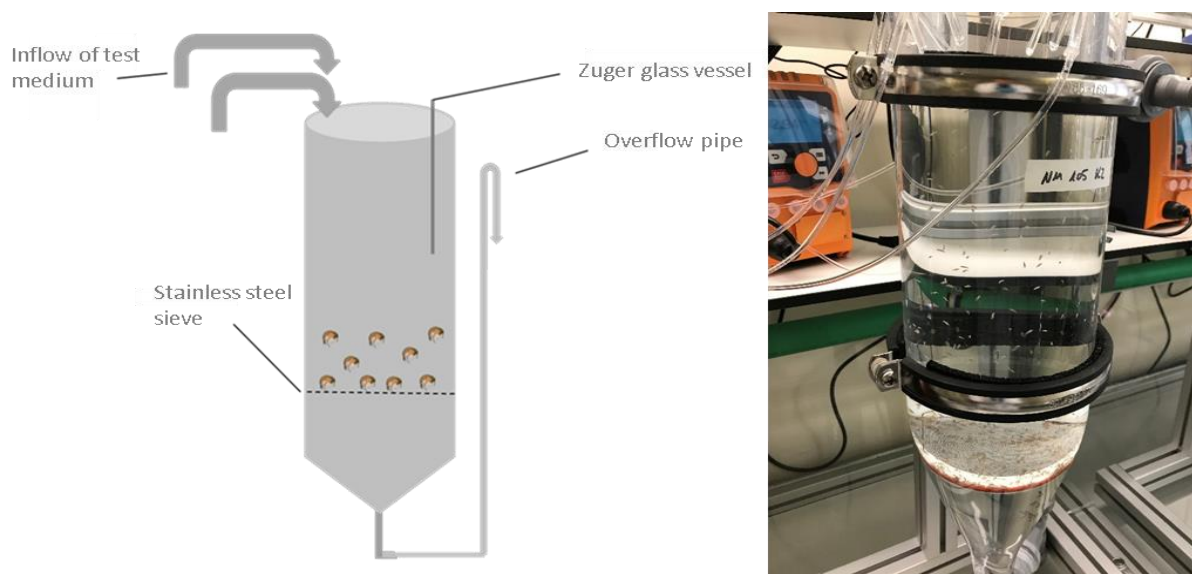
Source: EAWAG, Switzerland, in Kuehr et al. (2020a).

4.2 Test concepts for testing nanomaterials

4.2.1 Bioconcentration test

High NM concentrations were applied in the exposure media to allow good analytical investigations, however, many NMs tend to agglomerate and thus to sedimentation in the test media. In previous studies classical glass aquaria were used to expose fish to NMs like e.g. NM105 (Zeumer et al., 2020a; Zeumer et al., 2020b). A strong decrease (between 58 and 75 %) of the NM concentrations in the test media were observed (R. Zeumer personal communication). That was explained by the strong sedimentation and thus accumulation of the NMs in the lower part of the water body or at the bottom of the aquarium. Thus the flow-through studies for bioaccumulation testing carried out as part of this project were carried out in a modified test system (Figure 25) as described by Kuehr et al. (2020c), to avoid the local accumulation (“sink”) of nanomaterials within the test system that may cause inhomogeneous exposure conditions of the test animals. The system consisted of a Zuger glass jar test vessel providing a volume of 8 L for test medium. A sieve made from stainless steel and Teflon was fixed at the bottom of the glass body to prevent the loss of amphipods through the outlet pipe and to serve as substrate. A stainless steel mesh was added into the test system to serve as refuge for the animals.

Figure 25: Schematic overview of the flow-through test system for testing nanomaterials.



Source: Fraunhofer IME, in Kuehr et al. (2020a).

The stock solution of the test substance was added into a mixing vessel using peristaltic pumps (IPC High Precision Multichannel Dispenser, ISMATEC®) and further diluted with dilution water supplied by a membrane pump (gamma/ X, ProMinent®) to produce the test medium which was supplied into the zuger glass jar by TYGON® tubes (E-3603, TYGON®). The dilution water was aerated and heated to 25 °C before pumped into the mixing vessel. The complete system including the outlet pipe had a volume of around 10 L. As described in Chapter 2.3.2 at least five volume replacements through each test chamber per day should be achieved according to the protocol of the HYBIT method (Schlechtriem et al., 2019; Kosfeld et al., 2020). To achieve a sufficient medium exchange, a flow rate of 3 L/h was chosen which allowed an easy handling of the volumes of NM stock suspensions needed to reach the gained exposure concentrations. The test media left the test system at the bottom of the zuger glass jar by an overflow pipe. The working suspension of NM 105 was applied directly to the test vessel to avoid sedimentary processes in the mixing vessel. The preparation of the working suspension is described in Chapter 4.4.4. Animals were fed ad libitum with agar-agar cubes (DECOTABS) manufactured as described in Chapter 4.5 without the addition of NMs.

Before the start of the bioaccumulation test the system was allowed to equilibrate for at least 48 h until stable media concentrations with a variation of $\leq 20\%$ were reached for at least three consecutive sampling times (separated by at least 3 h).

During the test water parameters like pH-value, temperature and dissolved oxygen (mg/L and saturation in %) were monitored daily. Measurements of ammonia, nitrite and nitrate were carried out at the start, end of the uptake and end of elimination phase using a test kit for photometric measurements (NANOCOLOR® 500D, Machery-Nagel).

The animals were exposed for up to 336 h before being transferred into a clean system that was prepared identically but without the test substance for the depuration phase. The animals were washed with HDW before being placed into the new system to avoid the transfer of test substance from the exposure medium.

4.2.2 Biomagnification test

The Zuger glass system described above was also used for the biomagnification tests. The design of the test system including the stainless steel sieve allowed removal of i) feces, and ii) potentially leached ions and suspended NMs from the feces or experimental feed (DECOTABs; Chapter 4.5) from the test chamber with the water flow to avoid co-exposure of the amphipods via the aqueous pathway. This could not be guaranteed if aquaria without flow-through would have been used for the tests. For each test item two biomagnification tests were carried out using two different concentrations to allow the determination of potential concentration dependent effects on the uptake and elimination of metals from the NMs. Test animals were fed DECOTABs containing NMs every morning following the removal of feed residues.

Water samples were taken during the uptake period to determine any potential contamination of the test water. The duration of the uptake and depuration phase as well as the schedule of the animal samplings were adjusted depending on the experiences gained during the bioconcentration tests. A depuration phase was only carried out in the tests with the high exposure concentration to gain information on the elimination of the previously accumulated metals/NMs.

4.3 Analytics

4.3.1 Inductively coupled plasma mass spectrometry (ICP-MS)

The tissue samples and samples of the experimental food were acid digested using microwaves. A MLS turbo Wave® was used for the digestion of Ag and Au samples (30 min at 220 °C and 40 bar). Aqua regia (3:1, nitric acid:hydrochloric acid) was added (8 mL) to the samples before vortex stirring (VORTEX GENIE 2, Si™ Scientific Industries) and the digestion process. The TiO₂ samples were digested in a MLS Ultra Clave following addition of nitric acid by the method described by Kuehr et al. (2020c). All digested samples were diluted up to 15 mL with nitric acid (10 %) before measurements.

The additional samples taken to determine the amount of Ag that can be extracted by liquefaction of the animals' proteins using proteinase K (Sigma Aldrich) were enzymatically digested as described below. The digestion solution was filtered using 0.45 µm syringe filters (Minisart® NML, 0.45 µm). The filtrate (3 mL) was digested using 5 mL aqua regia and microwave treatment as described above. All microwave digested samples were filtered using 0.45 µm syringe filters (Minisart® NML, 0.45 µm) before measurements.

The test media samples (20 mL) which were acidified after sampling and stored at 4 °C were measured directly. Total concentrations of Ag, Au and Ti (as equivalent to TiO₂) in the aqueous test media were determined by inductively coupled plasma mass spectrometry (ICP-MS, Agilent 7700 ICP-Q-MS, Agilent Technologies, Waldbronn, Germany). The instrument calibration and method verification were carried out as described by Kuehr et al. (2018) using certified element, multi-element standards (Merck and Sigma Aldrich) and reference water (TM 25.4; Environment Canada). A rhodium standard solution (Merck KGaA; CertiPUR) was applied as internal standard for compensation of instrumental fluctuations. At least three measurements were recorded for each standard and sample and the mean concentration was determined by the ICP-MS software.

4.3.2 Single particle inductively coupled plasma mass spectrometry (sp-ICP-MS)

For the examination of *Hyalella* tissue samples by single particle ICP-MS (sp-ICP-MS) a gentle sample preparation method was applied using the enzyme proteinase K (Schmidt et al., 2011; Loeschner et al., 2013) which is known not to dissolve the particles and which affects the particle properties as little as possible (Kuehr et al., 2020b; Kuehr et al., 2020c). The dried animals (10 per replicate) were transferred into a 50 mL glass beaker and gently pestled using a glass rod. The glass rod was rinsed with 10 mL of the digestion solution (45 mg proteinase K in 1 L buffer solution + 0.5 % SDS + 50 mM NH_4HCO_3 , pH adjusted to 8.0 - 8.2) which was collected in the glass beaker containing the crushed tissue samples. The samples were incubated in the 10 mL digestion solution for 3 h at 50 °C and 100 rpm. As shown by Kuehr et al. (2020c) this process has no or only a negligible impact on the dissolution and size distribution of the present NPs. The solution was filtered using 0.45 μm syringe filters (Minisart® NML, 0.45 μm) and then measured using an ICP-QQQ-MS (Agilent 8900, Agilent Technologies, Waldbronn, Germany). The dwell time in the single particle measurement mode of the ICP-MS was set to 100 μs and time resolved signals were recorded on the selected isotope for 60 s. Peak detection and integration were conducted automatically by the Agilent MassHunter software and converted into particle sizes. Dispersions of 60 nm gold nanoparticles (AuNMs 60 nm, BBI solutions, UK) were used for the determination of the nebulization efficiency and prepared freshly on the day of measurement. The samples were diluted in UHQ by a factor of 10^2 - 10^5 for measurement to reach a particle concentration of 200-2,000 particle events per minute. According to Sannac et al. (2013) and Mitrano et al. (2014) this correlates to an element concentration in the range of ng/L. Ag was measured as the isotope ^{107}Ag . The threshold between background and particle signals was defined based on visual inspection of the measured signal distributions (Kuehr et al. 2020c). After measurement of particle concentrations in the digested fraction using sp-ICP-MS, the filtrated solution was further digested by aqua regia to allow analysis of the total Ag content. To do this, 2 mL of aqua regia were added to 5 mL of the filtered solution prior to digestion in a microwave as described above (turboWave® Inert, MLS; max temperature 220 °C, max pressure 40 bar). Aqueous media samples collected during the studies were measured following the same procedure but without enzymatic digestion (Kuehr et al. 2020b).

4.4 Bioconcentration tests with NMs and AgNO₃

Three bioconcentration tests with AgNO₃ were carried out to identify the impact of the i) exposure concentration and ii) sexes of the test animals on the bioaccumulation of the metal. The studies were carried out simultaneously allowing usage of the same stock solutions for each test and thus to minimize the variation of the test conditions.

4.4.1 Bioconcentration test with AgNO₃

4.4.1.1 Test design of the bioconcentration test with AgNO₃

The bioconcentration studies with AgNO₃ were conducted using the Zuger glass test system. The system was run with a flow rate of 3 L/h HDW which was mixed with AgNO₃ stock solution in a mixing chamber. The tests with AgNO₃ were carried out as described above (Chapter 4.2.1) using only male (AgNO_{3-ML}) and only female individuals (AgNO_{3-FL}) in order to investigate potential effects of the animals sex on the bioaccumulation of metals or ions released from NPs during the tests. In addition, a third, extended test was carried out with females testing a higher exposure concentration (2-3 times higher) that was gained by a higher supply of the stock solution to the mixing vessel to investigate the potential concentration dependence of the bioaccumulation (AgNO_{3-FH}).

In all tests the uptake phase was lasting for 336 h with animal and medium samplings at regular intervals. Triplicate tissue samples, each consisting of 20 individuals, were taken from the test system at different times during the uptake and elimination phases. Sampled animals were rinsed with HDW and blotted dry using lint free paper towels and stored at -20 °C.

The medium samples were acidified by adding 200 µL of nitric acid (69 %, suprapure grade, Roth) and stored at 4 °C. Media samples for sp-ICP-MS were not acidified and measured directly. Animal samples were rinsed with HDW, blotted with lint free paper, weighted (AUW220D, SHIMADZU) and stored at -20 °C. Tissue samples for sp-ICP-MS were shock frozen using liquid nitrogen and subsequently stored at -20 °C. In the test with the lower exposure concentration and using female *H. azteca*, the remaining test animals were washed and transferred to a clean test system after the uptake phase for a depuration phase lasting 336 h with several sampling points.

4.4.1.2 Analytics of the bioconcentration tests with AgNO₃

The sampled animals were digested and investigated to determine the total Ag content as described in Chapter 4.3.1. The medium samples were measured directly without previous digestion as mentioned above.

4.4.1.3 Results of the bioconcentration tests with AgNO₃

Three bioconcentration tests with AgNO₃ were carried out to identify the impact of the exposure concentration and the sex of the test animals on the bioaccumulation of the metal.

The TWA concentrations of total Ag in the test on bioaccumulation in male and female animals were 0.64 for females (AgNO_{3-FL}) and 0.67 µg Ag/L for males (AgNO_{3-ML}). In the related test on the concentration dependent bioaccumulation of Ag carried out with female animals a 2.5 times higher TWA of 1.64 µg Ag/L (AgNO_{3-FH}) was measured (Table 8). The concentration time courses are presented in Figures 26 - 28.

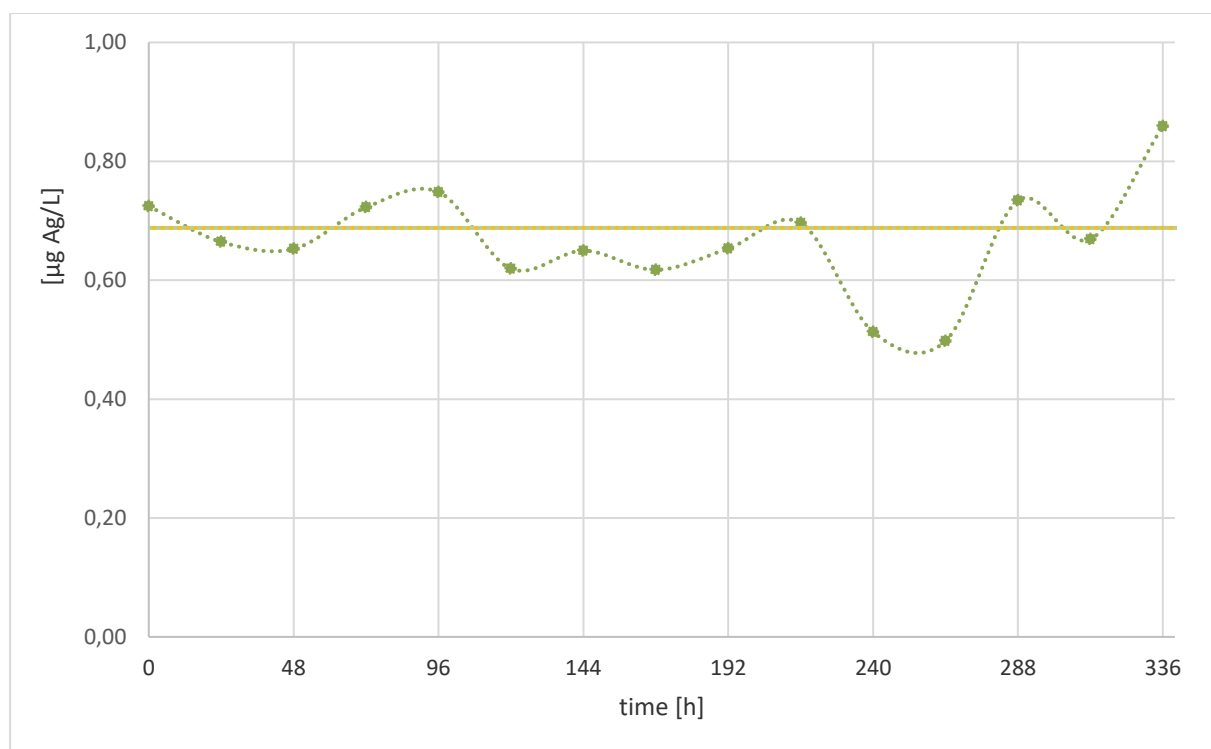
The steady state tissue concentrations were calculated as an average of the values measured in the samples taken between 240 and 336 h of exposure. Male and female animals exposed to the

AgNO₃ treatments revealed tissue concentrations of 3.40 ± 0.34 mg Ag/kg and 3.14 ± 0.09 mg Ag/kg, respectively. The steady state tissue concentration measured in the AgNO_{3-FH} treatment, in animals taken between 288 and 336 h of exposure (not between 240 and 336 h), was 7.70 ± 0.59 mg Ag/kg. Considering the measured tissue and water concentrations, BCF_{SS} values of 4,900 (AgNO_{3-ML}), 5,100 (AgNO_{3-FL}) and 4,700 (AgNO_{3-FH}) were calculated (Table 8). The course of the tissue concentrations measured during the uptake and depuration phases are presented in Figures 29 - 30.

Table 8: Characteristics of the bioconcentration tests with AgNO₃ and calculated BCF values.

Study	Test item	Sex	TWA [µg Ag/L]	BCF _{SS}
AgNO _{3-FL}	AgNO ₃	female	0.64	5,094
AgNO _{3-ML}	AgNO ₃	male	0.67	4,883
AgNO _{3-FH}	AgNO ₃	female	1.64	4,695

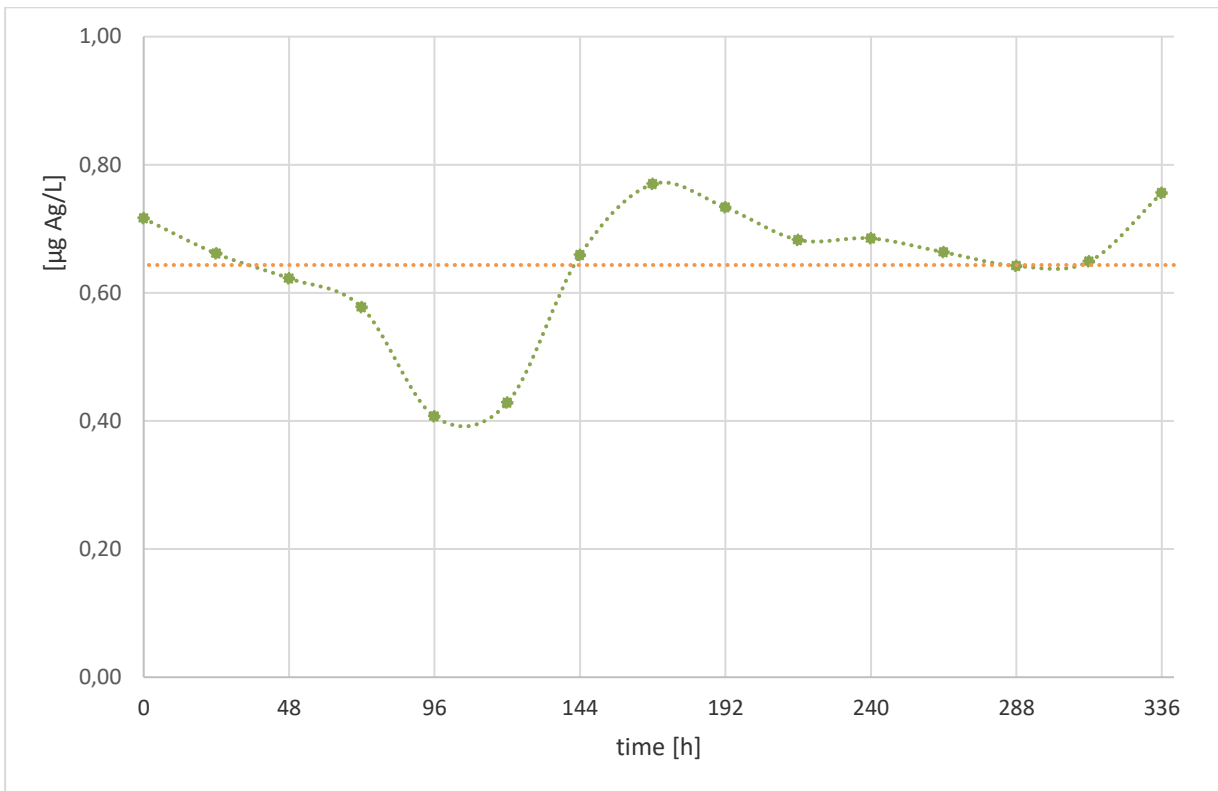
Figure 26: Total Ag medium concentration in bioconcentration test AgNO_{3-ML} using males.*



*TWA = 0.67 µg Ag/L.

Source: Fraunhofer IME, own diagram.

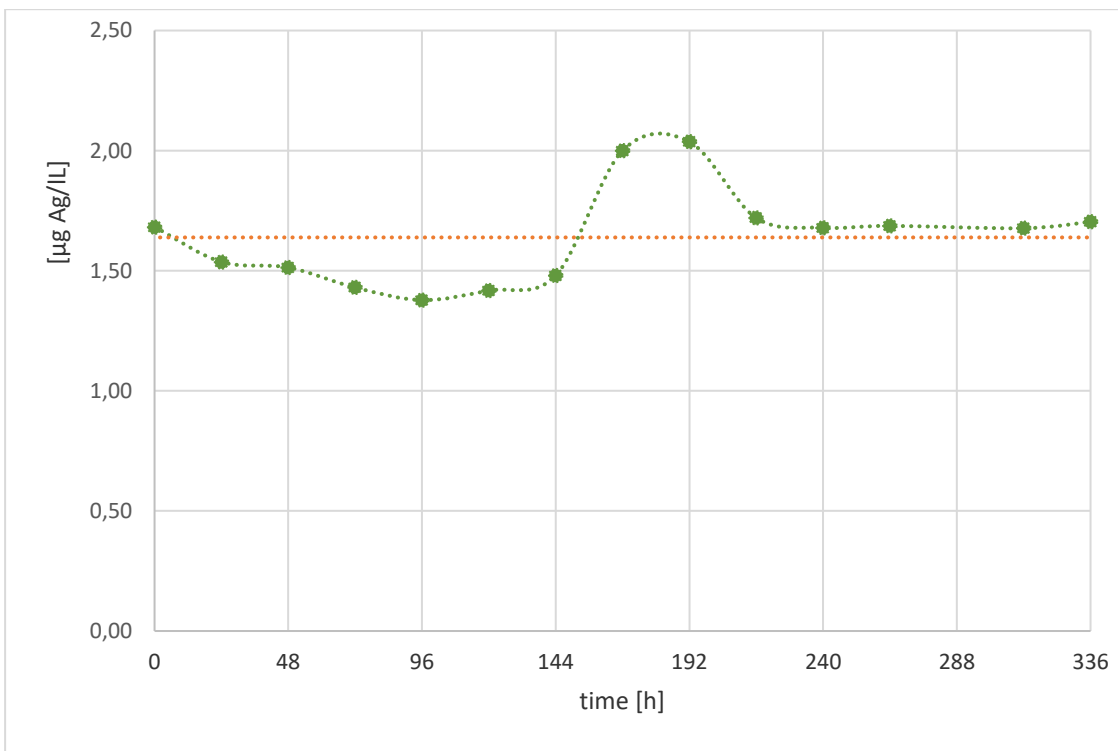
Figure 27: Total Ag medium concentration in bioconcentration test AgNO_{3-FL} using females.*



*TWA = 0.64 µg Ag/L.

Source: Fraunhofer IME, own diagram.

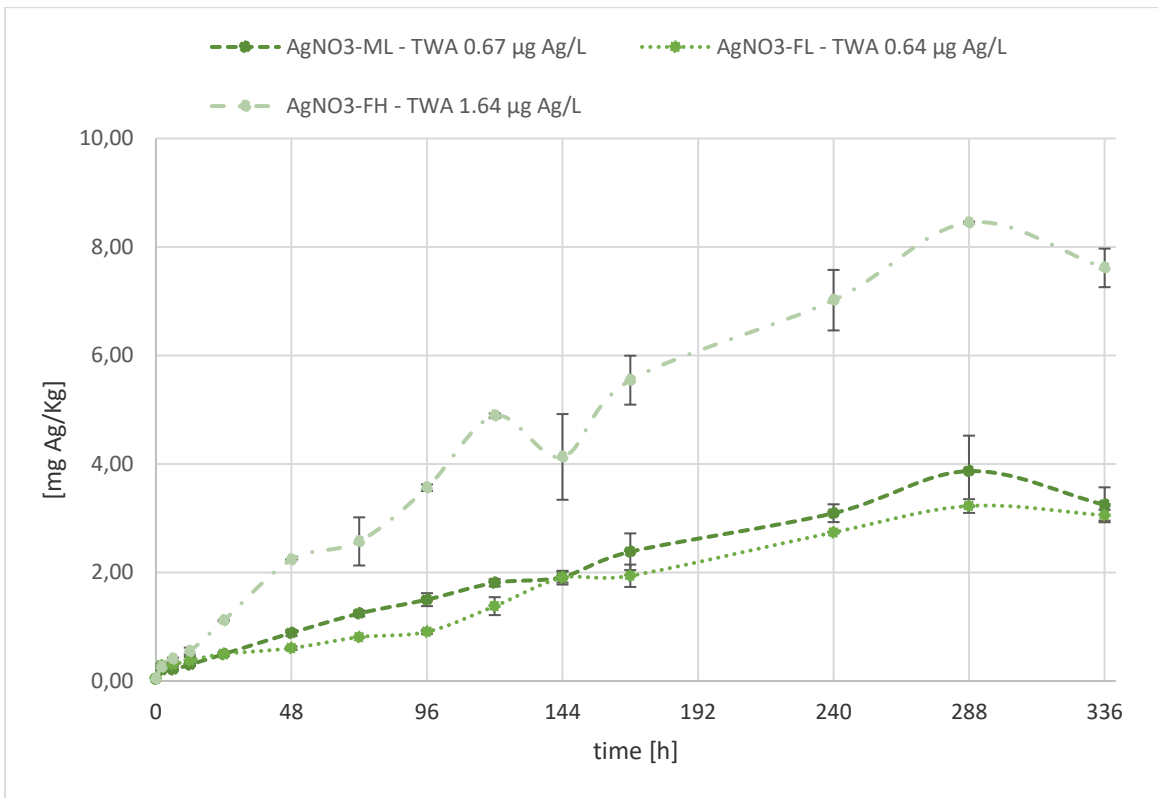
Figure 28: Total Ag medium concentration in bioconcentration test AgNO_{3-FH} using females.*



*TWA = 1.64 µg Ag/L.

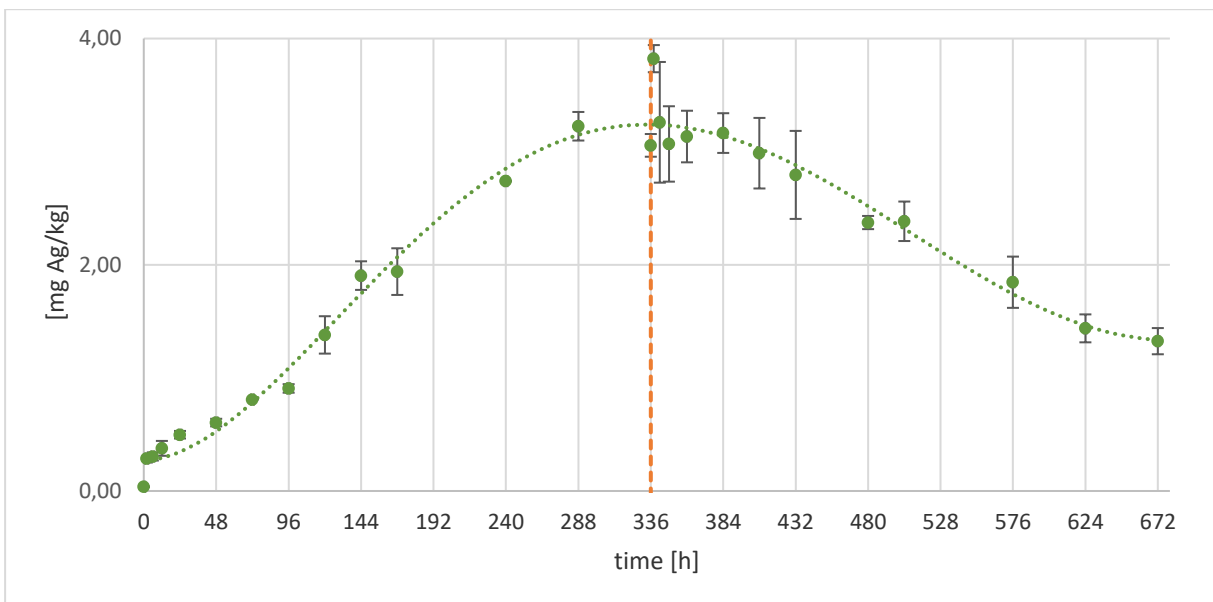
Source: Fraunhofer IME, own diagram.

Figure 29: Total Ag tissue concentrations in bioconcentration tests with AgNO₃ (uptake phase).



Source: Fraunhofer IME, own diagram.

Figure 30: Total Ag tissue concentrations in females during bioconcentration test AgNO₃-FL.



Source: Fraunhofer IME, own diagram.

4.4.1.4 Evaluation of the bioconcentration tests with AgNO₃

The tests with AgNO₃ showed that Ag from AgNO₃ is available for *H. azteca* if exposed via the aqueous medium. We were able to determine the uptake and elimination kinetics of the metal or its ions and to calculate BCF values. The calculated BCF_{SS} values indicate a high bioaccumulation potential. A closer look at the elimination phase of the test using females exposed to the lower test concentration showed that the Ag body burden of the animals collected after 14 days of depuration was still at a level equivalent to 50 % of the steady state concentration measured at the end of the uptake phase.

It is not clear whether this observation was caused by a very low elimination rate or a “sink”, e.g. based on metal binding proteins like metallothioneins. Also detoxification processes like biomineralization or sequestration of Ag as e.g. phosphates or carbonates may have caused this as described by Ahearn et al. (2004).

The comparison of both sexes in the different tests at comparable TWA values (0.67 and 0.64 µg Ag/L) showed that the kinetics of the uptake (Figure 29) as well as the calculated BCF_{SS} of 5,094 (males) and 4,883 (females) for both sexes are comparable (Table 8). Also for the following tests using metal or metal oxide-based NPs both sexes were used. To minimize artefacts due to reproduction/ release of juveniles which may cause an elimination of previously ingested/accumulated metal or NMs animals of only one sex were used for each test.

Testing the higher exposure concentration (TWA 1.64 µg Ag/L) with females and comparing the gained BCF_{SS} value of 4,695 with those from the test with females and an exposure TWA concentration of 0.64 µg Ag/L (BCF_{SS} 5,094) shows that there is no or only a slightly negative concentration dependency for the bioaccumulation of Ag present as Ag⁺ in *H. azteca*.

Bioconcentration tests with AgNO₃ were carried out in addition to the studies with AgNMs to allow a comparison of the bioaccumulation potential of ionic and particulate Ag. The tests with AgNO₃ showed that Ag⁺ exposed via the water is available for *H. azteca*. Uptake and elimination kinetics of the ions measured as total Ag were determined. The calculated BCF_{SS} values indicate a high bioaccumulation potential. The trend of the Ag concentrations in *H. azteca* during the elimination phase of the AgNO_{3-FL} test showed that the Ag body burden after 14 days of depuration was still at a level of 50 % of the steady state concentration. It is not clear if this observation was caused by a very low elimination rate, the binding of Ag⁺ by metal binding proteins like metallothioneins or the sequestration of Ag as solids (concretions) as discussed below.

The bioconcentration of AgNO₃ was tested in two independent bioconcentration studies with male and female amphipods to investigate potential gender-specific differences. The comparison of both groups exposed to comparable test concentrations showed that the uptake kinetics of total silver as well as the calculated BCF_{SS} are comparable for both sexes. Therefore, both male and female *H. azteca* seem to be suitable for testing metal or metal oxide based NMs, but further investigations with more different types of NMs are required. Nevertheless, test animals need to be separated and only male or female animals should be used per test to avoid elimination of accumulated test item through the release of juveniles.

The uptake of metals in crustaceans may be at least partly regulated (Viarengo, 1989; Rainbow, 1995, 1997). Due to the underlying mechanism, it is anticipated that the metal uptake in crustaceans is dependent on the metal concentration in the water. Therefore, it was necessary that at least two concentrations were tested. Comparing the BCF_{SS} values calculated for the high and low treatment, a negative concentration dependency for the bioaccumulation of Ag⁺ was observed, with the animals exposed to the higher test concentration showing a lower BCF_{SS} value.

4.4.2 Preliminary bioconcentration test with NM 300K

A preliminary bioconcentration test using NM 300K was applied to gain information about the availability of Ag from NM 300K and the suitability of this system for conducting bioconcentration tests with NMs in *H. azteca*.

4.4.2.1 Preliminary bioconcentration test with NM 300K: Test design and analytics

The preliminary bioconcentration test with NM 300K was carried out as described for AgNO₃ (Chapter 4.4). The uptake phase of 168 h and was followed by an equally long depuration phase. Tissue and media samples were taken, processed and stored as described in Chapter 4.4.1.

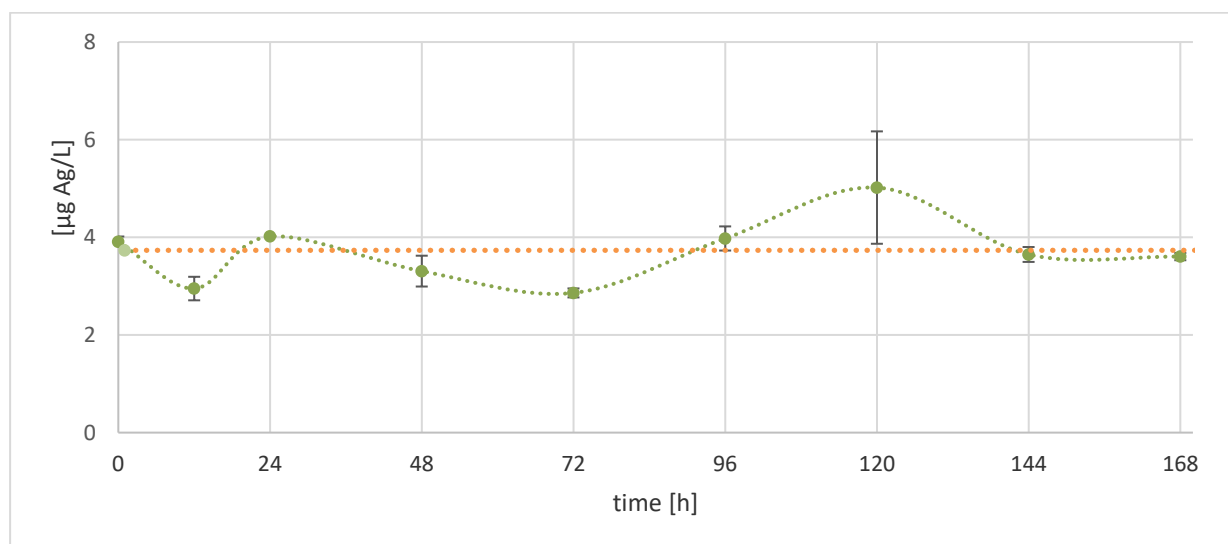
The analytics for the total Ag content in the animals' tissue and medium samples were carried out as described in Chapter 4.3.

4.4.2.2 Results of the preliminary bioconcentration test with NM 300K

During the time course of the uptake phase constant exposure conditions with a total Ag concentration (TWA) of 3.734 µg Ag/L were reached (Figure 31). Kuehr et al. (2020c) estimated the percentage of Ag⁺ of the measured total Ag concentration in a NM 300K exposure medium produced in the same way as applied in this study, to be between 1.6 and 21.5 % under static conditions. Therefore, the measured total Ag concentration supposedly consists of nanoparticulate as well as ionized Ag present in the exposure medium.

During the uptake phase a constant increase of the Ag body burden was detected in the sampled animals without reaching a steady state within the 168 h of exposure (Figure 32). Following the transfer of the remaining animals into a clean system running with HDW a slow decrease of the total Ag body burden was observed that did not lead to a complete depuration of the previously accumulated Ag until the end of the depuration phase.

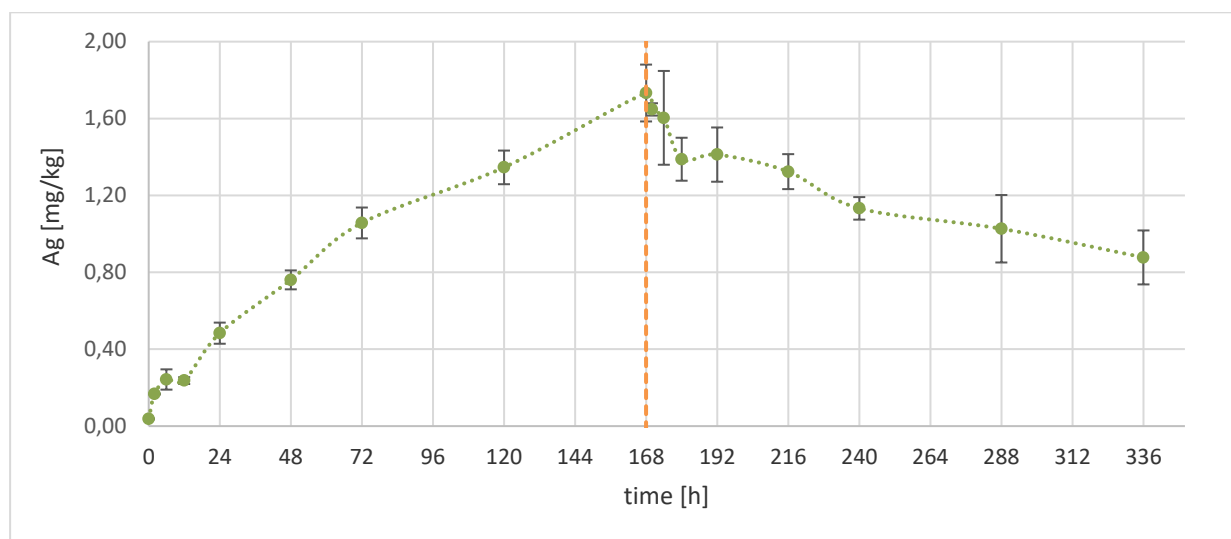
Figure 31: Total Ag medium concentration in NM 300K preliminary bioconcentration test.*



*TWA = 3.734 µg Ag/L.

Source: Fraunhofer IME, own diagram.

Figure 32: Preliminary bioconcentration test with NM 300K: Total Ag tissue concentrations.



Source: Fraunhofer IME, own diagram.

4.4.2.3 Evaluation of the preliminary bioconcentration test with NM 300K.

The results of the preliminary bioconcentration test with NM 300K indicate that *H. azteca* seems to be suitable for testing the bioconcentration potential of Ag from AgNMs, even though it was not possible to calculate a BCF_{SS} value because steady state conditions were not reached at the end of the uptake phase. The following tests were carried out to show that the *Hyalella* bioconcentration test can be used to investigate the bioaccumulation potential of different NMs.

In case of NM 300K no negative impact like e.g. toxic effects or higher mortality of the used total Ag concentration (TWA = 3.734 µg Ag/L) was observed. The following bioaccumulation tests with NM 300K were thus carried out under the same exposure conditions. However, the duration of the exposure and depuration phase was extended to check whether steady state conditions as well as a complete elimination can be reached at the end of the uptake and depuration phase, respectively.

4.4.3 Bioconcentration test with NM 300K

For testing the bioaccumulation of NM 300K, three bioconcentration tests were carried out to identify the impact of i) the test system used (classic aquarium or Zuger glass jar) and ii) the composition of the test medium for NM exposure (dilution water or culture medium). To identify the influence of the test media composition two tests were carried out (NM 300K_{Cm} and NM 300K_{Aq}). Aquaria were used in a test design as described in Chapter 2.3.2.1. Peristaltic pumps were used to apply the stock solution of NM 300K. The test which was carried out with test medium (NM 300K_{Cm}) based on culture medium (Table 1) was carried out at UBA / Berlin Marienfelde. The other test using test medium (NM 300K_{Aq}) which was prepared by using dilution water was carried out at Fh IME in Schmallenberg.

To identify the impact of the used test system, two tests were carried out simultaneously using the same stock solution for each test allowing to minimize the variation of the test conditions. One of the tests (NM 300K_{Aq}) was conducted using a normal aquarium as described in Chapter 2.3.2.2. The Zuger glass-based test system for the other test (NM 300K_{Zg}) was used as described in Chapter 4.2.1 (Figure 25). Table 8 describes the specifications of the bioconcentration studies with NM 300K and presents the calculated BCF values.

4.4.3.1 Bioconcentration tests with NM 300K: Test design and analytics

The uptake and depuration phases of the bioconcentration tests with NM 300K were lasting 336 h each. The analytics to measure the total Ag content in test media and tissue samples as well as the examinations using the sp-ICP-MS were carried out as described above in chapters 4.3.1 and 4.3.2.

Additional samples (triplicates of 10 animals) were taken at the end of the uptake and depuration phase of study NM 300K_{Aq}, each, to determine the total Ag content associated with the protein fraction of the animals. The samples were digested enzymatically as described in Chapter 4.3.2. Following filtration, the digested samples were mixed with aqua regia and digested again using the microwave method as described in Chapter 4.3.1 and finally measured for total Ag content. This allowed to compare the content of Ag in the protein fraction of the animals with the whole amount of Ag in the complete samples.

The pH (WTW, inolab® pH 7310) and the conductivity as indication for the ionic strength (WTW, Multi 3320 at 24.6 °C) were measured in the culture media and the dilution water.

Table 9: Specifications of the bioconcentration studies with NM 300K and calculated BCF values.

Study	Test item	Test system	Exposure Medium	TWA [$\mu\text{g Ag/L}$]	BCF
NM 300K _{Cm}	NM 300K / AgNM	aquarium	culture medium	3.00	604
NM 300K _{Aq}	NM 300K / AgNM	aquarium	dilution water	6.73	480
NM 300K _{Zg}	NM 300K / AgNM	Zuger glass system	dilution water	6.83	453

4.4.3.2 Results of the bioconcentration tests with NM 300K

The media samples collected during the uptake phase of test NM 300K_{Cm} lasting 336 h, which was carried out in an aquarium using a physiological culture medium had a total Ag TWA concentration of 3.00 $\mu\text{g Ag/L}$ (Table 9; Figure 33). In this study a fast increase of the total Ag body burden was observed (Figure 34) which slowed down after 288 h of exposure and remained nearly constant at a level of appr. $1.81 \pm 0.13 \text{ mg Ag/kg}$ until the end of the uptake phase (336 h). Considering the average total Ag concentration measured for the last three samplings as the steady state concentration, a BCF_{SS} value of 604 could be calculated for the NM 300K_{Cm} test (Table 9). During the depuration phase the total Ag body burden decreased within 72 h to a level of appr. 1.5 mg Ag/kg and remained stable on this level until the end of the study.

Media samples collected during the uptake phase of the other tests performed in dilution water and carried out in different test systems (aquarium vs. Zuger glass) were measured and total Ag TWA values of 6.73 (NM 300K_{Aq}), and 6.83 $\mu\text{g Ag /L}$ (NM 300K_{Zg}) were determined (Table 9). Media samples taken from NM 300K_{Zg} were further analyzed using sp-ICP-MS. Median particle sizes for Ag particles were determined to be 15 nm and thus identical to the size of the stock material.

The Ag body burden of the animals increased during the uptake phase and reached stable concentrations of 3.22 ± 0.07 (NM 300K_{Aq}) and $3.09 \pm 0.09 \text{ mg Ag/kg}$ (NM 300K_{Zg}) after 288 h of exposure (Figure 36). Based on the calculated steady state tissue concentrations reached after

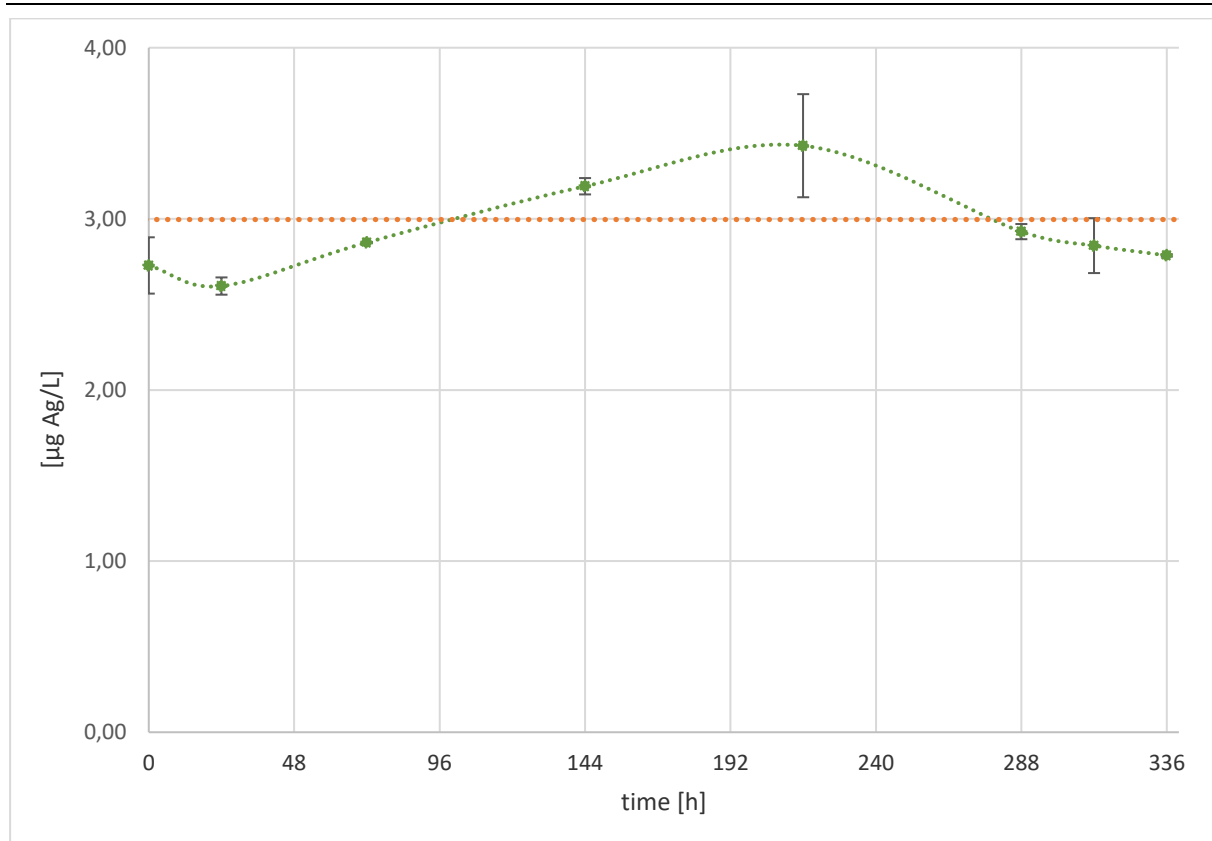
288 h of exposure and the calculated total Ag TWA of the test media (Figure 35), BCF_{SS} values of 480 and 453 were determined for the test using the aquarium (NM 300K_{Aq}) and the Zuger glass system (NM 300K_{Zg}), respectively (Table 9). In both tests, a similar decrease of the Ag tissue concentration was observed during the depuration phase leading to a final tissue concentration of approximately 1.5 mg Ag/kg (Figure 36).

Additional animal samples were collected at the end of the uptake and depuration phase of the NM 300K_{Aq} test to determine the Ag burden of the protein fraction of the animals. At the end of the uptake and depuration phase concentrations of approximately 1.87 and 1.58 mg Ag/kg were measured, respectively, equivalent to 59.3 and 112 % of the total Ag measured for the complete samples that were taken at the same time.

Particles extracted from animals collected at the end of the uptake phase of the NM 300K_{Aq} test were measured using sp-ICP-MS and had a median particle size of 22.6 ± 0.6 nm.

The pH of the different exposure media were determined to be 8.6 and 8.0 for the culture medium and the dilution water, respectively. The conductivity values were 401 (culture medium) and 264 µS/cm (dilution water) at 24 °C.

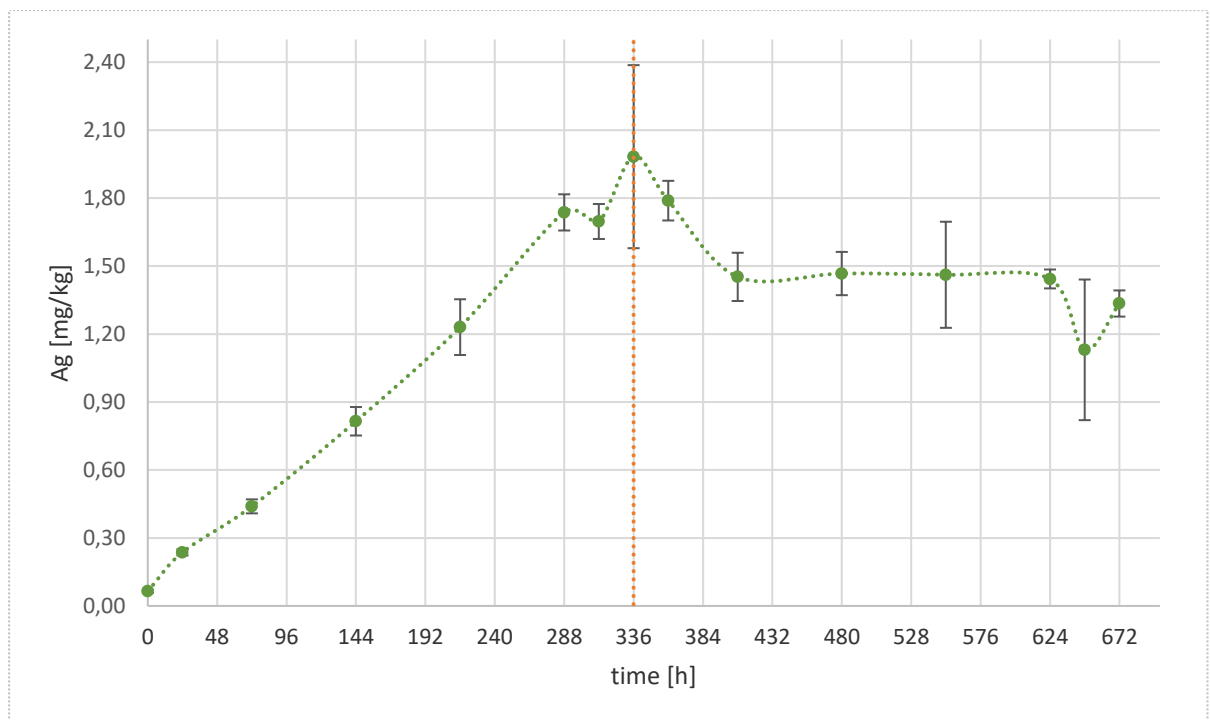
Figure 33: Total Ag medium concentration in NM 300K_{Cm} bioconcentration test (Test medium based on culture medium).*



*TWA of 3.00 µg Ag/L.

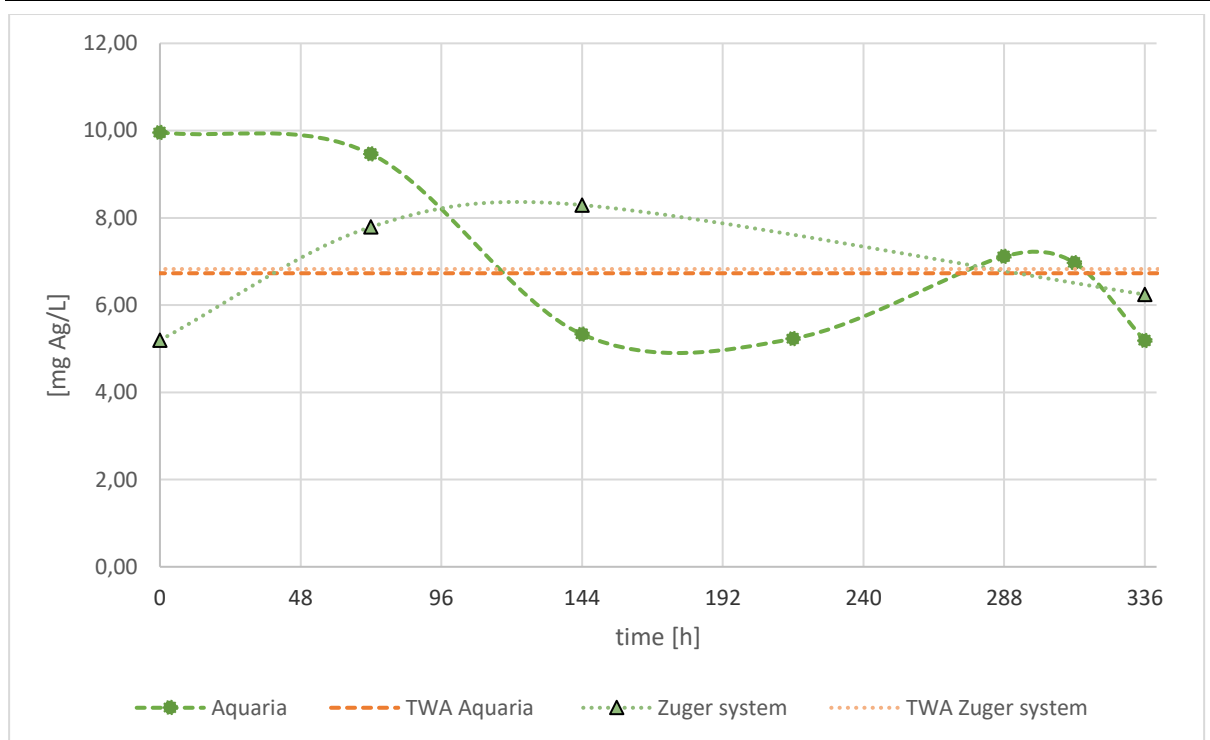
Source: Fraunhofer IME, own diagram.

Figure 34: Total Ag tissue concentrations in NM 300K_{cm} bioconcentration test (Test medium based on culture medium).



Source: Fraunhofer IME, own diagram.

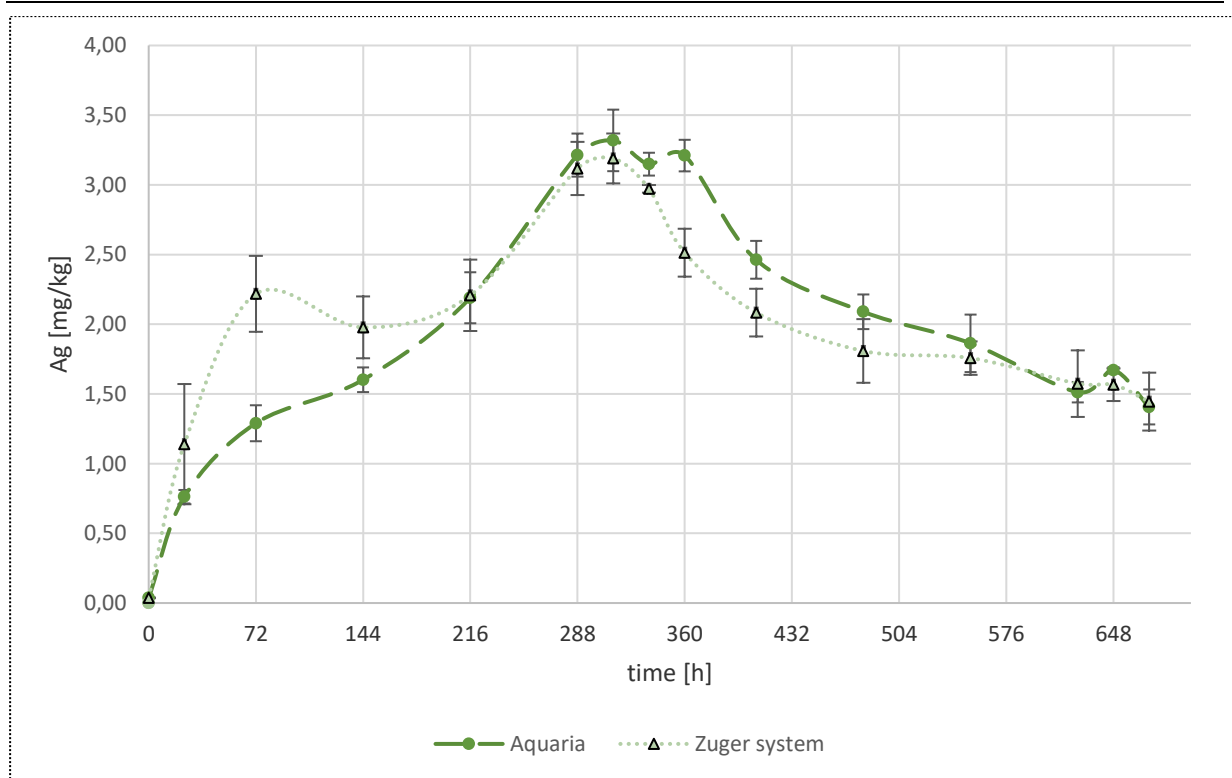
Figure 35: Total Ag medium concentration in bioconcentration tests with NM 300K_{Aq} and NM 300K_{Zg}.*



*Test NM 300K_{Aq} (TWA of 6.729 µg Ag/L) and test NM 300K_{Zg} (TWA of 6.827 µg Ag/L).

Source: Fraunhofer IME, own diagram.

Figure 36: Total Ag tissue concentrations in NM 300K bioconcentration test using Aquarium (NM 300K_{Aq}) and Zuger glass system (NM 300K_{Zg}).



Source: Fraunhofer IME, own diagram.

4.4.3.3 Evaluation of the bioconcentration tests with NM 300K

All bioconcentration tests using NM 300K proved that *H. azteca* can be used for bioconcentration tests with AgNMs, allowing to derive the uptake and elimination kinetics of the metal as well as to calculate BCF_{SS} values. The results of the tissue examinations using sp-ICP-MS indicate that AgNMs are ingested or at least attached to the animals' body, even after rinsing with clean water and blotting the animals dry after sampling.

The measurement of the median particle sizes of AgNMs that were detected and measured using sp-ICP-MS showed that the AgNMs in the exposure medium were obviously not affected by the test system showing nearly the same median size as measured for the feed stock material. It can be only speculated whether the difference in size of the measured particles in the test media of 0.01 nm was the result of slight dissolution and release of Ag⁺ or caused by the inaccuracy of the analytical method. The calculated medium size of 22.6 ± 0.6 nm of particles found in the liquefied proteins shows that the particles seemed to become bigger following ingestion. This may be explained by processes like agglomeration of the particles or by an artefact caused by the measurement of Ag associated with inorganic or organic Ag complexes. Another explanation for the bigger particles measured in the protein extracts might be the formation of solid concretion granules. Baccaro et al. (2018) found AgNMs in earthworms (*Eisenia fetida*) that were bigger than the AgNMs used for exposure. They hypothesized that the measured AgNMs were granules actively formed by the earthworms to sequester Ag⁺ as also observed in intestinal fish cells exposed to AgNO₃ (Minghetti and Schirmer, 2016). Methods like TEM and EDX, e.g. as described by Kühn et al. (2020c) for AgNMs in *H. azteca* are required to further elucidate the mechanisms involved.

The stable total Ag concentrations measured in the animals even after 336 h of depuration might be explained by the binding of Ag⁺ to proteins like metallothioneins, after being taken up from the exposure media or being released within the organisms after ingestion of AgNMs. This may also explain why the total Ag concentration measured in the protein fraction of animals collected at the end of the depuration phase was about 100 % of the concentration found in the complete animals. The increased percentage (> 100 %) could be explained by the comparison of different samples, the variation between the samples and the accuracy of the measurements.

The result of test NM 300K_{Cm} using culture medium shows that the presence of comparatively higher levels of chloride, bromide, carbonate and sulfate in the test medium did not inhibit the uptake of Ag from NM 300K from the exposure medium, e.g. by passivation of the NMs surface or sequestering potentially releases Ag⁺ as chlorides, bromides or carbonates.

A higher BCF_{SS} value of 604 was calculated for the test NM 300K_{Cm} which was conducted with culture medium in comparison for the other tests which were carried out with HDW. This might be explained by the low negative correlation of BCF_{SS} values and the exposure concentration as previously described for the exposure with AgNO₃ (Chapter 4.4.1) but probably not by the composition of the exposure medium. Similar observations of a negative correlation between the bioaccumulation of metals and their exposure level have been described several times also for crustaceans (DeForest et al., 2007; Lebrun et al., 2014; Verschoor et al., 2012). This finding was explained by mechanisms like sequestration, binding of the metals to proteins, their excretion as well as by a saturation of the uptake capacities at high exposure concentrations (DeForest et al., 2007; Rainbow, 2007).

The impact of the test system used for the bioconcentration studies on the resulting BCF_{SS} of total Ag following exposure to AgNMs was investigated using conical and cubic shaped test vessels. The results of the flow-through tests using the same stock solution (NM 300K_{Zg} and NM 300K_{Aq}) showed that both test systems lead to comparable outcomes even though the Zuger glass system is limiting the risks associated with the accumulation of NPs within the system which may result in an inhomogeneous exposure scenario. However, this kind of artefact should be of higher relevance for the testing of NMs that show a higher tendency to sediment in the aquatic environment than NM 300K. The following tests with NM 105 and AuNPs were thus carried out using the Zuger glass system.

All bioconcentration tests with AgNM (NM 300K) carried out as part of this study showed that *H. azteca* is suitable to be used as test organism for bioconcentration tests with stable dispersed NMs. The monitoring of the uptake and elimination kinetics of the metal in the amphipods as well as the calculation of BCF_{SS} values were possible. The BCF_{SS} values derived from the bioconcentration tests with NM 300K were all in a similar range (453 to 604) and indicate a certain bioavailability or even bioaccumulation of Ag from NM 300K.

4.4.4 Bioconcentration test with NM 105

The titanium dioxide NM 105 was tested in two bioconcentration tests using two different exposure concentrations (high, NM 105_H; and low, NM 105_L) to determine a potential concentration dependence of the bioconcentration process.

4.4.4.1 Test design and analytics of the bioconcentration tests with NM 105

The tests were carried out using a Zuger glass system (Figure 25). During the uptake and depuration phases lasting 168 h each samples were taken, processed and measured as described in Chapter 4.3 and by Kuehr et al. (2020c). To gain a stable working suspension of NM 105 the feed stock nano powder was suspended in UHQ in a 3 L glass beaker and diluted using UHQ to a volume of 3 L. The diluted suspension (1 mg TiO₂/L) was allowed to settle for 72 h at room temperature. After decanting, the suspension with the remaining stable dispersed fraction was used as the working suspension. The working suspension was introduced into the test system at three (lower exposure concentration) or six (higher exposure concentration) different surface positions of the water body to ensure an even distribution of the TiO₂NMs in the test medium which was constantly supplied into the test vessels at a flow rate of 3 L/h. Every 72 h a new working suspension was used to ensure the stability of the working suspension during the study as recommended by Kuehr et al. (2020c). The studies with the two test concentrations were carried out simultaneously allowing to use the same stock solution for both tests and thus to minimize the variation of the test conditions.

4.4.4.2 Results of the bioconcentration tests with NM 105

In the bioconcentration test with NM 105, TWA values of 1.49 (NM 105_L) and 3.30 µg TiO₂/L (NM 105_H) were determined for the test media applied during the uptake phase lasting 168 h (Table 10, Figure 37 - 38).

Media samples were analyzed using sp-ICP-MS. The median particle size for TiO₂ particles present in the test medium was determined to be 56.3 ± 6.2 nm which is similar to the median size of the particles in the working suspension of 55.7 ± 1.3 nm.

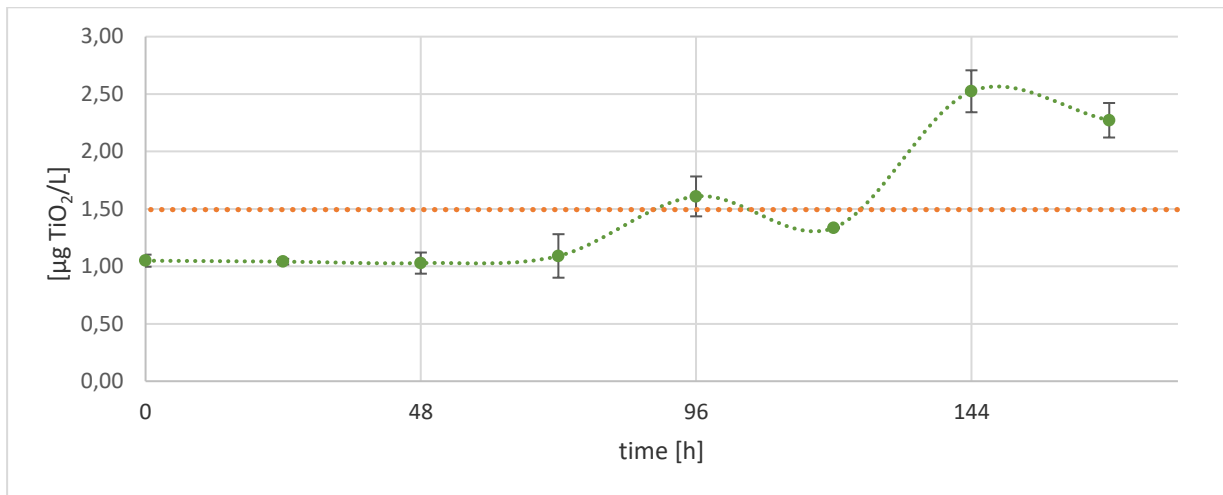
Animals collected from both treatments showed that no significant increase of tissue concentrations during the test occurred. For both treatments the measured concentrations of total Ti in the acid digested animals, as equivalent to the TiO₂ body burden, were mostly lower than the limit of quantification (LOQ, 1.390 µg Ti/L) and the limit of detection (LOD, 0.463 µg Ti/L). As an example, the results of the test with the higher concentrated exposure are presented in Figure 38.

Particles extracted from animals sampled at the end of the exposure were measured to have a median particle size of 107.0 ± 3.9 nm.

Table 10: Specifications of the bioconcentration studies with NM 105 and calculated BCF values.

Study	Test item	Exposure Medium	TWA [µg TiO ₂ /L]	BCF
NM 105 _L	NM 105 / TiO ₂ NM	dilution water	1.49	--
NM 105 _H	NM 105 / TiO ₂ NM	dilution water	3.3	--

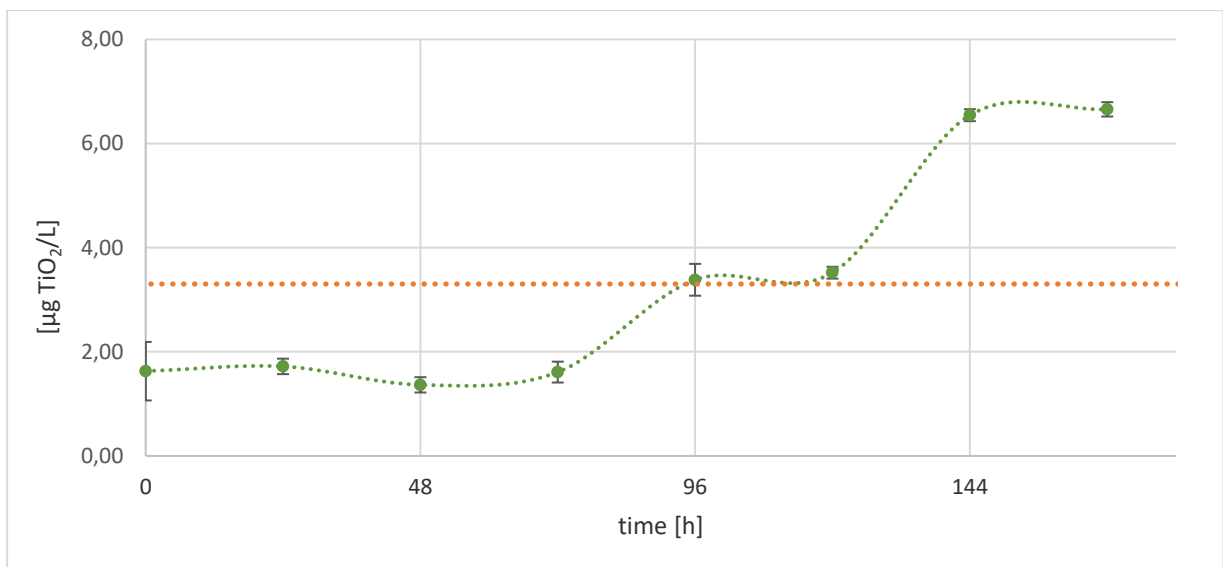
Figure 37: Total TiO₂ medium concentration in bioconcentration test NM 105_L.*



*TWA of 1.49 µg TiO₂/L.

Source: Fraunhofer IME, own diagram.

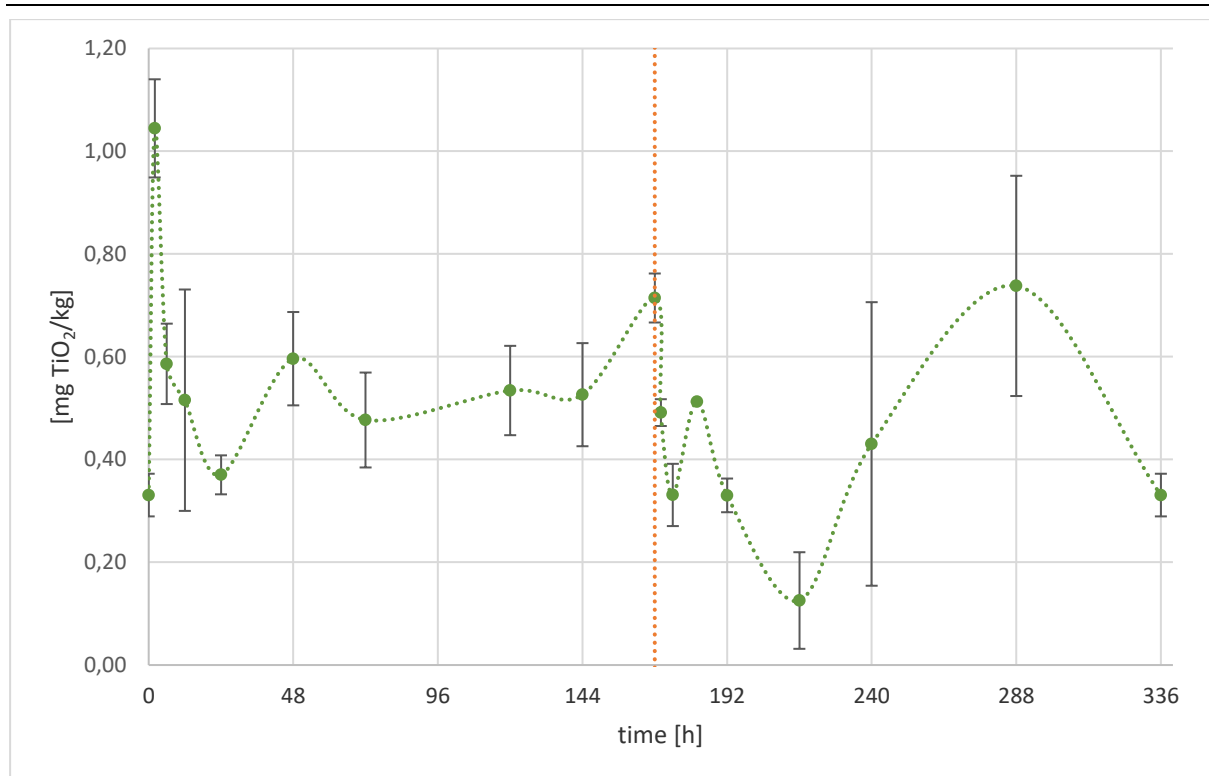
Figure 38: Total TiO₂ medium concentration in bioconcentration test NM 105_H.*



*TWA of 3.30 µg TiO₂/L.

Source: Fraunhofer IME, own diagram.

Figure 39: Exemplary total TiO₂ tissue concentrations in NM 105_H bioconcentration test (all data below LOQ).



Source: Fraunhofer IME, own diagram.

4.4.4.3 Evaluation of the bioconcentration tests with NM 105

The variation of the exposure concentrations observed during the uptake phase were presumably caused by the different working suspensions used. Following the bioconcentration tests, the calculation of BCF_{SS} values was not possible because no significant increase of tissue concentrations during the test occurred.

Animals collected during the bioconcentration studies with TiO₂ showed low tissue concentrations and gave evidence of at least limited bioavailability of the test item. Even in the test with the higher exposure concentration only a slight increase of the total tissue concentration in comparison to the control animals (0 h, all data below LOQ) could be observed. Due to limitations given by the production of the working suspension only a narrow range of possible medium concentrations could be tested. The lack of TiO₂ uptake during aqueous exposure to TiO₂NMs is in accordance with the results of TiO₂NM exposure tests using *H. azteca* carried out under flow-through conditions (Wallis et al., 2014).

An explanation for the low bioavailability could be that the particles are settling down and leaving the system too fast to be taken up by the amphipods. However, the lack of bioavailability of the TiO₂ particles may also be the result of their size. Agglomeration of TiO₂ particles was shown by TEM examinations. According to the sp-ICP-MS investigations, the TiO₂ particles in the working suspension and exposure medium had a calculated median particle size of 55.7 and 56.3 nm, respectively, and thus seemed not to be highly agglomerated. In contrast, particles measured in animals collected during the bioconcentration studies with NM 105 using sp-ICP-MS showed a calculated median particle size of > 100 nm providing clear indications for particle agglomeration. Even though the amount of TiO₂ particles attached to or ingested by the amphipods did not affect the measurable body burden at a significant level, the low amount was

sufficient to be detected by the very sensitive method of sp-ICP-MS. Particles measured by sp-ICP-MS were obviously attached to the carapace or ingested by *H. azteca* but presumably not incorporated into their tissues as indicated by the rapid and complete elimination of TiO₂ from the organisms during the depuration phase. Thus, it can only be speculated whether the agglomeration of the TiO₂ particles occurred in the animals gut after ingestion. Also the potential impact of the flow rate in the test system on the bioavailability of the TiO₂ particles requires further investigations.

4.4.5 Bioconcentration test with AuNMs

The AuNMs were tested in two bioconcentration tests using two different exposure concentrations to determine a potential concentration dependence of the bioconcentration process.

4.4.5.1 Test design and analytics of the bioconcentration tests with AuNMs

The tests with AuNMs were carried out as described for NM 300K (Chapter 4.4). The tests using two different exposure concentrations (high, AuNM_H; and low, AuNM_L) were carried out simultaneously allowing the usage of the same stock solutions for both tests and thus to minimize the differences in the applied test conditions. Analytics were carried out as described above (Chapter 4.3).

4.4.5.2 Results of the bioconcentration tests with AuNMs

The TWA concentrations of Au measured in the test media applied in the bioconcentration study with AuNM were 0.085 (AuNM_L) and 0.704 µg Au/L (AuNM_H) and thus 10 times lower than the target exposure concentrations. Media concentrations showed high variations in the course of the study (Table 11; Figure 40; Figure 42). A strong adsorption of Au was observed at the inner surface of the glass system and tubes. Median particle sizes for AuNMs present in the test medium were determined to be 56.9 ± 1.0 nm by sp-ICP-MS. The median size of the feed stock material was measured to be 56.2 ± 0.5 nm. According to the supplier the percentage of ionic Au in the initial stock solution should be appr. 0.01 % and being present as AuCl. Due to the high dilution rate of the stock solution in the test medium, and no expectable dissolution processes of the AuNMs under the applied test conditions, the amount of ionic Au in the test medium should have been insignificant.

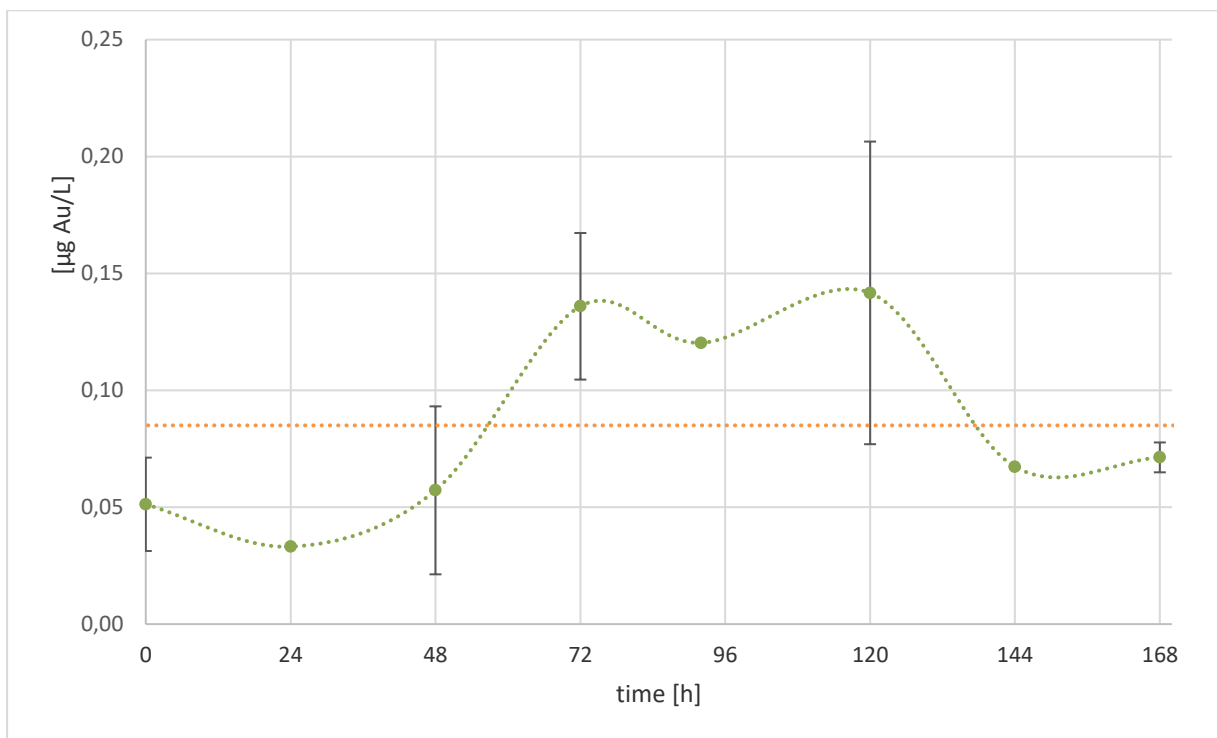
No real accumulation of Au was detected by the measurement of total Au concentrations in the animal samples (Figure 41; Figure 43). In both treatments the highest Au body burden was reached within 48 h of exposure. In the AuNM_L treatment the tissue concentration remained more or less stable until the end of the uptake phase (168 h). The average tissue concentration of 0.036 ± 0.006 mg Au/kg (48 h to 168 h) was used as steady state concentration resulting in a calculated BCF_{SS} of around 424 (Table 11) An average steady state tissue concentration of 0.117 ± 0.015 mg Au/kg was reached after 120 h for the AuNM_H treatment resulting in a calculated BCF_{SS} of around 166. During the depuration phase of the AuNM_H test lasting 168 h a rapid decrease of the total Au body burden was observed. After 48 h of depuration the total Au body burden reached the initial background concentration of the control animals measured at 0 h (Figure 43).

Particles extracted from animals sampled at the end of the uptake phase were measured to have a median particle size of 56.9 ± 0.7 nm.

Table 11: Specifications of the bioconcentration studies with AuNMs and calculated BCF values.

Study	Test item	Exposure Medium	TWA [µg Au/L]	BCF
AuNM _L	AuNM	dilution water	0.085	424
AuNM _H	AuNM	dilution water	0.704	166

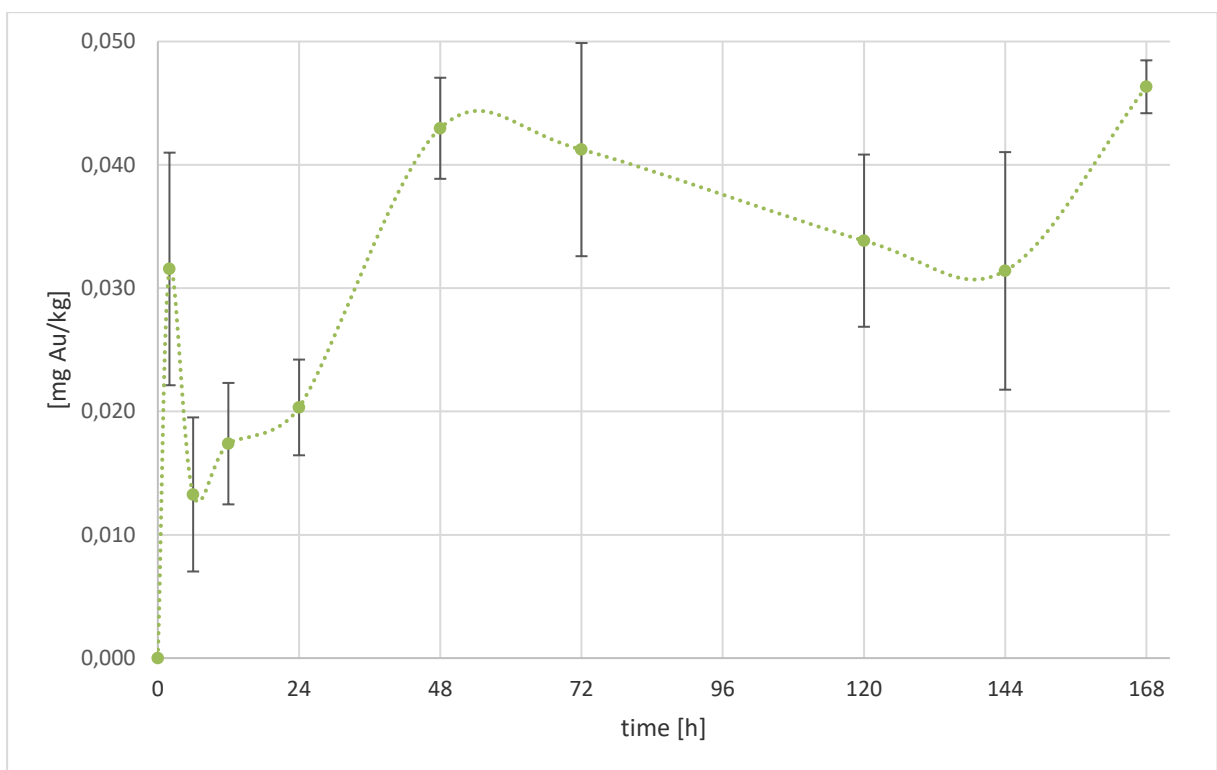
Figure 40: Total Au medium concentration in the bioconcentration test AuNM_L.*



*TWA of 0.085 µg Au/L.

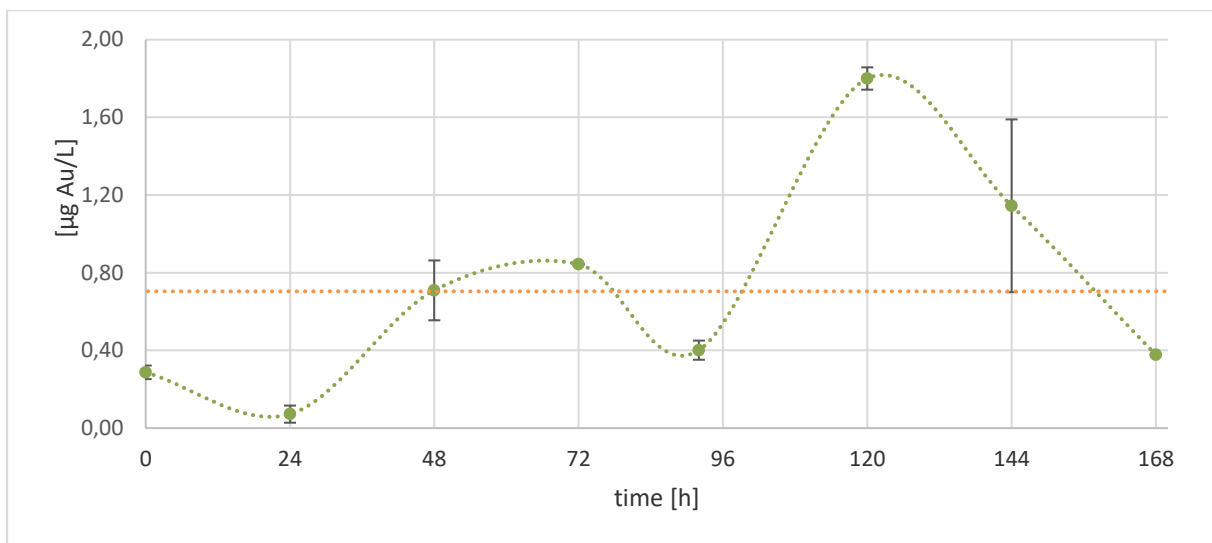
Source: Fraunhofer IME, own diagram.

Figure 41: Total Au tissue concentrations in the bioconcentration test AuNM_L.



Source: Fraunhofer IME, own diagram.

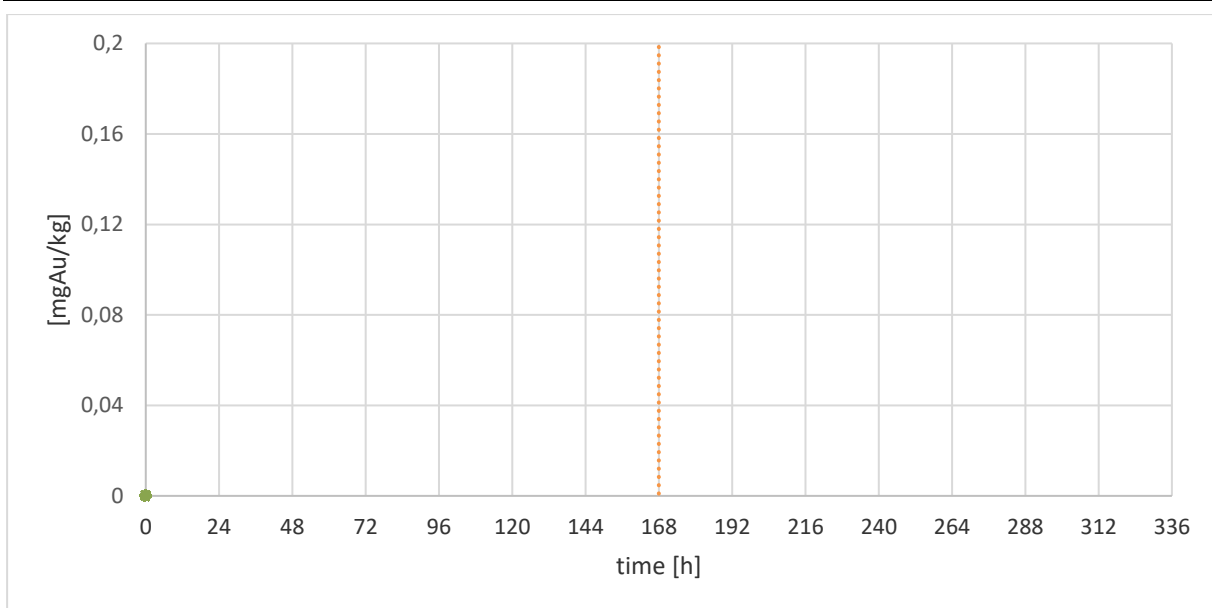
Figure 42: Total Au medium concentration in the bioconcentration test AuNM_H.*



*TWA of 0.704 µg Au/L.

Source: Fraunhofer IME, own diagram.

Figure 43: Total Au tissue concentrations in the bioconcentration test AuNM_H.



Source: Fraunhofer IME, own diagram.

4.4.5.3 Evaluation of the bioconcentration tests with AuNMs

Similar to the results obtained during the bioconcentration test with NM 105, AuNMs were obviously ingested by the amphipods, however no indications for an incorporation or transport within the animal tissue were provided. This may also explain the rapid elimination of AuNMs during the depuration phase. Therefore, calculated BCF values rather provide a rough indication for the “loading capacity” of the test animals exposed to AuNMs rather than the real bioconcentration potential of the NMs. The fast and effective elimination is comparable to that observed for the non-ion releasing NM 105 in the bioaccumulation tests using mussels from Kuehr et al. (2020c).

4.5 Biomagnification tests with NMs

4.5.1 Experimental feed for biomagnification tests and leaching test with NM 300K

4.5.1.1 Production

The method for the production of agar-agar cubes (DECOTABs) described by Kampfraath et al. (2012) was modified to produce nanomaterial enriched DECOTABs as experimental diet that allows the controlled exposure of NMs via the magnification pathway at stable concentrations with minimal risk of NPs or ions leaching that may lead to a secondary and uncontrolled uptake path.

For each nanomaterial own DECOTABs were produced. Therefore, 500 mg agar-agar were dissolved in 23 mL boiling UHQ under constant stirring using a magnet stirrer. 500 µL of the respective NM stock solutions (ca. 50 mg NPs/L) were added and heated and stirred for 1 min before 1,500 mg ground TetraMin® flakes were added under constant stirring. The suspension was stirred for 2 min and transferred into silicon ice trays to form cubes of 1 mL. The trays were stored at 4 °C until DECOTABs were completely hardened. 5 DECOTABs of each treatment were taken as 5 replicates for metal content analysis to check the homogeneity of the experimental food. Further samples were taken and frozen with liquid nitrogen and stored at -20 °C for the analysis with spICP-MS and TEM. The DECOTABs for feeding were stored at 4 °C during the time of the respective study.

4.5.1.2 Leaching test with NM 300K

4.5.1.2.1 Test design of the leaching test with NM 300K

A leaching test was conducted to determine the leaching of ions or NMs from the experimental diet enriched with NMs. The DECOTABs enriched with NM 300K were placed in 500 mL HDW in 600 mL glass beakers with 20 *H. azteca* for 7 days without water exchange. The test was carried out in 3 replicates for the treatment with enriched DECOTABs and 3 control groups with clean DECOTABs. Water samples were taken at the test start and on day 3 and 7, acidified and measured to determine the total Ag content as described in Chapter 4.3.

4.5.1.2.2 Results and Evaluation of the leaching test with NM 300K

The highest measured total Ag content in the water samples was 0.08 µg Ag/L, whereby the measured total Ag concentration in the water samples from the control triplicates was 0.04 µg Ag/L. The continuous flow of the HDW in the test system washes off potentially leached ions or NMs and thus helps to keep the concentrations of Ag in the test medium to a minimum. DECOTABs used as control feed were shown to be suitable for the feed borne exposure of NMs without causing the risk of NMs or ions from the diet leaching into the surrounding medium.

4.5.2 Biomagnification test with NM 300K

Two biomagnification tests with NM 300K (Figure 44) were carried out using two different Ag concentrations to determine potential concentration depending effects on the uptake, elimination or bioaccumulation of Ag from the AgNMs.

4.5.2.1 Test design and analytics of the biomagnification test with NM 300K

The biomagnification tests were carried out as described above (Chapter 4.2.2). Animals were exposed to NM 300K by the experimental diet during the 168 h (7 days) lasting uptake phase. Following application of the experimental diet enriched with the higher concentration of Ag a depuration phase of 192 h followed where the animals were fed with uncontaminated DECOTABs. Animal samples were taken for the determination of the total Ag body burden and for examination of ingested particles using sp-ICP-MS (Chapter 4.3.2). Water samples were taken to check the media for unintended exposure.

4.5.2.2 Results of the biomagnification test with NM 300K

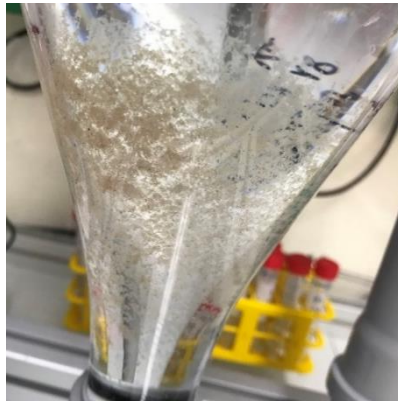
Total Ag concentrations of 0.07 ± 0.00 and 0.751 ± 0.01 mg Ag/ kg were measured in DECOTABs enriched with low (NM 300K_L) and high (NM 300K_H) concentration of NM 300K (Table 12). Non-enriched DECOTABs containing a total Ag concentration of 0.01 ± 0.00 mg Ag/kg were fed to the animals during the depuration phase.

Samples of the applied DECOTABs were digested using proteinase K (Chapter 4.3.2) to allow the examination of the embedded AgNMs using sp-ICP-MS. The median particle size of Ag particles present in the experimental diet was determined to be 14.1 ± 0.8 nm. The animals accepted the experimental diets as the control diet and thus a constant exposure of the test animals was ensured. Examinations on the experimental food using TEM and EDX (Chapter 4.1.1) proved the presence of AgNPs within the enriched food as shown in Figure 45.

In the NM 300K_L treatment of the biomagnification study an increasing total Ag body burden was observed in animals collected during the first 72 h of the uptake phase finally reaching a plateau which was stable until the end of the uptake phase (168 h) with an average tissue concentration of 0.07 ± 0.01 mg Ag/kg (Figure 46). A BMF_{SS} value of 0.25 was calculated. In the NM 300K_H treatment a stable body burden was also reached after 72 h of exposure (Figure 47) which remained stable until the end of the uptake phase (168 h). With an average tissue concentration of 0.18 ± 0.01 mg Ag/kg a BMF_{SS} value of 0.93 was calculated (Table 12). Particles extracted from animals collected at the end of the uptake phase were analyzed to have a median particle size of 17.1 ± 1.3 nm.

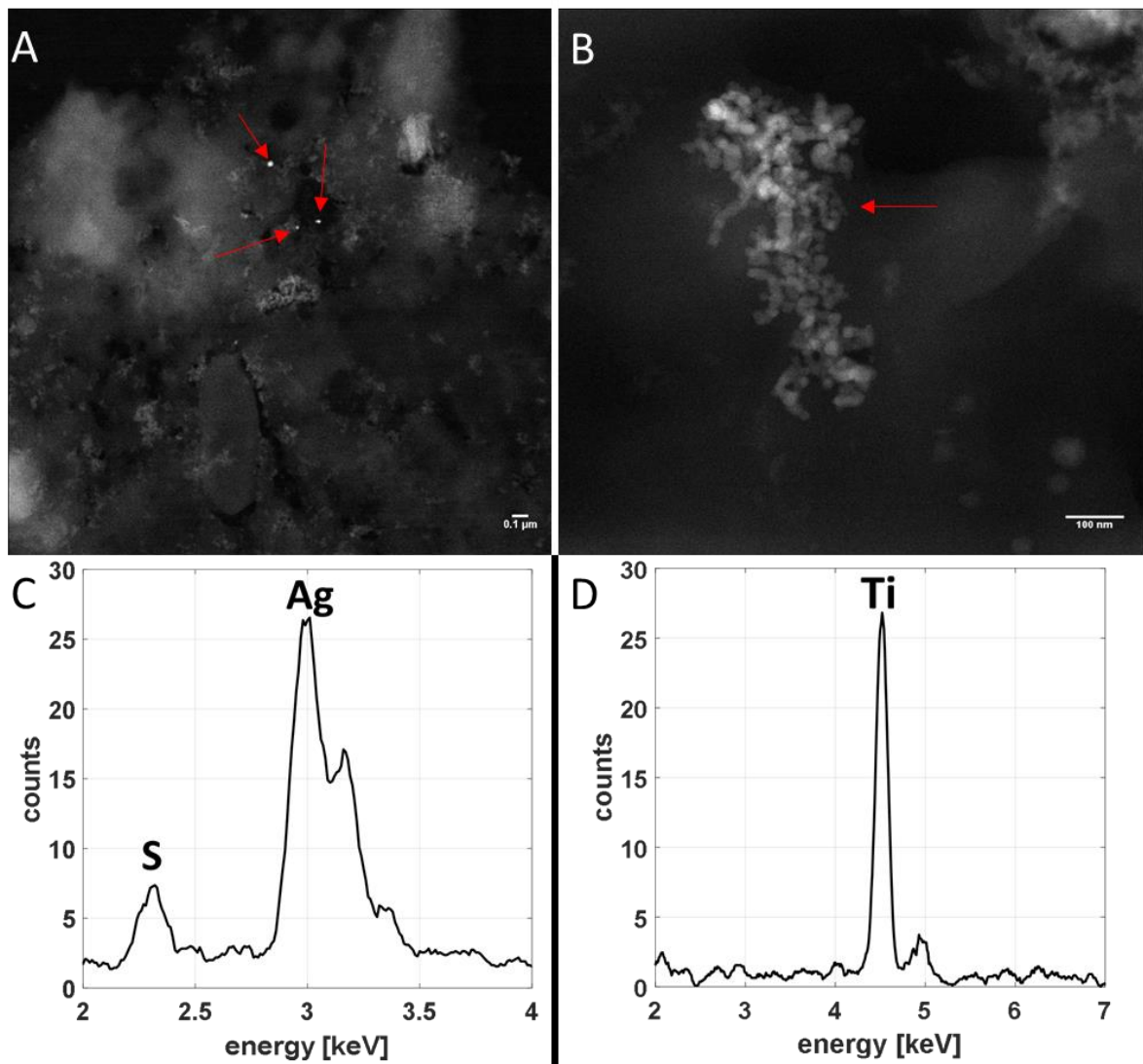
During the first 96 h of the depuration phase following the NM 300K_H treatment nearly no elimination of Ag was observed. Until the end of the depuration phase lasting 192 h, the tissue concentration reached a level of 0.14 mg Ag/kg representing 75 % of the previously determined steady state tissue concentration.

Figure 44: Feces at the ground of the Zuger glass test system 24 h after the start of the biomagnification test with NM 300K.



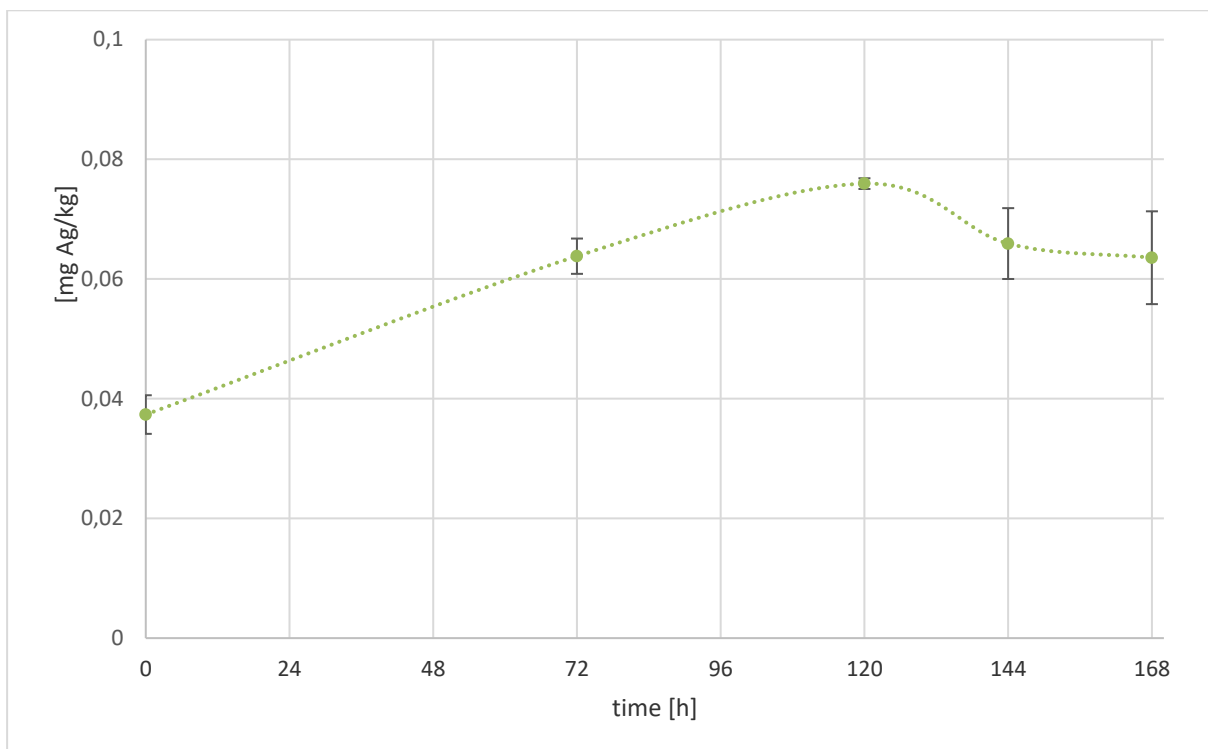
Source: Fraunhofer IME.

Figure 45: TEM HAADF images and the corresponding EDX signals of NPs enriched in the experimental feed.



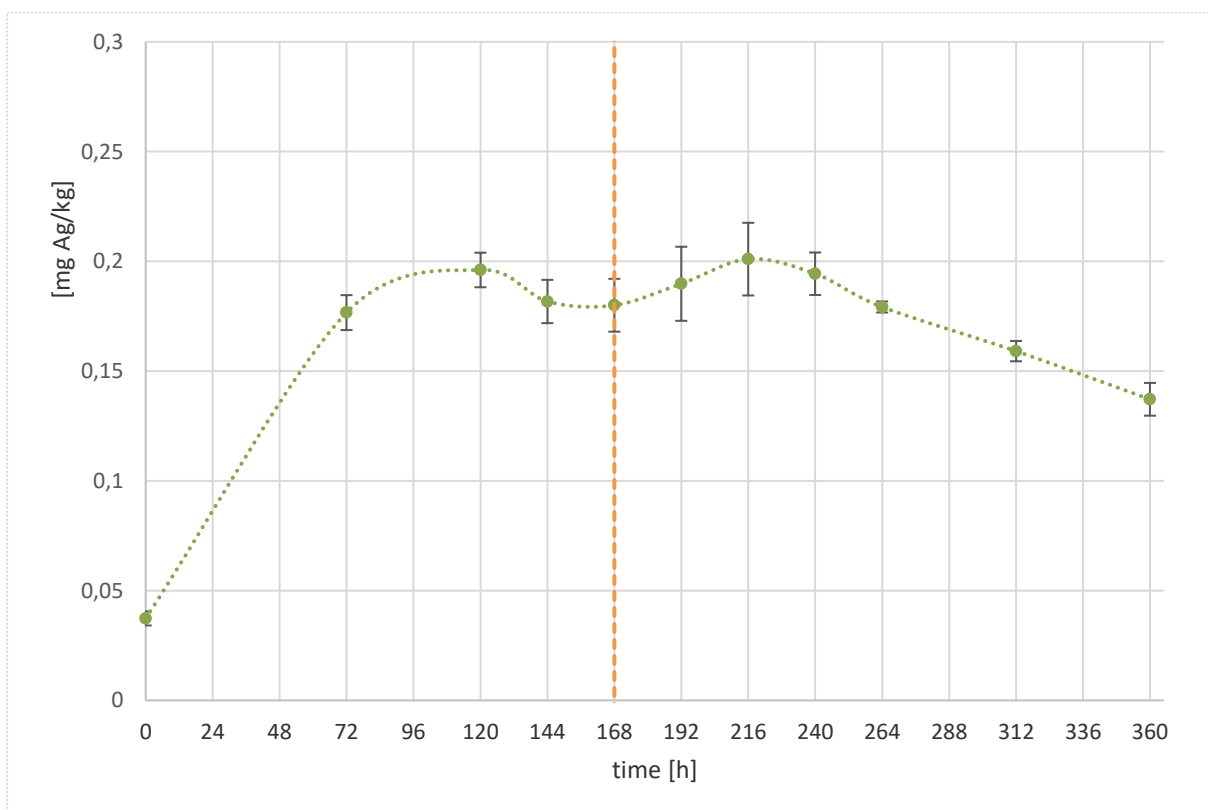
A: NM 300K, magnification 30 kx; B: NM 105, magnification 100 kx; C: NM 300K, EDX signals; D: NM 105, EDX signals.
Source: EAWAG, Switzerland in Kuehr et al. (2020a).

Figure 46: Total Ag tissue concentrations in NM 300K_L biomagnification test.*



*Feed concentration 0.072 mg Ag/kg. Source: Fraunhofer IME, own diagram.

Figure 47: Total Ag tissue concentrations in NM 300K_H biomagnification test.*



*Feed concentration 0.751 mg Ag/kg. Source: Fraunhofer IME, own diagram.

4.5.2.3 Evaluation of the biomagnification test with NM 300K

The investigation of the AgNMs supplemented to the experimental diet revealed that the NMs had a median particle size (14.1 ± 0.8 nm) that was slightly smaller than that of the feed stock material (around 15 nm). However, the observed difference in median size may be explained by the inaccuracy of the applied method. Particles extracted from the animal samples were around 3 nm bigger than the stock material which could be explained by the same mechanisms as discussed for the bigger AgNMs extracted from the animals of the NM 300K bioconcentration tests (Chapter 4.4.3).

DECOTABs supplemented with NM 300K as well as the feces released by the animals did not lead to a measurable Ag burden in the water of the test system. AgNMs embedded in the DECOTABs were detectable under TEM. The examination of the AgNMs using EDX showed that the particles were present in a sulfidized form as indicated by the ratio of the signals from Ag and S ($\sim 2:1$).

However, Ag from the presumably sulfidized AgNMs has been demonstrated to be still bioavailable as shown by the increasing total Ag body burden during the course of the uptake phase of the biomagnification test with NM 300K. This is in accordance with the observations made by (Kampe et al., 2018) where the terrestrial isopod *Porcellio scaber* was able to accumulate Ag from sulfidized AgNMs (NM 300K) present in sediment enriched with sewage treatment plant sludge. Kuehr et al. (2018) and Kuehr et al. (2020b) observed the accumulation of Ag in *H. azteca* which were exposed to wastewater and sewage sludge containing presumably sulfidized AgNMs (NM 300K).

Similar to the observations made during the bioconcentration tests with AgNM, a delayed and incomplete elimination of previously accumulated Ag from the animals during the depuration phase of the biomagnification test with NM 300K_H was observed. This may be explained by ions taken up during exposure associating with structural proteins in tissues and mucus or with functional proteins present in the haemolymph or cells. In a study to investigate the intestinal uptake of Ag⁺ in rainbow trout (Khan et al., 2017) observed that up to 92 % of the total Ag content measured in fish was bound to the intestine mucus layer, whereas only small amounts of Ag were found in the blood of the fish. Functional proteins like metallothioneins (MTs) are present in nearly all species and their expression is triggered by the presence of free Ag⁺ and several other metal ions. In this study the Ag⁺ ions were supposed to be released from the NM 300K particles in the gut after ingestion of the experimental diet. The Ag⁺ ions may have also been released during feed production. Bound to the feed matrix they were potentially released in the gut during the biomagnification tests. The presence and role of proteins like MTs as part of a detoxifying strategy has been described for several species including crustaceans, e.g. by Ahearn et al. (2004); Roesijadi (1992); Sterling et al. (2007). MTs that are present in intestinal cells are described to bind metals taken up from the lumen of the gastro intestinal tract by the epithelial transport mechanism (Roesijadi, 1992). In invertebrate groups like crustaceans, the digestive gland combines the functional role of liver and intestines of vertebrates and has abilities of intracellular digestion and phagocytosis (Gardiner, 1972). Thus, metals ingested with feed are expected to bind first in the cells of the digestive gland and may then be transferred to other organs (Engel and Brouwer, 1984). The binding to MTs may be seen as a barrier to prevent rapid transfer of metals to other organs and tissues due to the reduced and retarded transfer of metals across the intestinal epithelium (Roesijadi, 1992). MTs loaded with associated metals may accumulate in the lysosomes and thus represent a sink for (heavy-) metals like Ag, but may also be transported to the nucleus and intermembrane space of mitochondria (Ye et al., 2001). Mitochondria, endoplasmatic reticulum and lysosomes are sites of a second detoxifying strategy that may lead to the reduction of metals solved in the cytoplasm by sequestration of

metal concretions using sulfate, phosphate and carbonate (Al-Mohanna and Nott, 1985; Chavez-Crooker et al., 2003; Mandal et al., 2006, 2005; Sterling et al., 2007). The formation of concretions has been examined in a wide range of invertebrates and also plays a key role in the accumulation of metals (Sterling et al., 2007). These processes are very effective and the metals remain within the organism until necrosis or apoptosis of the cells or active excretion of the concretions as granules via the lumen of the digestive gland occur (Nott and Nicolaidou, 1990).

The feces released by the amphipods were removed from the test system with the water current preventing that the amphipods could get in contact with the highly contaminated feces, making the Zuger glass system more suitable for biomagnification testing than using an aquarium. Although only low BMF values were calculated, Ag seems to be bioavailable for *H. azteca*. Ag⁺ ions released from the AgNP may be potentially be trapped by protein binding leading to the slow and incomplete elimination of Ag from the animals during the depuration phase as also observed in the bioconcentration tests using NM 300K. This is in accordance with Kuehr et al. (2020b) who examined *H. azteca* showing a significant Ag body burden, after exposure to sewage sludge containing AgNMs. No evidence for an incorporation of AgNMs into the tissue was given by tissue examinations using the methods of correlative microscopy providing further indications for a primary role of Ag⁺ in the uptake and accumulation of Ag by *H. azteca* being exposed to AgNMs.

Table 12: Characteristics of the biomagnification studies with NM 300K and calculated BMF values.

Study	Test item	Concentration [mg/kg]	BMF
NM 300K _L	NM 300K / AgNM	0.07	0.25
NM 300K _H	NM 300K / AgNM	0.751	0.93

4.5.3 Biomagnification test with NM 105

4.5.3.1 Test design of the biomagnification test with NM105

The biomagnification tests with NM 105 were conducted as described for NM 300K. Due to the missing information regarding the time required to reach steady state tissue concentrations, the uptake phase was extended to 240 h (10 days), which was followed by a depuration phase of the same time period.

4.5.3.2 Results of the biomagnification test with NM 105

Total TiO₂ concentrations of 3.67 ± 0.05 (NM 105_L) and 19.43 ± 0.60 mg TiO₂/kg (NM 105_H) were measured in the two experimental diets (Table 13). A background concentration of total TiO₂ of 2.17 ± 0.34 mg TiO₂/kg was determined for the control DECOTABs that were applied during the depuration phase of the study with NM 105_H. As described above, NM 105 particles in the experimental diets were highly agglomerated as shown by TEM (Figure 45). Particles extracted from the experimental feed were examined by sp-ICP-MS and a median particle size of 55.9 ± 8.4 nm was determined (NM 105_H).

In the NM 105_L treatment a slight increase of the total TiO₂ concentration in the animal tissue was observed during the uptake phase lasting 240 h (Figure 48). The initial concentration of the animals (0 h) was 0.59 ± 0.07 mg TiO₂/kg. An average body burden of 1.03 ± 0.46 mg TiO₂/kg was observed at the end of the uptake phase (168 to 240 h) resulting in an BMF_{SS} value of 0.12 considering the observed increase of the total TiO₂ concentration in the animals of around 0.44 mgTiO₂/kg.

In the NM 105_H treatment a relatively stable body burden was reached after 72 h of the uptake phase (Figure 49). The total TiO₂ tissue concentration increased by 0.48 mg TiO₂/kg to an average concentration level of 1.07 ± 0.03 mg TiO₂/kg, resulting in a BMF_{SS} value of 0.02. (Table 13).

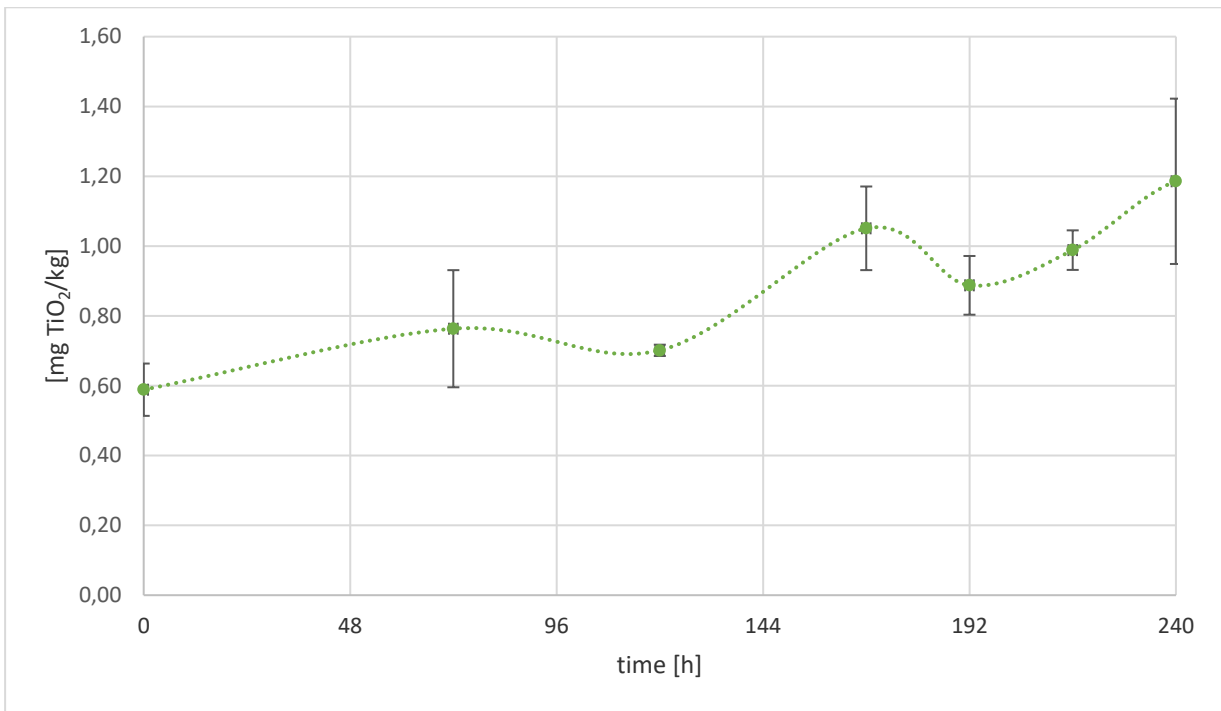
The median size of the particles in animals collected at the end of the uptake phase and determined by sp-ICP-MS was 62.2 ± 10.7 nm.

In the NM 105_H treatment, during the depuration phase (240 h) a nearly stable tissue concentration of 0.74 ± 0.06 mg TiO₂/kg was reached after 24 h of elimination and remained on this level until the end of the study (Figure 49).

Table 13: Characteristics of the biomagnification studies with NM 105 and calculated BMF values.

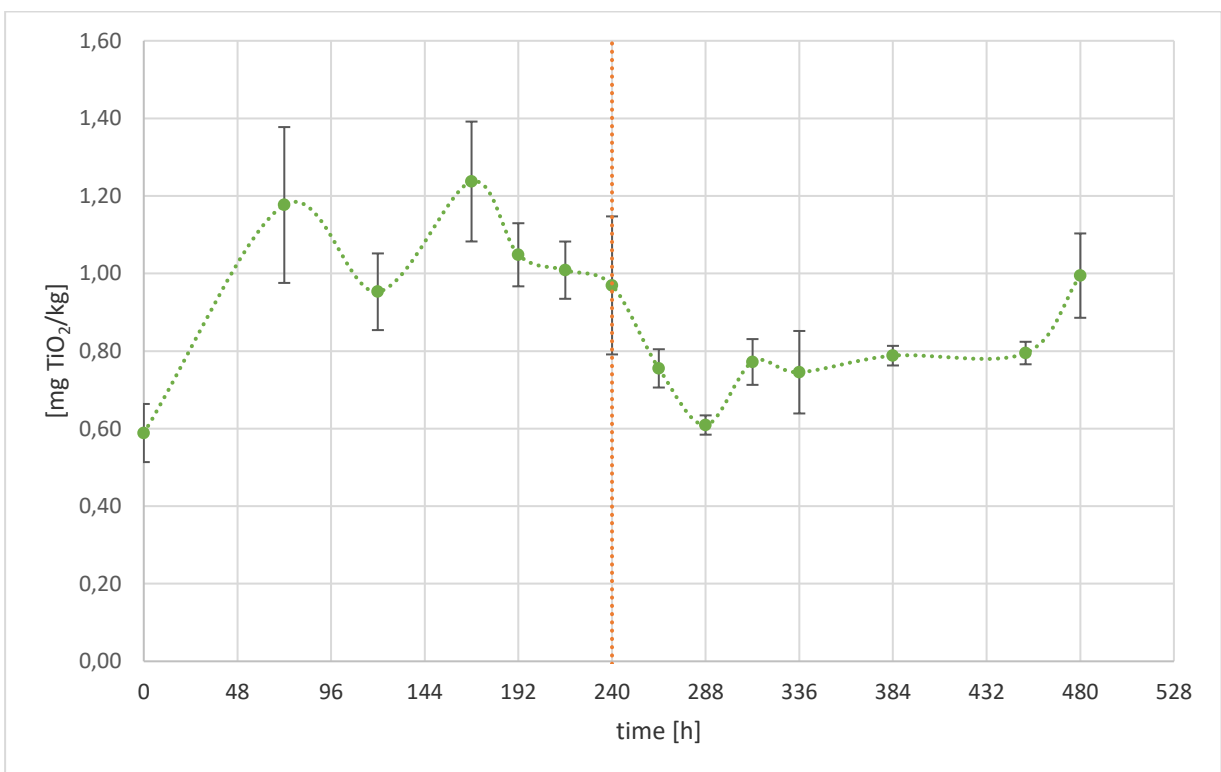
Study	Test item	Concentration [mg/kg]	BMF
NM 105 _L	NM 105 / TiO ₂ NM	3.67	0.12
NM 105 _H	NM 105 / TiO ₂ NM	19.43	0.02

Figure 48: Total TiO₂ tissue concentrations in NM 105_L biomagnification test.*



*Feed concentration 3.667 mg TiO₂/kg. Source: Fraunhofer IME, own diagram.

Figure 49: Total TiO₂ tissue concentrations in NM 105_H biomagnification test.*



*Feed concentration 19.43 mg TiO₂/kg. Source: Fraunhofer IME, own diagram.

4.5.3.3 Evaluation of the biomagnification test with NM 105

In the biomagnification tests with NM 105 a high initial background concentration of TiO₂ was measured in the control animals collected at 0 h which may be explained by the TiO₂ contamination of the diet used for the husbandry of the test animals and which was equivalent to the control diet (DECOTABs) used for the biomagnification study with NM 105 having a Ti / TiO₂ concentration of 2.167 mg TiO₂/kg. However, it needs to be borne in mind that ICP-MS measurements can only quantify the content of Ti but not TiO₂. Therefore, we cannot be sure that the measured concentrations of Ti in the diets and animals' tissues consisted of TiO₂ only.

The low increase of the body burden observed during the biomagnification tests with NM 105 indicates a limited bioavailability of the TiO₂NMs. Results from the experimental feed using TEM showed that the TiO₂ particles present in the experimental diet were highly agglomerated. However, it can only be speculated whether or not the size and form of the particles / agglomerates in the diet led to the limited uptake and accumulation of TiO₂ observed in the biomagnification test with NM 105. Following the uptake phase, a concentration which was slightly higher than the initial background concentration of Ti was reached quickly during the depuration phase. This was probably due to a fast elimination of the previously ingested but non-internalized TiO₂ particles/agglomerates. The slightly increased concentration in the animals' organism during the depuration phase may be the result of the Ti contaminated control feed (2.17 ± 0.34 mg TiO₂/kg).

4.5.4 Biomagnification test with AuNMs

4.5.4.1 Test design of the biomagnification test with AuNMs

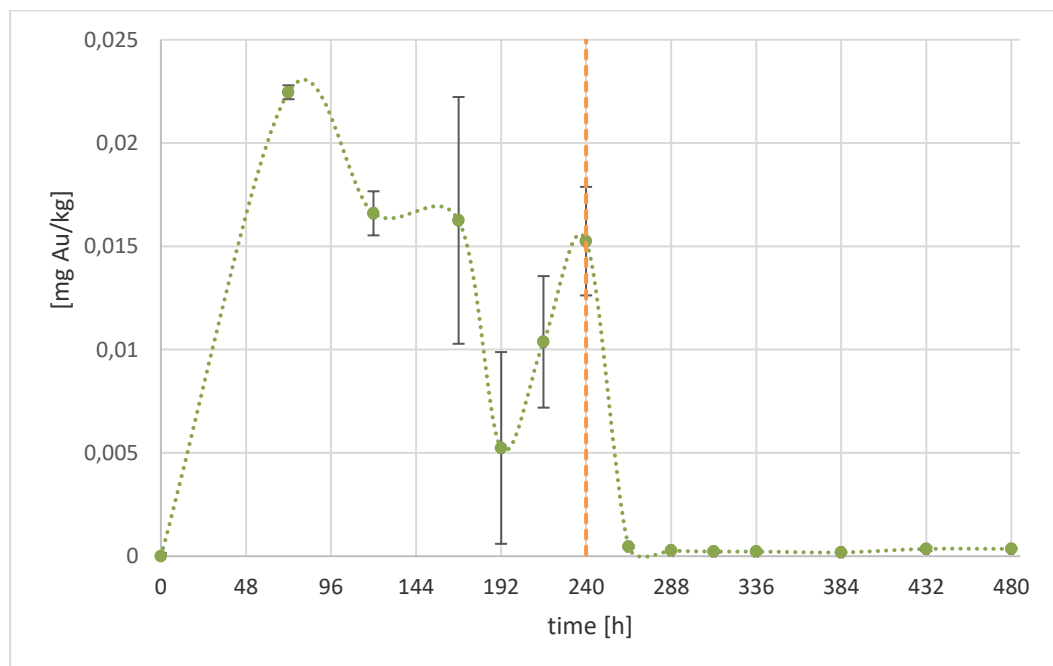
The biomagnification test with AuNMs and the analysis of the total Au concentrations were carried out as described for the other NMs. The uptake and depuration phase were lasting 240 h, each.

4.5.4.2 Results of the biomagnification test with AuNMs

The total Au concentrations in the experimental diet were determined to be 0.003 ng Au/kg in the control feed (DECOTABs fed during depuration phase), and 3.9 ± 0.004 ng Au/kg and 0.889 ± 0.096 mg Au/kg in the low (AuNM_L) and high treatment (AuNM_H), respectively (Table 14). AuNM concentrations in the two enriched experimental diets were too low to be detected by TEM. However, AuNMs could be extracted from the experimental diets as well as the animals collected at the end of the uptake phase and measured by sp-ICP-MS. Median particle sizes of 57.0 ± 1.4 nm and 51.2 ± 0.4 nm for feed and animals were determined, respectively.

Tissue concentrations of animals collected during the test from the AuNM_L treatment were all below the limit of quantification for Au (0.002 µg/L, in the digested samples). However, measurable Au tissue concentrations were measured in animals collected during the uptake phase of the AuNM_H treatment. The course of the measured Au body burden is presented in Figure 50. After washing the animals with dilution water and their transfer into a new test system for the depuration phase, the initial Au body burden was almost reached within 24 h (Figure 50). Because there was no clear steady state of the body burden, we used the highest Au body burden (around 0.0225 mg Au/kg) measured after 48 h of exposure and the tissue concentration present at the end of the uptake phase (0.0153 ± 0.003 mg Au/kg) to calculate magnification factor between 0.03 of 0.02 based on the Au concentration in the diet of 0.889 mg Au/kg.

Figure 50: Total Au tissue concentrations in AuNM_H biomagnification test.*



* Feed concentration 0.889 mg Ag/kg. Source: Fraunhofer IME, own diagram.

Table 14: Characteristics of the biomagnification studies with AuNM and calculated BMF values.

Study	Test item	Concentration [mg/kg]	BMF
AuNML	AuNM	< 0.00*	--
AuNMH	AuNM	0.889	0.02 - 0.03

* Au concentration in the AuNML treatment was 3.9 ng/kg.

4.5.4.3 Evaluation of the biomagnification test with AuNMs

The low Au concentration in the experimental feed of the AuNML treatment might be explained by the loss of particles during the diet preparation process due to adsorption of the AuNMs to the glass surface of the mixing beakers. In contrast, the Au concentration in the higher concentrated feed could be measured by ICP-MS. The presence of AuNMs was confirmed using sp-ICP-MS. However, the concentration in the feed was obviously too low to allow the detection of the AuNMs using TEM. Thus, further biomagnification tests should include a pretest for determination of the necessary concentration of NMs needed to be used for production of the experimental diet without generating too low NM burden in the diet.

The fast elimination of the Au concentrations measured in the animal samples indicates that the measured body burden probably primarily reflected the gut content of the animals containing the ingested particles and which were quickly eliminated by defecation.

4.6 Conclusions

The presented results show that *H. azteca* is suitable for testing the bioaccumulation of NMs. Further tests with a broader range of NPs representing further “character groups” (e.g. carbon-based NMs) are needed to be able to make clear statements on the suitability of the bioconcentration or biomagnification pathways for testing the bioaccumulation of NMs in *H. azteca*. Both test systems, Zuger glass and aquarium, are principally suitable to establish constant exposure conditions, with the Zuger glass system providing further benefits regarding media exchange and feces removal. The test system used should be generally tested prior to a bioaccumulation test to prove the establishment of constant exposure conditions and to carry out adjustments if required.

Generally, the *H. azteca* bioaccumulation test has two key benefits:

- ▶ In comparison to other bioaccumulation tests with invertebrate organisms such as bivalves (Kühr et al., 2020c), using *H. azteca* allows exposure via an aqueous test medium or a supplemented diet and thus allows to derive BCF or BMF values.
- ▶ The risk of artefacts due to active protection mechanisms as observed during the test using bivalves (reduction of the filtration rate and thus limited uptake of the test substance) as shown by Kuehr et al. (2020c) is not given.

5 Workpackage 3: Development of an OECD Guideline

5.1 Critical evaluation of the HYBIT protocol for testing highly hydrophobic and ionic substances and nanomaterials

The HYBIT allows the use of different test media, e.g. tap water or Borgmann medium (Borgmann, 1996) and provides the choice between male or female test organisms. The use of solvents and dispersants (solubilizing agents) is not generally recommended. However, the use of these materials may be acceptable in *Hyalella* bioconcentration studies, as in fish flow-through studies, in order to produce suitably concentrated stock solutions. In agreement with the flow-through fish test, steady state or kinetic BCF values depending on the experimental design can be derived. In contrast to the fish flow-through test according to OECD 305, the HYBIT also describes an alternative test concept following a semi-static exposure scenario.

5.1.1 UV-compounds

UV compounds are difficult to apply due to their very low solubility in water. In this study we tested the suitability of the *Hyalella* test system to elucidate the bioaccumulation potential of UVs. Two phenolic benzotriazoles (UV 234 and UV 329) which are highly hydrophobic ($\log K_{ow} > 6$) were tested following the HYBIT flow-through protocol. As expected only very low exposure concentrations ($\leq 1 \mu\text{g/L}$) could be established. Nevertheless, the measurement of substance concentrations in the test media and *H. azteca* samples collected during the uptake and depuration phase was still possible and allowed the determination of BCF_{ss} and BCF_k values for both compounds. The results reveal the high bioaccumulation potential of the two test compounds. The BCF studies showed that the new test system using a non-vertebrate organism is also suitable for the testing of phenolic benzotriazoles which are difficult to test in fish flow-through tests due to their high hydrophobicity. The use of solvents may be acceptable in *Hyalella* bioconcentration studies, as in fish flow-through studies, in order to produce suitably concentrated stock solutions. However, the use of solvents and dispersants (solubilizing agents) is not generally recommended due to the enhanced microbial growth as observed in this study. Alternatively, a solid phase desorption dosing system can be applied allowing to derive column generated concentrations without using solubilizing agents.

5.1.2 Ionizable organic compounds

So far, mostly lipid accumulating substances have been tested with *H. azteca*. A further objective of this study was to evaluate the suitability of HYBIT to estimate the bioconcentration potential of ionizable organic compounds by the example of perfluorooctane sulfonate (PFOS) and GenX. The HYBIT provides a certain degree of flexibility with regard to the experimental procedure. Therefore, several *Hyalella* BCF tests were carried out under different experimental conditions to elucidate potential effects on the result obtained. Generally, the suitability of HYBIT for testing ionizable organic compounds was demonstrated, however, the test conditions may affect the bioconcentration of PFOS as shown for the use of different test media, or the performance of bioconcentration experiments with male or female test animals.

In all experiments constant exposure conditions were established. Due to the low dissociation constant ($\text{pK}_a < 1.0$) of the test substance, it can be expected that PFOS was present in the test media (pH 6.9 - 8.5) exclusively in its ionized form for which, depending on the experimental design, kinetic and/or steady state BCF values could be calculated. However, as long as the bioaccumulation mechanisms of ionizable organic compounds such as PFOS are mostly unknown, the simple prediction of B or non-B classification in the standard fish test based on

Hyalella BCF values as suggested for hydrophobic substances is not possible. However, the HYBIT can still help to further elucidate the bioaccumulation potential of emerging compounds in aquatic organisms and provide BCF values for regulatory purposes.

Cu-reduced tap water (HDW) was compared with culture medium, a common medium for *Hyalella* culture. Both media were shown to be appropriate for bioconcentration testing since no adverse effects on animal performance or exposure conditions were observed. However, the use of different test media may lead to differences in bioconcentration as shown in this study testing PFOS in *H. azteca*. Anionic surfactants such as PFOS may form precipitates with the calcium and magnesium ions contained in hard water (Shinoda and Hirai, 1977; Wen et al., 2016). The formation of precipitates in HDW may potentially influenced the uptake of PFOS leading to the reduced bioconcentration observed for HDW compared to culture medium. For standardization of bioaccumulation tests through time and across laboratories, the use of standardized artificial media such as BM is thus recommended. This applies in particular to metals and ionizable organic compounds. However, testing the bioconcentration of hydrophobic compounds in both media may well lead to comparable results as shown during the international multi-laboratory ring trial.

Steady state bioconcentration factors (BCF_{ss}) and kinetic bioconcentration factors (BCF_K) for PFOS and GenX were derived from this study leading to constantly higher kinetic than steady state bioconcentration factors. This may simply point to the fact that the uptake phase was not sufficient to reach steady state conditions. However, the use of the kinetic approach for PFASs bioaccumulation was critically discussed by Liu et al., 2011. They criticize the fact that the previous assumption of “first order uptake reaction” is inappropriate in the case of PFASs bioaccumulation which appears to follow an adsorption rather than a partitioning model. In this context, the kinetic BCF values derived from this study obtained by calculating the ratio of the uptake rate constant k_1 to the depuration rate constant k_2 should thus be treated with caution.

Over the last 50 years a steady increase of the commercial use of PFAS occurred and there are currently more than 3,000 PFASs on the global market (Wang et al., 2017). With the replacement of long-chain PFASs by a wide range of fluorinated alternatives (e.g. GenX), as observed during the last years (Scheringer et al., 2014), there is a need to make sure that the new compounds are less persistent, bioaccumulative and toxic than PFOS, PFOA and related compounds. However, for most emerging PFASs little is known of their bioaccumulation potential (Shi et al., 2020) even if there are indications that short-chain PFAS are less hydrophobic and more mobile in aquatic systems compared to the long-chain perfluorinated surfactants (Ahrens and Bundschuh, 2014). A methodology for large-scale screening of PFASs has not yet been developed, though some initial work indicates that in-silico docking methods may hold promise (Ng and Hungerbuehler, 2015). Predicted interactions between PFAS and proteins could be used as a proxy for bioaccumulation potential.

As an alternative in vivo method for bioaccumulation testing, the *Hyalella* BCF may help to further elucidate the bioaccumulation process of PFASs in aquatic organisms and can provide BCF values for regulatory purposes. All *Hyalella* BCF_{ss} values for PFOS (and GenX) derived from this study were < 500 and thus clearly below the regulatory B criterion ($BCF > 2,000$, i.e., REACH) in accordance with the corresponding fish BCF values described in the literature for rainbow trout ($BCF = 1,100$) and common carp ($BCF = 720 - 1,300$) (Martin et al., 2003; Inoue et al., 2012). However, as long as the bioaccumulation mechanisms and exposure routes of PFAS are unknown, the transfer of *Hyalella* bioconcentration test results to other species should be avoided. The simple prediction of B or non-B classification of ionizable organic compounds in the standard fish test based on *Hyalella* BCF values as suggested for hydrophobic substances (Schlechtriem et al., 2019) is currently not possible.

5.1.3 Nanomaterials

For all bioaccumulation tests a previous characterization of the test item is necessary and the results should be considered in the study design. The generally special properties of NMs in comparison to (soluble) organic components require different application procedures to enable continuous and homogeneous exposure scenarios. In this context, the tendency of NMs to sediment in the test basin must be avoided as shown by Zeumer et al. (2020a, 2020b). The described Zuger glass system may help to avoid the accumulation of sedimenting NMs in the test system and thus allow to generate stable exposure conditions which may be difficult to achieve in the commonly used aquarium set-up.

Total metal concentrations in exposed animals could be measured allowing the calculation of the established endpoints BCF and BMF. However, tissue concentrations should not be used without considering the specific uptake and elimination mechanisms involved in the potential accumulation of metal/metal oxide NMs which are known to be different to those of soluble test items. Completely different physical processes are involved in the uptake of NMs as well as in the possible formation of potential steady state conditions (Derjaguin et al., 1987; Handy et al., 2018, 2008; Petersen et al., 2019).

Regarding the specific uptake mechanisms of NMs and potential artefacts caused by the simple attachment of the particles to the animals' surface the assessment of the bioaccumulation potential should not be based on the concentration ratios between organism and exposure medium. The review by Kuehr et al. (2021) describes a proposal for alternative endpoints which consider the residue in the organism following depuration and the time required to reach the initial natural exposure level after the end of exposure. Guidance for the weighting and use of data from nanomaterial bioaccumulation studies and an assessment scheme are provided.

5.2 Development of an OECD test guideline

The ultimate decisive bioaccumulation criterion as part of the regulatory chemical safety assessment of pesticides, biocides, pharmaceuticals, and other chemicals is the bioconcentration factor (BCF). HYBIT is a non-vertebrate alternative for bioaccumulation studies and will thus provide the opportunity to reduce the use of fish for BCF testing in accordance to the "3R"-principles. Following validation of the HYBIT test protocol a part of an international ring test (Schlechtriem et al., in prep.), the development of a new test guideline is planned.

The new test guideline will be developed largely following the test design described in OECD TG 305-I (OECD, 2012). As in the fish test, aqueous bioconcentration studies with *H. azteca* are conducted to assess the bioaccumulation potential of chemicals measured by the chemical's bioconcentration factor (BCF).

H. azteca are exposed to the chemical dissolved in water. Hyalella and water samples are collected and analyzed at certain intervals during the course of the test to ultimately determine uptake and depuration rate constants and to calculate bioconcentration factors. The BCF is calculated as the ratio of the concentration in the amphipod to the dissolved concentration in water at steady state bioconcentration factors (BCF_{ss}), or by the ratio of the uptake and depuration rate constants (BCF_k). A broad range of compounds of different hydrophobicity ($\log K_{ow}$ 0.7 - 7.8) was tested. However, further studies are required to elucidate the bioaccumulation of non-lipid accumulating compounds in *H. azteca* as shown in this study.

In contrast to juvenile fish, Hyalella has a comparatively low sample size and the pooling of test animals (~20 animals/sample) is required to obtain sufficient biomass to allow chemical analysis. Considering all sample replicates and the series of sampling times required to estimate

the kinetics of substance uptake and elimination, large test populations of up to 1,500 organisms may result (Schlechtriem et al., 2019).

Populations of adult amphipods consist of male and female animals. However, mixed test groups should be avoided to prevent the reproduction of the animals during the study which would cause elimination of the previously accumulated test item by the release of juvenile amphipods. Sexing of adult amphipods is simple and can be carried out based on a few characteristics such as female eggs and male claws (Schlechtriem et al., 2019).

The lipid content in *H. azteca* may vary depending on the size and age of the amphipods and tends to be lower compared to the lipid levels measured in fish used for bioaccumulation testing. Therefore, lipid normalization of the estimated BCF values is required to allow the comparison with BCF estimates derived from fish studies. Lipid normalization to a lipid level of 5 % can be carried out as recommended by OECD 305 (Schlechtriem et al., 2019). However, only the use of suitable extraction techniques guarantees the complete extraction of total lipids from collected test organisms which is required to ensure a correct lipid normalization of BCF values. A standard protocol for lipid measurements of small size samples will be part of the new OECD Test Guideline.

Biotransformation processes can be a key factor affecting bioaccumulation. General biotransformation pathways in freshwater crustaceans have been described (Kosfeld et al., 2020; Fu et al., 2019). However, additional investigations are required to further elucidate the metabolism of xenobiotic compounds in *H. azteca*, to identify species specific metabolites and to assess the impact of biotransformation processes on the outcome of bioconcentration studies (Schlechtriem et al., 2019).

The results of the tests carried out as part of this study show that the basic principles of the HYBIT also allow the assessment of the bioaccumulation potential of NMs, however, specific adjustments of the test system may be required in order to take into account the special physico-chemical properties of the test compounds. The different application approaches and pretreatments (such as the Zuger glass system allowing to avoid the sedimentation of NMs or the equilibration approach used here for TiO₂ NMs) required to enable continuous and homogeneous exposure of the test items should be described in an independent guidance document for testing nanomaterials supporting the new technical guideline. The guidance document should also include information on how to perform dietary exposure studies to elucidate the biomagnification of NMs which cannot be applied by aqueous exposure, for instance due to agglomeration of the particles. However, due to the lack of regulatory threshold values for BMF estimates and the missing acceptance of the fish biomagnification approach, an alternative non-vertebrate method for dietary testing needs to be critically discussed.

In conclusion, the *Hyalella* bioconcentration test provides several advantages with respect to the testing of difficult to test compounds, due to the shorter exposure periods required, and the smaller experimental units used in comparison to the flow-through fish test. As a non-vertebrate test, the *Hyalella* bioconcentration (biomagnification) test may help to further reduce the amount of fish required for the regulatory testing of chemicals.

6 References

- Ahearn, G.A., Mandal, P.K., Mandal, A., 2004. Mechanisms of heavy-metal sequestration and detoxification in crustaceans: a review. *J. Comp. Physiol. B* 174, 439–452. <https://doi.org/10.1007/s00360-004-0438-0>
- Ahrens, L., Bundschuh, M., 2014. Fate and effects of poly- and perfluoroalkyl substances in the aquatic environment: A review. *Environ. Toxicol. Chem.* 33 (9), 1921–1929. <https://doi.org/10.1002/etc.2663>
- Al-Mohanna, S.Y., Nott, J.A., 1985. The accumulation of metals in the hepatopancreas of the shrimp *Penaeus semisulcatus* de Haan (Crustacea: Decapoda) during the moult cycle. *Mar. Environ. Pollut.* 195–209.
- Alves, L.C., Borgmann, U., Dixon, D.G., 2009. Kinetics of uranium uptake in soft water and the effect of body size, bioaccumulation and toxicity to *Hyalella azteca*. *Environ. Pollut.* 157, 2239–2247. <https://doi.org/10.1016/j.envpol.2009.04.006>
- American Society for Testing and Materials, 2003. ASTM E1022 - 94(2013) Standard Guide for Conducting Bioconcentration Tests with Fishes and Saltwater Bivalve Mollusks.
- Aschberger, K., Micheletti, C., Sokull-Klüttgen, B., Christensen, F.M., 2011. Analysis of currently available data for characterising the risk of engineered nanomaterials to the environment and human health — Lessons learned from four case studies. *Environ. Int.* 37, 1143–1156. <https://doi.org/10.1016/J.ENVINT.2011.02.005>
- Baccaro, M., Undas, A.K., de Vriendt, J., van den Berg, J.H.J., Peters, R.J.B., van den Brink, N.W., 2018. Ageing, dissolution and biogenic formation of nanoparticles: how do these factors affect the uptake kinetics of silver nanoparticles in earthworms? *Environ. Sci. Nano* 5, 1107–1116. <https://doi.org/10.1039/C7EN01212H>
- Bachelot, M., Li, Z., Munaron, D., Le Gall, P., Casellas, C., Fenet, H., Gomez, E., 2012. Organic UV filter concentrations in marine mussels from French coastal regions. *Sci. Total Environ.* 420, 273–279. <https://doi.org/10.1016/J.SCITOTENV.2011.12.051>
- Balbi, T., Smerilli, A., Fabbri, R., Ciacci, C., Montagna, M., Grasselli, E., Brunelli, A., Pojana, G., Marcomini, A., Gallo, G., Canesi, L., 2014. Co-exposure to n-TiO₂ and Cd²⁺ results in interactive effects on biomarker responses but not in increased toxicity in the marine bivalve *M. galloprovincialis*. *Sci. Total Environ.* 493, 355–364. <https://doi.org/10.1016/J.SCITOTENV.2014.05.146>
- Ball, A.L., Borgmann, U., Dixon, D.G., 2006. Toxicity of a cadmium-contaminated diet to *Hyalella azteca*. *Environ. Toxicol. Chem.* 25, 2526–2532. <https://doi.org/10.1897/05-650R.1>
- Berthiaume, J., Wallace, K.B., 2002. Perfluorooctanoate, perfluorooctanesulfonate, and N-ethyl perfluorooctanesulfonamido ethanol; peroxisome proliferation and mitochondrial biogenesis. *Toxicol. Lett.* 129, 23–32.
- Blaser, S.A., Scheringer, M., MacLeod, M., Hungerbühler, K., 2008. Estimation of cumulative aquatic exposure and risk due to silver: Contribution of nano-functionalized plastics and textiles. *Sci. Total Environ.* 390, 396–409. <https://doi.org/http://dx.doi.org/10.1016/j.scitotenv.2007.10.010>
- Bone, A.J., Colman, B.P., Gondikas, A.P., Newton, K.M., Harrold, K.H., Cory, R.M., Unrine, J.M., Klaine, S.J., Matson, C.W., Di Giulio, R.T., 2012. Biotic and abiotic interactions in aquatic microcosms determine fate and toxicity of Ag nanoparticles: Part 2–Toxicity and Ag speciation. *Environ. Sci. Technol.* 46, 6925–6933. <https://doi.org/10.1021/es204683m>
- Borgmann, U., 2002. Toxicity test methods and observations using the freshwater amphipod, *Hyalella*. Environment Canada.
- Borgmann, U., 1996. Systematic analysis of aqueous ion requirements of *Hyalella azteca*: A standard artificial medium including the essential bromide ion. *Arch. Environ. Contam. Toxicol.* 30, 356–363. <https://doi.org/10.1007/BF00212294>
- Borgmann, U., Norwood, W.P., Dixon, D.G., 2004. Re-evaluation of metal bioaccumulation and chronic toxicity in *Hyalella azteca* using saturation curves and the biotic ligand model. *Environ. Pollut.* 131, 469–484. <https://doi.org/10.1016/J.ENVPOL.2004.02.010>

- Bossi, R., Riget, F.F., Dietz, R., Sonne, C., Fauser, P., Dam, M., Vorkamp, K., 2005. Preliminary screening of perfluorooctane sulfonate (PFOS) and other fluorochemicals in fish, birds and marine mammals from Greenland and the Faroe Islands. *Environ. Pollut.* 136, 323–329. <https://doi.org/10.1016/J.ENVPOL.2004.12.020>
- Bousfield, E.L., 1958. Freshwater amphipod crustaceans of glaciated North America. *Can. Fld Nat.* 72, 55–113.
- Bragg, P.D., Rainnie, D.J., 1974. The effect of silver ions on the respiratory chain of *Escherichia coli*. *Can. J. Microbiol.* 20, 883–889. <https://doi.org/10.1139/m74-135>
- Carpinteiro, I., Abuín, B., Ramil, M., Rodríguez, I., Cela, R., 2012. Matrix solid-phase dispersion followed by gas chromatography tandem mass spectrometry for the determination of benzotriazole UV absorbers in sediments. *Anal. Bioanal. Chem.* 402, 519–527. <https://doi.org/10.1007/s00216-011-5386-4>
- Casado, J., Rodríguez, I., Carpinteiro, I., Ramil, M., Cela, R., 2013. Gas chromatography quadrupole time-of-flight mass spectrometry determination of benzotriazole ultraviolet stabilizers in sludge samples. *J. Chromatogr. A* 1293, 126–132. <https://doi.org/10.1016/J.CHROMA.2013.03.050>
- Chavez-Crooker, P., Garrido, N., Pozo, P., Ahearn, G.A., 2003. Copper transport by lobster (*Homarus americanus*) hepatopancreatic lysosomes. *Comp. Biochem. Physiol. Part C Toxicol. Pharmacol.* 135, 107–118. [https://doi.org/10.1016/S1532-0456\(03\)00103-0](https://doi.org/10.1016/S1532-0456(03)00103-0)
- Dai, Z., Xia, X., Guo, J., Jiang, X., 2013. Bioaccumulation and uptake routes of perfluoroalkyl acids in *Daphnia magna*. *Chemosphere* 90, 1589–1596. <https://doi.org/10.1016/J.CHEMOSPHERE.2012.08.026>
- de March, B.G.E., 1978. The effects of constant and variable temperatures on the size, growth, and reproduction of the freshwater amphipod *Hyalella azteca* (Saussure). *Can. J. Zool.* 56, 1801–1806. <https://doi.org/10.1139/z78-246>
- de Vos, M.G., Huijbregts, M.A.J., van den Heuvel-Greve, M.J., Vethaak, A.D., Van de Vijver, K.I., Leonards, P.E.G., Van Leeuwen, S.P.J., De Voogt, P., Hendriks, A.J., 2008. Accumulation of perfluorooctane sulfonate (PFOS) in the food chain of the Western Scheldt estuary: Comparing field measurements with kinetic modeling. *Chemosphere* 70, 1766–1773.
- de Wolf, W., Comber, M., Douben, P., Gimeno, S., Holt, M., Léonard, M., Lillicrap, A., Sijm, D., van Egmond, R., Weisbrod, A., Whale, G., 2007. Animal use replacement, reduction, and refinement: development of an integrated testing strategy for bioconcentration of chemicals in fish. *Integr. Environ. Assess. Manag.* 3, 3–17. [https://doi.org/10.1897/1551-3793\(2007\)3\[3:AURRAR\]2.0.CO;2](https://doi.org/10.1897/1551-3793(2007)3[3:AURRAR]2.0.CO;2)
- DeForest, D.K., Brix, K.V., Adams, W.J., 2007. Assessing metal bioaccumulation in aquatic environments: The inverse relationship between bioaccumulation factors, trophic transfer factors and exposure concentration. *Aquat. Toxicol.* 84, 236–246. <https://doi.org/10.1016/j.aquatox.2007.02.022>
- Derjaguin, B.V., Churaev, N.V., Muller, V.M., 1987. The Derjaguin—Landau—Verwey—Overbeek (DLVO) theory of stability of lyophobic colloids, in: *Surface Forces*. Springer, pp. 293–310.
- Dreaden, E.C., Alkilany, A.M., Huang, X., Murphy, C.J., El-Sayed, M.A., 2012. The golden age: gold nanoparticles for biomedicine. *Chem. Soc. Rev.* 41, 2740–2779. <https://doi.org/10.1039/C1CS15237H>
- ECHA, 2021. Registered substances. <https://echa.europa.eu/de/information-on-chemicals/registered-substances>. Last updated 09 März 2021.
- ECHA, 2017. Guidance on Information Requirements and Chemical Safety Assessment, Part C: PBT/vPvB assessment, Version 3.0, June 2017. https://echa.europa.eu/documents/10162/13643/information_requirements_part_c_en.pdf/e56a6015-807e-46eb-b808-e5a7dc9fd572
- Engel, D.W., Brouwer, M., 1984. Cadmium-binding proteins in the blue crab, *Callinectes sapidus*: laboratory-field comparison. *Mar. Environ. Res.* 14, 139–151. [https://doi.org/10.1016/0141-1136\(84\)90075-8](https://doi.org/10.1016/0141-1136(84)90075-8)
- Environment Canada, 2013. Biological test method: test for survival and growth in sediment and water using the freshwater amphipod *Hyalella azteca*. *Environ. Prot. Ser.*, 1/RM/33.

- European Parliament Council, 2006. Regulation (EC) No 1907/2006 of the European Parliament and of the Council of 18 December 2006 concerning the Registration, Evaluation, Authorisation and Restriction of Chemicals (REACH), establishing a European Chemicals Agency, amending Directive 1999/4. Off. J Eu.
- Fabrega, J., Luoma, S.N., Tyler, C.R., Galloway, T.S., Lead, J.R., 2011. Silver nanoparticles: Behaviour and effects in the aquatic environment. *Environ. Int.* 37, 517–531. <https://doi.org/http://dx.doi.org/10.1016/j.envint.2010.10.012>
- Fan, W., Liu, L., Peng, R., Wang, W.X., 2016. High bioconcentration of titanium dioxide nanoparticles in *Daphnia magna* determined by kinetic approach. *Sci. Total Environ.* 569–570, 1224–1231. <https://doi.org/10.1016/j.scitotenv.2016.06.197>
- Farkas, J., Bergum, S., Nilsen, E.W., Olsen, A.J., Salaberria, I., Ciesielski, T.M., Bączek, T., Konieczna, L., Salvenmoser, W., Jenssen, B.M., 2015. The impact of TiO₂ nanoparticles on uptake and toxicity of benzo(a)pyrene in the blue mussel (*Mytilus edulis*). *Sci. Total Environ.* 511, 469–476. <https://doi.org/10.1016/J.SCITOTENV.2014.12.084>
- Feng, Q.L., Wu, J., Chen, G.Q., Cui, F.Z., Kim, T.N., Kim, J.O., 2000. A mechanistic study of the antibacterial effect of silver ions on *Escherichia coli* and *Staphylococcus aureus*. *J. Biomed. Mater. Res.* 52, 662–668. [https://doi.org/10.1002/1097-4636\(20001215\)52:4<662::AID-JBM10>3.0.CO;2-3](https://doi.org/10.1002/1097-4636(20001215)52:4<662::AID-JBM10>3.0.CO;2-3)
- Franco, A., Ferranti, A., Davidsen, C., Trapp, S., 2010. An unexpected challenge: ionizable compounds in the REACH chemical space. *Int. J. Life Cycle Assess.* 15, 321–325. <https://doi.org/10.1007/s11367-010-0165-6>
- Gardiner, M.S., 1972. The biology of invertebrates. McGraw-Hill Book Company, New York.
- Ghosh, P., Han, G., De, M., Kim, C.K., Rotello, V.M., 2008. Gold nanoparticles in delivery applications. *Adv. Drug Deliv. Rev.* 60, 1307–1315.
- Goeritz, I., Falk, S., Stahl, T., Schäfers, C., Schleichriem, C., 2013. Biomagnification and tissue distribution of perfluoroalkyl substances (PFASs) in market-size rainbow trout (*Oncorhynchus mykiss*). *Environ. Toxicol. Chem.* 32, 2078–2088. <https://doi.org/10.1002/etc.2279>
- Hainfeld, J.F., Slatkin, D.N., Focella, T.M., Smilowitz, H.M., 2006. Gold nanoparticles: a new X-ray contrast agent. *Br. J. Radiol.* 79, 248–253. <https://doi.org/10.1259/bjr/13169882>
- Handy, R.D., Henry, T.B., Scown, T.M., Johnston, B.D., Tyler, C.R., 2008. Manufactured nanoparticles: Their uptake and effects on fish - A mechanistic analysis. *Ecotoxicology*. <https://doi.org/10.1007/s10646-008-0205-1>
- Handy, R.D., Ahtiainen, J., Navas, J.M., Goss, G., Bleeker, E.A.J., von der Kammer, F., 2018. Proposal for a tiered dietary bioaccumulation testing strategy for engineered nanomaterials using fish. *Environ. Sci. Nano* 5, 2030–2046. <https://doi.org/10.1039/C7EN01139C>
- Hankin, S.M., Peters, S.A.K., Poland, C.A., Foss Hansen, S., Holmqvist, J., Ross, B.L., Varet, J., Aitken, R.J., 2011. Specific Advice on Fulfilling Information Requirements for Nanomaterials under REACH (RIP-oN 2) - Final Project Report.
- Hassell, K.L., Coggan, T.L., Cresswell, T., Kolobaric, A., Berry, K., Crosbie, N.D., Blackbeard, J., Pettigrove, V.J., Clarke, B.O., 2020. Dietary uptake and depuration kinetics of Perfluorooctane Sulfonate, Perfluorooctanoic Acid, and Hexafluoropropylene Oxide Dimer Acid (GenX) in a benthic fish. *Environ. Toxicol. Chem.* 39, 595–603.
- Heerden, D. van, Vosloo, A., Nikinmaa, M., 2004. Effects of short-term copper exposure on gill structure, metallothionein and hypoxia-inducible factor-1 α (HIF-1 α) levels in rainbow trout (*Oncorhynchus mykiss*). *Aquat. Toxicol.* 69, 271–280. <https://doi.org/10.1016/J.AQUATOX.2004.06.002>
- Heydebreck, F., Tang, J., Xie, Z., Ebinghaus, R., 2015. Alternative and Legacy Perfluoroalkyl Substances: Differences between European and Chinese River/Estuary Systems. *Environ. Sci. Technol.* 49, 8386–8395. <https://doi.org/10.1021/acs.est.5b01648>
- Hoff, P.T., Van de Vijver, K., Van Dongen, W., Esmans, E.L., Blust, R., De Coen, W.M., 2003. Perfluorooctane sulfonic acid in bib (*Trisopterus luscus*) and plaice (*Pleuronectes platessa*) from the Western Scheldt and the Belgian North Sea: distribution and biochemical effects. *Environ. Toxicol. Chem. An Int. J.* 22, 608–614.

- Hoke, R.A., Ferrell, B.D., Sloman, T.L., Buck, R.C., Buxton, L.W., 2016. Aquatic hazard, bioaccumulation and screening risk assessment for ammonium 2, 3, 3, 3-tetrafluoro-2-(heptafluoropropoxy)-propanoate. *Chemosphere* 149, 336–342.
- Hu, W., Jones, P.D., Upham, B.L., Trosko, J.E., Lau, C., Giesy, J.P., 2002. Inhibition of gap junctional intercellular communication by perfluorinated compounds in rat liver and dolphin kidney epithelial cell lines in vitro and Sprague-Dawley rats in vivo. *Toxicol. Sci.* 68, 429–436.
- Huang, X., Jain, P.K., El-Sayed, I.H., El-Sayed, M.A., 2008. Plasmonic photothermal therapy (PPTT) using gold nanoparticles. *Lasers Med. Sci.* 23, 217–228. <https://doi.org/10.1007/s10103-007-0470-x>
- Inoue, Y., Hashizume, N., Yakata, N., Murakami, H., Suzuki, Y., Kikushima, E., Otsuka, M., 2012. Comparison of bioconcentration and biomagnification factors for poorly water-soluble chemicals using common carp (*Cyprinus carpio* L.). *Arch. Environ. Contam. Toxicol.* 63(2), 241–248. <https://doi.org/10.1007/s0024-012-9761-8>
- Kameda, Y., Kimura, K., Miyazaki, M., 2011. Occurrence and profiles of organic sun-blocking agents in surface waters and sediments in Japanese rivers and lakes. *Environ. Pollut.* 159, 1570–1576. <https://doi.org/10.1016/J.ENVPOL.2011.02.055>
- Kampe, S., Kaegi, R., Schlich, K., Wasmuth, C., Hollert, H., Schlechtriem, C., 2018. Silver nanoparticles in sewage sludge: Bioavailability of sulfidized silver to the terrestrial isopod *Porcellio scaber*. *Environ. Toxicol. Chem.* <https://doi.org/10.1002/etc.4102>
- Kampfraath, A.A., Hunting, E.R., Mulder, C., Breure, A.M., Gessner, M.O., Kraak, M.H.S., Admiraal, W., 2012. DECOTAB: a multipurpose standard substrate to assess effects of litter quality on microbial decomposition and invertebrate consumption. *Freshw. Sci.* 31, 1156–1162. <https://doi.org/10.1899/12-075.1>
- Kannan, K., Koistinen, J., Beckmen, K., Evans, T., Gorzelany, J.F., Hansen, K.J., Jones, P.D., Helle, E., Nyman, M., Giesy, J.P., 2001. Accumulation of perfluorooctane sulfonate in marine mammals. *Environ. Sci. Technol.* 35, 1593–1598.
- Kannan, K., Newsted, J., Halbrook, R.S., Giesy, J.P., 2002. Perfluorooctanesulfonate and related fluorinated hydrocarbons in mink and river otters from the United States. *Environ. Sci. Technol.* 36, 2566–2571.
- Khan, F.R., Boyle, D., Chang, E., Bury, N.R., 2017. Do polyethylene microplastic beads alter the intestinal uptake of Ag in rainbow trout (*Oncorhynchus mykiss*)? Analysis of the MP vector effect using in vitro gut sacs. *Environ. Pollut.* 231, 200–206. <https://doi.org/10.1016/j.envpol.2017.08.019>
- Kim, J.-W., Isobe, T., Ramaswamy, B.R., Chang, K.-H., Amano, A., Miller, T.M., Siringan, F.P., Tanabe, S., 2011. Contamination and bioaccumulation of benzotriazole ultraviolet stabilizers in fish from Manila Bay, the Philippines using an ultra-fast liquid chromatography–tandem mass spectrometry. *Chemosphere* 85, 751–758. <https://doi.org/10.1016/J.CHEMOSPHERE.2011.06.054>
- Kissa, E., 2001. Fluorinated surfactants and repellents. CRC Press.
- Klein, C.L., Stahlmecke, B., Romazanov, J., Kuhlbusch, T.A.J., Van Doren, E., De Temmerman, P.-J., Mast, J., Wick, P., Krug, H., Locoro, G., Hund-Rinke, K., Kördel, W., Friedrichs, S., Maier, G., Werner, J., Linsinger, T., Gawlik, B.M., Comero, S., Institute for Health and Consumer Protection., European Commission. Joint Research Centre. Institute for Environment and Sustainability., Institute for Reference Materials and Measurements., 2011. NM-Series of representative manufactured nanomaterials: NM-300 Silver Characterisation, Stability, Homogeneity. Publications Office.
- Kobayashi, H., 2009. Bioconcentration Study of FRD903 with Carp. Yokohama, Japan, Mitsubishi Chemical Medience Corporation: pp. 113.
- Korea Ministry of Government Legislation, 2008. Korean Laws in English - Toxic Chemicals Control Act [WWW Document].
- Kosfeld, V., Fu, Q., Ebersbach, I., Esser, D., Schauerte, A., Bischof, I., Hollender, J., Schlechtriem, C., 2020. Comparison of alternative methods for bioaccumulation assessment: Scope and limitations of in vitro depletion assays with rainbow trout and bioconcentration tests in the freshwater amphipod *Hyalella azteca* (Hybit). *Environ. Toxicol. Chem.* 39, 1813–1825.

- Kuehr, S., Schneider, S., Meisterjahn, B., Schlich, K., Hund-Rinke, K., Schlechtriem, C., 2018. Silver nanoparticles in sewage treatment plant effluents: chronic effects and accumulation of silver in the freshwater amphipod *Hyalella azteca*. *Environ. Sci. Eur.* 30:7. <https://doi.org/10.1186/s12302-018-0137-1>
- Kuehr, S., Kaegi, R., Maletzki, D., Schlechtriem, C., 2020a. Testing the bioaccumulation potential of manufactured nanomaterials in the freshwater amphipod *Hyalella azteca*. *Chemosphere* 263, 127961. <https://doi.org/10.1016/j.chemosphere.2020.127961>
- Kuehr, S., Klehm, J., Stehr, C., Menzel, M., Schlechtriem, C., 2020b. Unravelling the uptake pathway and accumulation of silver from manufactured silver nanoparticles in the freshwater amphipod *Hyalella azteca* using correlative microscopy. *NanoImpact* 19, 100239. <https://doi.org/10.1016/j.impact.2020.100239>
- Kuehr, S., Meisterjahn, B., Schröder, N., Knopf, B., Völker, D., Schwirn, K., Schlechtriem, C., 2020c. Testing the bioaccumulation of manufactured nanomaterials in the freshwater bivalve: *Corbicula fluminea* using a new test method. *Environ. Sci. Nano* 7, 535-553. <https://doi.org/10.1039/c9en01112a>
- Kuehr, S., Kosfeld, V., Schlechtriem, C. 2021. Bioaccumulation assessment of nanomaterials using freshwater invertebrate species. *Environmental Sciences Europe*. 33:9. <https://doi.org/10.1186/s12302-020-00442>
- Lansdown, A.B.G., Sampson, B., Rowe, A., 1999. Sequential changes in trace metal, metallothionein and calmodulin concentrations in healing skin wounds. *J. Anat.* 195, 375–386. <https://doi.org/10.1017/S0021878299005518>
- Lebrun, J.D., Uher, E., Tusseau-Vuillemin, M.H., Gourlay-Francé, C., 2014. Essential metal contents in indigenous gammarids related to exposure levels at the river basin scale: Metal-dependent models of bioaccumulation and geochemical correlations. *Sci. Total Environ.* 466/467, 100–108. <https://doi.org/10.1016/j.scitotenv.2013.07.003>
- Legeay, A., Achard-Joris, M., Baudrimont, M., Massabuau, J.-C., Bourdineaud, J.-P., 2005. Impact of cadmium contamination and oxygenation levels on biochemical responses in the Asiatic clam *Corbicula fluminea*. *Aquat. Toxicol.* 74, 242–253. <https://doi.org/10.1016/j.aquatox.2005.05.015>
- Liu, C., Gin, K. Y. H., Chang, V. W. C., Goh, B. P. L., Reinhard, M., 2011. Novel perspectives on the bioaccumulation of PFCs—the concentration dependency. *Environ. Sci. Technol.* 45(22), 9758–9764.
- Liu, Y.-S., Shareef, A., Kookana, R.S., 2012. Occurrence and removal of benzotriazoles and ultraviolet filters in a municipal wastewater treatment plant. *Environ. Pollut.* 165, 225–232. <https://doi.org/10.1016/J.ENVPOL.2011.10.009>
- Liu, Y., Ruan, T., Lin, Y., Liu, A., Yu, M., Liu, R., Meng, M., Wang, Y., Liu, J., Jiang, G., 2017. Chlorinated polyfluoroalkyl ether sulfonic acids in marine organisms from Bohai Sea, China: Occurrence, temporal variations, and trophic transfer behavior. *Environ. Sci. Technol.* 51, 4407–4414. <https://doi.org/10.1021/acs.est.6b06593>
- Loeschner, K., Navratilova, J., Kjøbler, C., Mølhøve, K., Wagner, S., von der Kammer, F., Larsen, E.H., 2013. Detection and characterization of silver nanoparticles in chicken meat by asymmetric flow field flow fractionation with detection by conventional or single particle ICP-MS. *Anal. Bioanal. Chem.* 405, 8185–8195. <https://doi.org/10.1007/s00216-013-7228-z>
- Mandal, P.K., Mandal, A., Ahearn, G.A., 2005. Physiological characterization of $^{45}\text{Ca}^{2+}$ and $^{65}\text{Zn}^{2+}$ transport by lobster hepatopancreatic endoplasmic reticulum. *J. Exp. Zool. Part A: Comp. Exp. Biol.* 303A, 515–526. <https://doi.org/10.1002/jez.a.186>
- Mandal, P.K., Mandal, A., Ahearn, G.A., 2006. $^{65}\text{Zn}^{2+}$ transport by lobster hepatopancreatic lysosomal membrane vesicles. *J. Exp. Zool. Part A: Comp. Exp. Biol.* 305A, 203–214. <https://doi.org/10.1002/jez.a.246>
- Martin, J.W., Mabury, S.A., Solomon, K.R., Muir, D.C.G., 2003. Bioconcentration and tissue distribution of perfluorinated acids in rainbow trout (*Oncorhynchus mykiss*). *Environ. Toxicol. Chem.* 22, 196–204. <https://doi.org/10.1002/etc.5620220126>
- Martin, J.W., Smithwick, M.M., Braune, B.M., Hoekstra, P.F., Muir, D.C.G., Mabury, S.A., 2004. Identification of long-chain perfluorinated acids in biota from the Canadian Arctic. *Environ. Sci. Technol.* 38, 373–380.

- McGillicuddy, E., Murray, I., Kavanagh, S., Morrison, L., Fogarty, A., Cormican, M., Dockery, P., Prendergast, M., Rowan, N., Morris, D., 2017. Silver nanoparticles in the environment: Sources, detection and ecotoxicology. *Sci. Total Environ.* 575, 231–246. <https://doi.org/10.1016/J.SCITOTENV.2016.10.041>
- Minghetti, M., Schirmer, K., 2016. Effect of media composition on bioavailability and toxicity of silver and silver nanoparticles in fish intestinal cells (RTgutGC). *Nanotoxicology* 10, 1526–1534. <https://doi.org/10.1080/17435390.2016.1241908>
- Ministry of Environment and Urbanization(MoEU) of Turkey, 2017. Draft by-law on registration, evaluation, authorization and restriction of chemicals.
- Mitrano, D.M., Ranville, J.F., Bednar, A., Kazor, K., Hering, A.S., Higgins, C.P., 2014. Tracking dissolution of silver nanoparticles at environmentally relevant concentrations in laboratory, natural, and processed waters using single particle ICP-MS (spICP-MS). *Environ. Sci. Nano* 1, 248–259. <https://doi.org/10.1039/C3EN00108C>
- Naiki, Y., 2010. Assessing Policy Reach: Japan’s Chemical Policy Reform in Response to the EU’s REACH Regulation. *J. Environ. Law* 22, 171–195. <https://doi.org/10.1093/jel/eqq002>
- Nakata, H., Murata, S., Filatreau, J., 2009. Occurrence and concentrations of benzotriazole UV stabilizers in marine organisms and sediments from the Ariake Sea, Japan. *Environ. Sci. Technol.* 43, 6920–6926. <https://doi.org/10.1021/es900939j>
- Nakata, H., Shinohara, R.-I., Nakazawa, Y., Isobe, T., Sudaryanto, A., Subramanian, A., Tanabe, S., Zakaria, M.P., Zheng, G.J., Lam, P.K.S., Kim, E.Y., Min, B.-Y., We, S.-U., Viet, P.H., Tana, T.S., Prudente, M., Frank, D., Lauenstein, G., Kannan, K., 2012. Asia–Pacific mussel watch for emerging pollutants: Distribution of synthetic musks and benzotriazole UV stabilizers in Asian and US coastal waters. *Mar. Pollut. Bull.* 64, 2211–2218. <https://doi.org/10.1016/J.MARPOLBUL.2012.07.049>
- Norey, C.G., Cryer, A., Kay, J., 1990. Induction of metallothionein gene expression by cadmium and the retention of the toxic metal in the tissues of rainbow trout (*Salmo gairdneri*). *Comp. Biochem. Physiol. Part C: Comp. Pharmacol.* 97, 215–220. [https://doi.org/10.1016/0742-8413\(90\)90130-2](https://doi.org/10.1016/0742-8413(90)90130-2)
- Norwood, W.P., Borgmann, U., Dixon, D.G., 2007. Chronic toxicity of arsenic, cobalt, chromium and manganese to *Hyalella azteca* in relation to exposure and bioaccumulation. *Environ. Pollut.* 147, 262–272. <https://doi.org/10.1016/J.ENVPOL.2006.07.017>
- Norwood, W.P., Borgmann, U., Dixon, D.G., 2006. Saturation models of arsenic, cobalt, chromium and manganese bioaccumulation by *Hyalella azteca*. *Environ. Pollut.* 143, 519–528. <https://doi.org/10.1016/J.ENVPOL.2005.11.041>
- Nott, J.A., Nicolaidou, A., 1990. Transfer of metal detoxification along marine food chains. *J. Mar. Biol. Assoc. United Kingdom* 70, 905–912. <https://doi.org/10.1017/S0025315400059130>
- Organisation for Economic Co-operation and Development (OECD), 2012. Test No. 305: Bioaccumulation in fish: aqueous and dietary exposure. OECD Guidel. Test. Chem. Paris.
- Organisation for Economic Co-operation and Development (OECD), 2012. Test No. 211: *Daphnia magna* Reproduction Test. OECD Guidel. Test. Chem. Paris..
- Othman, M.S., Pascoe, D., 2001. Growth, development and reproduction of *Hyalella azteca* (Saussure, 1858) in laboratory culture. *Crustaceana* 74, 171–181.
- Pan, Y., Zhang, H., Cui, Q., Sheng, N., Yeung, L.W.Y., Guo, Y., Sun, Y., Dai, J., 2017. First report on the occurrence and bioaccumulation of hexafluoropropylene oxide trimer acid: An emerging concern. *Environ. Sci. Technol.* 51, 9553–9560. <https://doi.org/10.1021/acs.est.7b02259>
- Petersen, E.J., Mortimer, M., Burgess, R.M., Handy, R., Hanna, S., Ho, K.T., Johnson, M., Loureiro, S., Selck, H., Scott-Fordsmand, J.J., Spurgeon, D., Unrine, J., van den Brink, N.W., Wang, Y., White, J., Holden, P., 2019. Strategies for robust and accurate experimental approaches to quantify nanomaterial bioaccumulation across a broad range of organisms. *Environ. Sci. Nano* 6, 1619–1656. <https://doi.org/10.1039/C8EN01378K>
- Piccinno, F., Gottschalk, F., Seeger, S., Nowack, B., 2012. Industrial production quantities and uses of ten engineered nanomaterials in Europe and the world. *J. Nanoparticle Res.* 14, 1109.

<https://doi.org/10.1007/s11051-012-1109-9>

- Poynton, H.C., Chen, C., Alexander, S.L., Major, K.M., Blalock, B.J., Unrine, J.M., 2019. Enhanced toxicity of environmentally transformed ZnO nanoparticles relative to Zn ions in the epibenthic amphipod *Hyalella azteca*. *Environ. Sci. Nano.* <https://doi.org/10.1039/C8EN00755A>
- Rainbow, P.S., 2007. Trace metal bioaccumulation: Models, metabolic availability and toxicity. *Environ. Int.* <https://doi.org/10.1016/j.envint.2006.05.007>
- Rasmussen, K., Mast, J., De Tammernann, P.-J., Verleysen, E., Waegneers, N., Van Steen, F., Pizzolon, J., Institute for Health and Consumer Protection, 2014. Titanium dioxide, NM-100, NM-101, NM-102, NM-103, NM-104, NM-105 characterisation and physico-chemical properties. Publications Office of the European Union. <https://doi.org/10.2788/79760>
- Raths, J., Kühr, S., Schlechtriem, C., 2020. Bioconcentration, metabolism and spatial distribution of ¹⁴C-labelled laurate in the freshwater amphipod *Hyalella azteca*. *Environ. Toxicol. Chem.* 39 (2), 310–322. <https://doi.org/10.1002/etc.4623>
- Ringwood, A.H., McCarthy, M., Bates, T.C., Carroll, D.L., 2010. The effects of silver nanoparticles on oyster embryos. *Mar. Environ. Res.* 69, S49–S51. <https://doi.org/10.1016/J.MARENRES.2009.10.011>
- Roesijadi, G., 1992. Metallothioneins in metal regulation and toxicity in aquatic animals. *Aquat. Toxicol.* 22, 81–113. [https://doi.org/10.1016/0166-445X\(92\)90026-J](https://doi.org/10.1016/0166-445X(92)90026-J)
- Ruan, T., Liu, R., Fu, Q., Wang, T., Wang, Y., Song, S., Wang, P., Teng, M., Jiang, G., 2012. Concentrations and composition profiles of benzotriazole UV stabilizers in municipal sewage sludge in China. *Environ. Sci. Technol.* 46, 2071–2079. <https://doi.org/10.1021/es203376x>
- Russell, W.M.S., Burch, R.L., Hume, C.W., 1959. The principles of humane experimental technique. Methuen London.
- Sannac, S., Tadjiki, S., Moldenhauer, E., 2013. Single particle analysis using the Agilent 7700x ICP-MS. *Agil. Technol.*
- Scheringer, M., Trier, X., Cousins, I. T., de Voogt, P., Fletcher, T., Wang, Z., and Webster, T. F., 2014. Helsingør statement on poly- and perfluorinated alkyl substances (PFASs). *Chemosphere* 114, 337–339.
- Slechtriem, C., Fliedner, A., Schäfers, C., 2012. Determination of lipid content in fish samples from bioaccumulation studies: Contributions to the revision of guideline OECD 305. *Environ. Sci. Europe.* 24, 13.
- Slechtriem, C., Böhm, L., Bebon, R., Bruckert, H.J., Düring, R.A., 2017. Fish bioconcentration studies with column-generated analyte concentrations of highly hydrophobic organic chemicals. *Environ. Toxicol. Chem.* 36, 906–916. <https://doi.org/10.1002/etc.3635>
- Slechtriem, C., Kampe, S., Bruckert, H.-J., Bischof, I., Ebersbach, I., Kosfeld, V., Kotthoff, M., Schäfers, C., L'Haridon, J., 2019. Bioconcentration studies with the freshwater amphipod *Hyalella azteca*: are the results predictive of bioconcentration in fish? *Environ. Sci. Pollut. Res.* 26, 1628–1641. <https://doi.org/10.1007/s11356-018-3677-4>
- Schmidt, B., Loeschner, K., Hadrup, N., Mortensen, A., Sloth, J.J., Bender Koch, C., Larsen, E.H., 2011. Quantitative characterization of gold nanoparticles by field-flow fractionation coupled online with light scattering detection and inductively coupled plasma mass spectrometry. *Anal. Chem.* 83, 2461–2468. <https://doi.org/10.1021/ac102545e>
- Schreurs, W.J., Rosenberg, H., 1982. Effect of silver ions on transport and retention of phosphate by *Escherichia coli*. *J. Bacteriol.* 152, 7–13.
- Shi, Y., Vestergren, R., Nost, T. H., Zhou, Z., and Cai, Y., 2018. Probing the differential tissue distribution and bioaccumulation behavior of per- and polyfluoroalkyl substances of varying chain-lengths, isomeric structures and functional groups in crucian carp. *Environ. Sci. Technol.* 52(8), 4592–4600.
- Shinoda, K., Hirai, T. 1977. Ionic surfactant applicable in the presence of multivalent cations: physicochemical properties. *J. Phys.Chem.* 81, 1842–1845.
- Smedes, F., 1999. Determination of total lipid using non-chlorinated solvents. *Analyst* 124, 1711-1718.

- Sterling, K.M., Mandal, P.K., Roggenbeck, B.A., Ahearn, S.E., Gerencser, G.A., Ahearn, G.A., 2007. Heavy metal detoxification in crustacean epithelial lysosomes: role of anions in the compartmentalization process. *J. Exp. Biol.* 210, 3484–93. <https://doi.org/10.1242/jeb.008300>
- Taniyasu, S., Kannan, K., Horii, Y., Hanari, N., Yamashita, N., 2003. A survey of perfluorooctane sulfonate and related perfluorinated organic compounds in water, fish, birds, and humans from Japan. *Environ. Sci. Technol.* 37, 2634–2639.
- US EPA, 2000. Methods for measuring the toxicity and bioaccumulation of sediment-associated contaminants with freshwater invertebrates, EPA 600/R-99/064, second ed. ed. Office of Research and Development.
- US EPA, 2001. Perfluorooctyl sulfonates; proposed significant new use rule. *Fed Reg* 65, 62319–62333.
- US EPA, 2004. High Production Volume Challenge Program C.
- Uusimaeki, T., Wagner, T., Lipinski, H.-G., Kaegi, R., 2019. AutoEM: a software for automated acquisition and analysis of nanoparticles. *J. Nanoparticle Res.* 21, 122.
- Vale, G., Mehennaoui, K., Cambier, S., Libralato, G., Jomini, S., Domingos, R.F., 2016. Manufactured nanoparticles in the aquatic environment-biochemical responses on freshwater organisms: A critical overview. *Aquat. Toxicol.* 170, 162–174. <https://doi.org/10.1016/J.AQUATOX.2015.11.019>
- Verschoor, A.J., Hendriks, A.J., Vink, J.P.M., de Snoo, G.R., Vijver, M.G., 2012. Multimetal accumulation in crustaceans in surface water related to body size and water chemistry. *Environ. Toxicol. Chem.* 31, 2269–2280. <https://doi.org/10.1002/etc.1941>
- Wallis, L.K., Diamond, S.A., Ma, H., Hoff, D.J., Al-Abed, S.R., Li, S., 2014. Chronic TiO₂ nanoparticle exposure to a benthic organism, *Hyalella azteca*: Impact of solar UV radiation and material surface coatings on toxicity. *Sci. Total Environ.* 499, 356–362. <https://doi.org/10.1016/j.scitotenv.2014.08.068>
- Wang, D., Schaaf, P., 2012. Nanoporous gold nanoparticles. *J. Mater. Chem.* 22, 5344. <https://doi.org/10.1039/c2jm15727f>
- Wang, Z., DeWitt, J. C., Higgins, C. P., and Cousins, I. T., 2017. A never-ending story of per- and polyfluoroalkyl substances (PFASs)? ACS Publications.
- Wen, W., Xia, X., Chen, X., Wang, H., Zhu, B., Li, H., & Li, Y., 2016. Bioconcentration of perfluoroalkyl substances by *Chironomus plumosus* larvae in water with different types of dissolved organic matters. *Environ. Pollut.* 213, 299–307.
- Wood, C.M., La Point, T.W., Armstrong, D.E., Birge, W.J., Brauner, C.J., Brix, K.V., Call, D.J., Creclius, E.A., Davies, P.H., Gorsuch, J.W., 2002. Biological effects of silver. *Transp. Fate Eff. Silver Environ.* SETAC Press. Pensacola, FL, USA 27–63.
- Yang, C., Kalwei, M., Schüth, F., Chao, K., 2003. Gold nanoparticles in SBA-15 showing catalytic activity in CO oxidation. *Appl. Catal. A Gen.* 254, 289–296. [https://doi.org/10.1016/S0926-860X\(03\)00490-3](https://doi.org/10.1016/S0926-860X(03)00490-3)
- Ye, B., Maret, W., Vallee, B.L., 2001. Zinc metallothionein imported into liver mitochondria modulates respiration. *Proc. Natl. Acad. Sci.* 98, 2317–2322.
- Zeumer, R., Galhano, V., Monteiro, M.S., Kuehr, S., Knopf, B., Meisterjahn, B., Soares, A.M.V.M., Loureiro, S., Lopes, I., Schleichriem, C., 2020. Chronic effects of wastewater-borne silver and titanium dioxide nanoparticles on the rainbow trout (*Oncorhynchus mykiss*). *Sci. Total Environ.* 723, 137974. <https://doi.org/10.1016/j.scitotenv.2020.137974>
- Zeumer, R., Hermsen, L., Kaegi, R., Kühr, S., Knopf, B., Schleichriem, C., 2020. Bioavailability of silver from wastewater and planktonic food borne silver nanoparticles in the rainbow trout *Oncorhynchus mykiss*. *Sci. Total Environ.* 706, 135695. <https://doi.org/10.1016/j.scitotenv.2019.135695>
- Zhang, C., Hu, Z., Deng, B., 2016. Silver nanoparticles in aquatic environments: Physicochemical behavior and antimicrobial mechanisms. *Water Res.* 88, 403–427. <https://doi.org/10.1016/J.WATRES.2015.10.025>
- Zhang, X., Sun, H., Zhang, Z., Niu, Q., Chen, Y., Crittenden, J.C., 2007. Enhanced bioaccumulation of cadmium in carp in the presence of titanium dioxide nanoparticles. *Chemosphere* 67, 160–166. <https://doi.org/10.1016/J.CHEMOSPHERE.2006.09.003>

- Zhang, Z., Ren, N., Li, Y.-F., Kunisue, T., Gao, D., Kannan, K., 2011. Determination of benzotriazole and benzophenone UV filters in sediment and sewage sludge. *Environ. Sci. Technol.* 45, 3909–3916. <https://doi.org/10.1021/es2004057>
- Zhu, X., Zhou, J., Cai, Z., 2011. TiO₂ Nanoparticles in the marine environment: Impact on the toxicity of tributyltin to abalone (*Haliotis diversicolor supertexta*) Embryos. *Environ. Sci. Technol.* 45, 3753–3758. <https://doi.org/10.1021/es103779h>
- Žnidaršič, N., Tušek-Žnidarič, M., Falnoga, I., Ščančar, J., Štrus, J., 2005. Metallothionein-like proteins and zinc-copper interaction in the hindgut of *Porcellio scaber* (Crustacea: Isopoda) exposed to zinc. *Biol. Trace Elem. Res.* 106, 253–264.

A Annex

A.1 Lipophilic and ionic organic compounds

A.1.1 Instrumental parameters for analysis of IOCs

Table 15: Overview of chromatographical conditions for analysis of PFOS and GenX in medium and *H. azteca* samples.

	PFOS and GenX
LC-MS/MS system	Acquity UPLC System with TQD (Waters)
stationary phase	Waters Acquity UPLC BEH C8 Säule, 1.7 µm
mobile phase	PFOS: A: 95/5 vol% H ₂ O/Methanol with 2 mM ammonium acetate B: Methanol with 2 mM ammonium acetate GenX: A: 95/5 vol% H ₂ O/Methanol with 2 mM ammonium bicarbonate B: Methanol with 2 mM ammonium bicarbonate
injection volume	20 µL
column temperature	55 °C
flow rate	PFOS: 250 µL/min GenX: 350 µL/min
gradient	PFOS: initial: 90 % A – 10 % B 1.0 min – 90 % A – 10 % B (curve 6) 1.5 min – 5 % A – 95 % B (curve 6) 3.0 min – 5 % A – 95 % B (curve 6) 3.1 min – 90 % A – 10 % B (curve 1) GenX: initial: 95.0 % A – 5 % B 0.5 min – 95 % A – 5 % B 1.0 min – 40 % A – 60 % B 1.5 min – 40 % A – 60 % B 3.5 min – 10 % A – 90 % B 3.6 min – 95 % A – 5 % B 6.0 min – 95 % A – 5 % B

Table 16: MS parameter for PFOS and GenX.

c	PFOS	GenX
Type	MRM	MRM
Span [Da]	0.2	00
Ion mode	ES-	ES-
Capillary [kV]	0.5	2,4
Cone [V]	50	10
Source temp. [°C]	150	150
Desolv. temp. [°C]	450	450
Cone gas flow [L h ⁻¹]	150.0	150

Table 17: Mass transitions.

c	Parent ion [m z-1]	Daughter ion [m z-1]	Dwell time [sec]	Collision energy [eV]
PFOS (quan.)	498.98	79.81	0.075	40
PFOS (qual.)	498.98	98.99	0.075	40
IS MPFOS (quant.)	502.99	79.81	0.075	45
IS MPFOS (qual.)	502.99	98.99	0.075	45
GenX (quan.)	391.03	169.07	0.075	18
GenX (qual.)	391.03	285.06	0.075	8
IS GenX (quan.)	394.04	168.79	0.075	8
IS GenX (qual.)	394.04	286.94	0.075	10

quan. = quantifier, qual. = qualifier

A.1.2 Instrumental parameters for highly hydrophobic compounds

Table 18: Overview of chromatographical conditions for analysis of UV-234 and UV-329 in medium and *H. azteca* samples.

	solvent-facilitated: UV-234 and UV-329	solvent-free: UV-329
LC-MS/MS system	Acquity UPLC System with TQ-S	Acquity UPLC System with Xevo TQD
stationary phase	Waters Acquity UPLC BEH C8 Säule, 1.7 µm	
mobile phase	UV-234 A: 95/5 vol% H ₂ O/methanol with 0.1 % formic acid B: methanol with 0.1 % formic acid UV-329 A: 95/5 vol% H ₂ O/acetonitrile with 0.1 % formic acid B: acetonitrile with 0.1 % formic acid	UV-329 A: 95/5 vol% H ₂ O/acetonitrile with 0.1 % formic acid B: acetonitrile with 0.1 % formic acid
injection volume	20 µL	10 µL
column temperature	55 °C	40 °C
flow rate	150 µL/min	350 µL/min
gradient	UV-234: initial: 95.0 % A – 5 % B (curve 4) 0.1 min – 40 % A – 60 % B (curve 6) 8.0 min – 0 % A – 100 % B (curve 6) 10.0 min – 0 % A – 100 % B (curve 6) 10.1 min – 95 % A – 5 % B (curve 1) 12.0 min – 95 % A – 5 % B (curve 1) UV-329: initial: 50 % A – 50 % B 0.1 min – 50 % A – 50 % B (curve 6) 6.0 min – 0 % A – 100 % B (curve 6) 8.0 min – 0 % A – 100 % B (curve 6) 8.1 min – 50 % A – 50 % B (curve 6) 12.0 min – 50 % A – 50 % B (curve 1)	UV-329: initial: 70 % A – 30 % B (curve 6) 1 min – 70 % A – 30 % B (curve 6) 3.0 min – 0 % A – 100 % B (curve 6) 4.0 min – 0 % A – 100 % B (curve 6) 4.1 min – 70 % A – 30 % B (curve 1) 7.0 min – 70 % A – 30 % B (curve 1)

Table 19: MS parameter.

c	solvent-facilitated		solvent-free
	UV-234	UV-329	UV-329
Type	MRM	MRM	MRM
Span [Da]	0.2	0.2	0.2
Ion mode	ES+	ES+	ES+
Capillary [kV]	2.0	1.5	3.0
Cone [V]	70	35	55
Source temp. [°C]	150	150	150
Desolv. temp. [°C]	500	500	500
Cone gas flow [L h ⁻¹]	150	150	50

Table 20: Mass transitions.

c	Parent ion [m z-1]	Daughter ion [m z-1]	Dwell time [sec]	Collision energy [eV]
UV-234 (quan.)	448.18	119.03	0.100	29
UV-234 (qual.)	448.18	370.07	0.100	19
UV-329 (quan.; TQ-S)	324.07	211.97	0.100	22
UV-329 (qual.; TQ-S)	324.07	57.07	0.100	22
UV-329 (quan.; Xevo TQD)	324.20	212.07	0.163	29
UV-329 (qual.; Xevo TQD)	324.20	57.09	0.163	29

quan. = quantifier, qual. = qualifier

A.1.3 Bioconcentration tests with PFOS and GenX

Table 21: Bioconcentration test PFOS, TWA 49.4 µg PFOS/L, males: total PFOS concentration in *H. azteca* tissue and standard deviation.

Time [d]	Tissue conc. [mg PFOS/kg]	SD
0	< LOQ	
1	2.53	0.22
3	5.31	0.19
5	7.95	0.25
6	8.69	0.36
7*	9.51	1.01
8	8.81	0.10
9	6.56	0.70
10	6.86	0.96
14	3.40	0.33

* = end of uptake

Table 22: Bioconcentration test PFOS, TWA 49.98 µg PFOS/L, males: total PFOS concentration in *H. azteca* tissue and standard deviation (performed at UBA).

Time [d]	Tissue conc. [mg PFOS/kg]	SD
0	< LOQ	
1	2.81	1.01
3	2.26	0.90
5	5.17	0.59
6	5.89	0.47
7*	5.61	0.16
8	4.64	0.61
9	3.89	0.25
10	3.92	0.38
14	1.91	0.08

* = end of uptake

Table 23: Bioconcentration test PFOS, TWA 39.22 µg PFOS/L, females: total PFOS concentration in *H. azteca* tissue and standard deviation.

Time [d]	Tissue conc. [mg PFOS/kg]	SD
0	0.8	
2	5.19	0.52
4	7.84	0.45
6	9.89	0.09
8	10.42	0.62
10*	10.27	0.24
11	12.57	1.58
12	9.03	0.91
14	6.24	0.37
16	5.26	0.24
18	4.09	0.77
20	3.18	0.22
22	2.38	0.41
24	1.65	0.33

* = end of uptake

Table 24: Bioconcentration test GenX, TWA 49.4 µg GenX/L, total GenX concentration in *H. azteca* tissue and standard deviation.

Time [d]	Tissue conc. [mg GenX/kg]	SD
0	0.011	0.006
1	0.043	0.001
3	0.081	0.000
5	0.159	0.073
6	0.128	0.009
7*	0.136	0.002
8	0.109	0.003
9	0.091	0.016
10	0.097	0.002
14	0.071	0.006

* = end of uptake

A.1.4 Bioconcentration tests with UV-234 and UV-329 – solvent-facilitated application

Table 25: Bioconcentration test UV-234, TWA 0.997 µg UV-234/L, total UV-234 concentration in *H. azteca* tissue and standard deviation.

Time [h]	Tissue conc. [mg UV-234/kg]	SD
0	< LOQ	
4	0.136	0.0265
8	0.224	0.0215
24	0.326	0.0088
48	0.474	0.0771
72	0.440	0.0381
96	0.495	0.0221
144	0.470	0.0693
168*	0.540	0.0949
172	0.406	0.1037
176	0.360	0.0113
192	0.282	0.0396
216	0.269	0.0396
240	0.213	0.0101
264	0.170	0.0267
312	0.076	0.0436
360	0.055	0.0160

* = end of uptake

Table 26: Bioconcentration test UV-329, TWA 0.078 µg UV-329/L, total UV-329 concentration in *H. azteca* tissue and standard deviation.

Time [h]	Tissue conc. [mg UV-329/kg]	SD
0	< LOQ	
4	1.62	0.167
8	2.24	0.273
24	4.66	0.416
48	6.58	0.563
72	6.75	0.468
96	7.74	0.408
120	7.58	0.638
144	6.96	2.249
168*	6.45	2.909
172	5.38	0.574
176	3.05	0.174
192	2.24	0.117
216	1.45	0.490
240	0.73	0.073

* = end of uptake

A.1.5 Bioconcentration test with UV-329 – solvent-free application

Table 27: Solvent-free bioconcentration test UV-329, TWA 0.208 µg UV-329/L, total UV-329 concentration in *H. azteca* tissue and standard deviation.

Time [h]	Tissue conc. [mg UV-329/kg]	SD
0	< LOQ	
6	1.62	0.167
24	2.24	0.273
48	4.66	0.416
72	6.58	0.563
96	6.75	0.468
120	7.74	0.408
144	7.58	0.638
168*	6.96	2.249
172	6.45	2.909
176	5.38	0.574
192	3.05	0.174
216	2.24	0.117
240	1.45	0.490
96	0.73	0.073

* = end of uptake

A.1.6 Exemplary calibration curves and chromatograms

Figure 51: Exemplary calibration curve of PFOS used for quantification of medium and tissue samples.

Compound name: PFOS
 Correlation coefficient: $r = 0.999560$, $r^2 = 0.999120$
 Calibration curve: $0.685015 * x + 11.6693$
 Response type: Internal Std (Ref 2), Area * (IS Conc. / IS Area)
 Curve type: Linear, Origin: Exclude, Weighting: 1/x, Axis trans: None

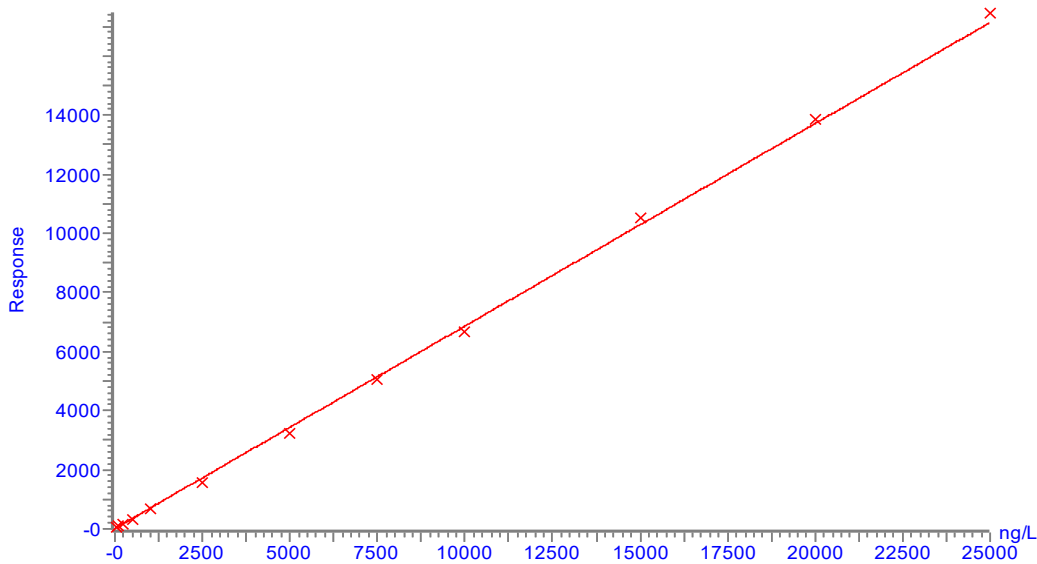


Figure 52: Exemplary chromatogram of PFOS standard (5 µg/L).

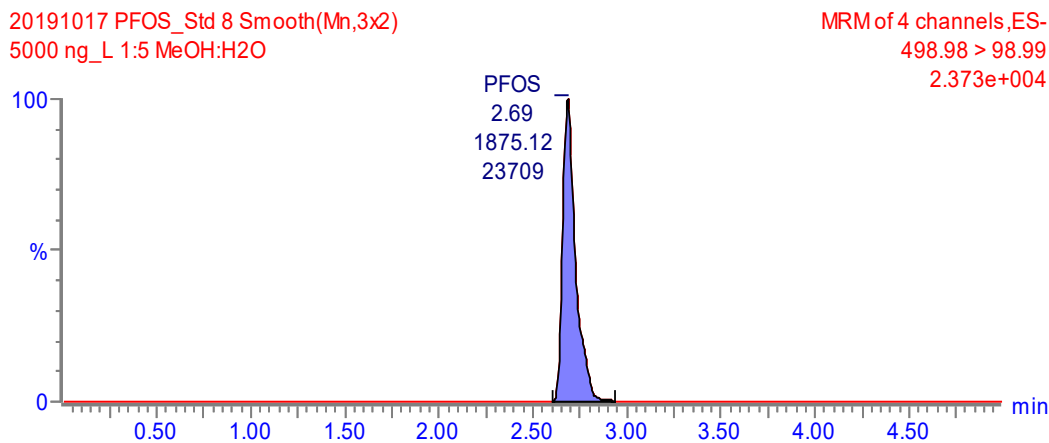
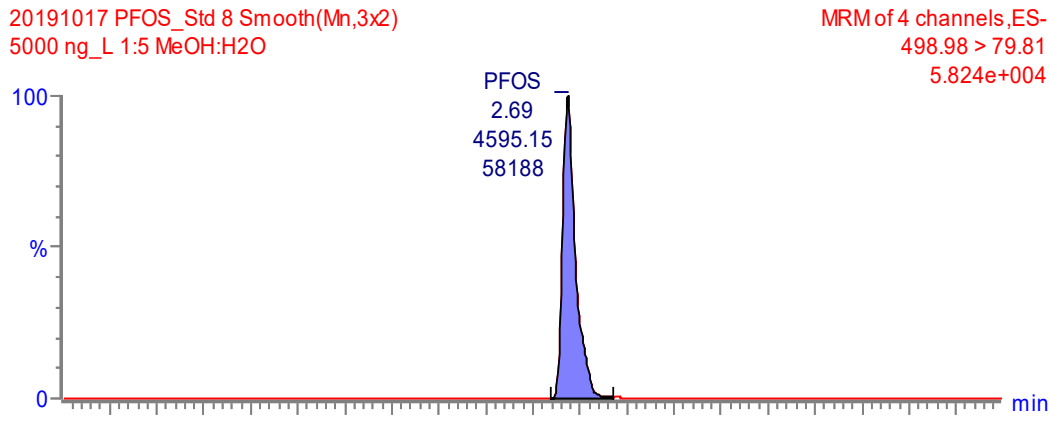


Figure 53: Exemplary calibration curve of GenX used for quantification of medium and tissue samples.

Compound name: GenX
 Correlation coefficient: $r = 0.998103$, $r^2 = 0.996210$
 Calibration curve: $8.49323 * x + 131.726$
 Response type: Internal Std (Ref 2), Area * (IS Conc. / IS Area)
 Curve type: Linear, Origin: Exclude, Weighting: 1/x, Axis trans: None

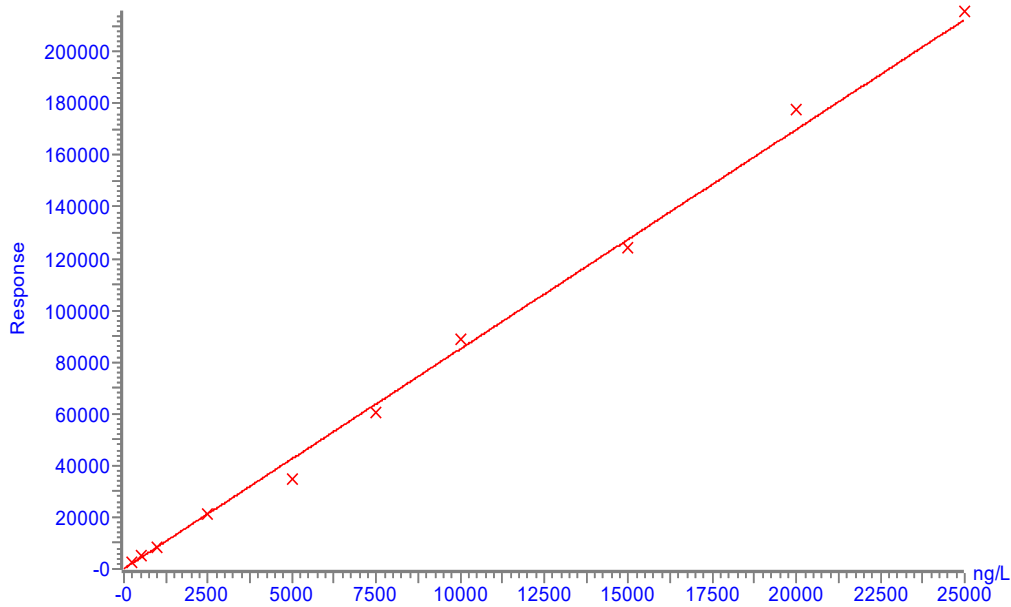


Figure 54: Exemplary chromatogram of GenX standard (5 µg/L).

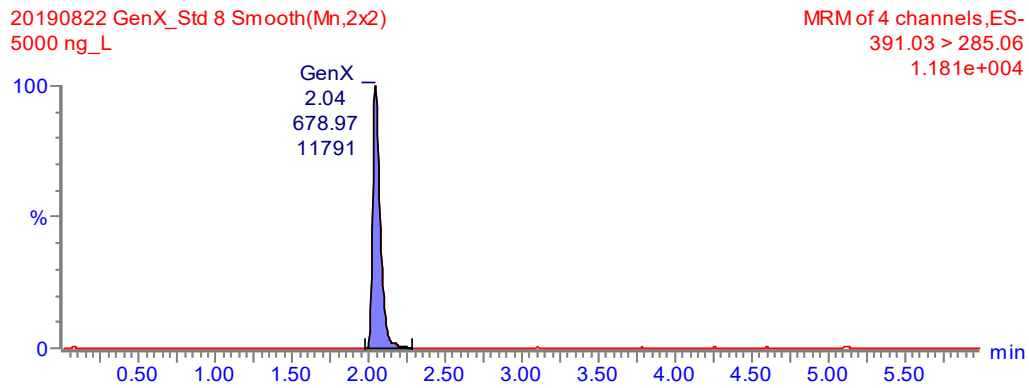
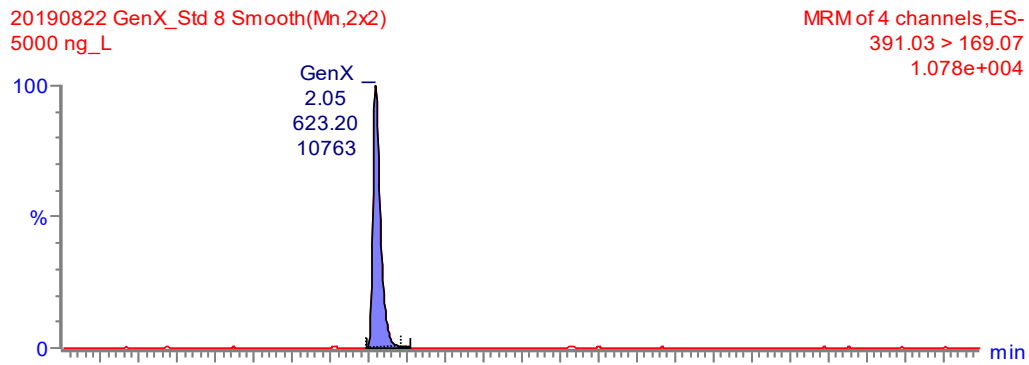


Figure 55: Exemplary calibration curve of UV-234 used for quantification of medium samples.

Compound name: UV-234
 Correlation coefficient: $r = 0.997527$, $r^2 = 0.995060$
 Calibration curve: $63414.4 * x + -19757.5$
 Response type: External Std, Area
 Curve type: Linear, Origin: Exclude, Weighting: 1/x, Axis trans: None

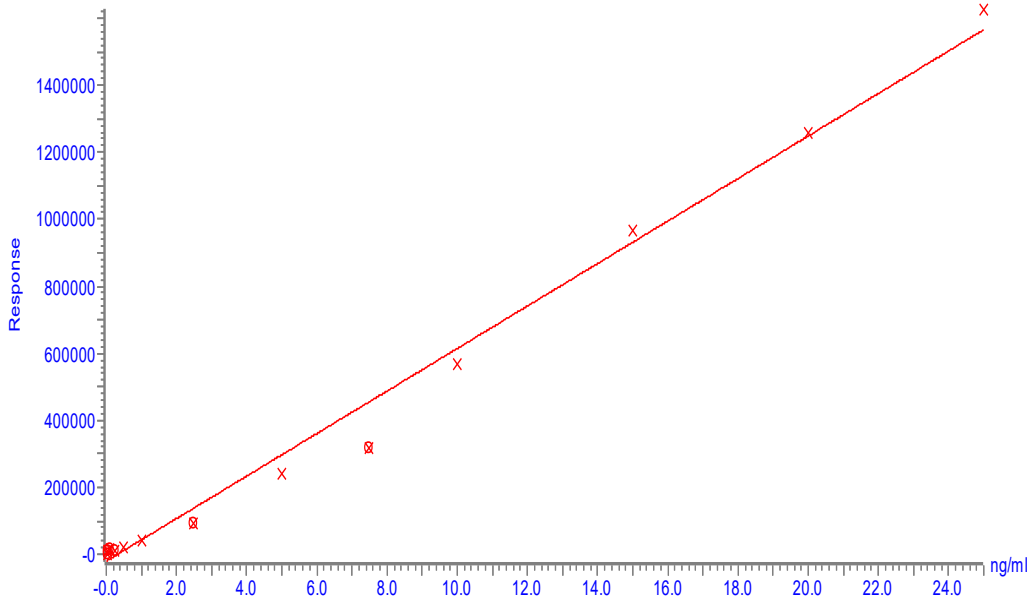


Figure 56: Exemplary chromatogram of UV-234 standard (5 µg/L).

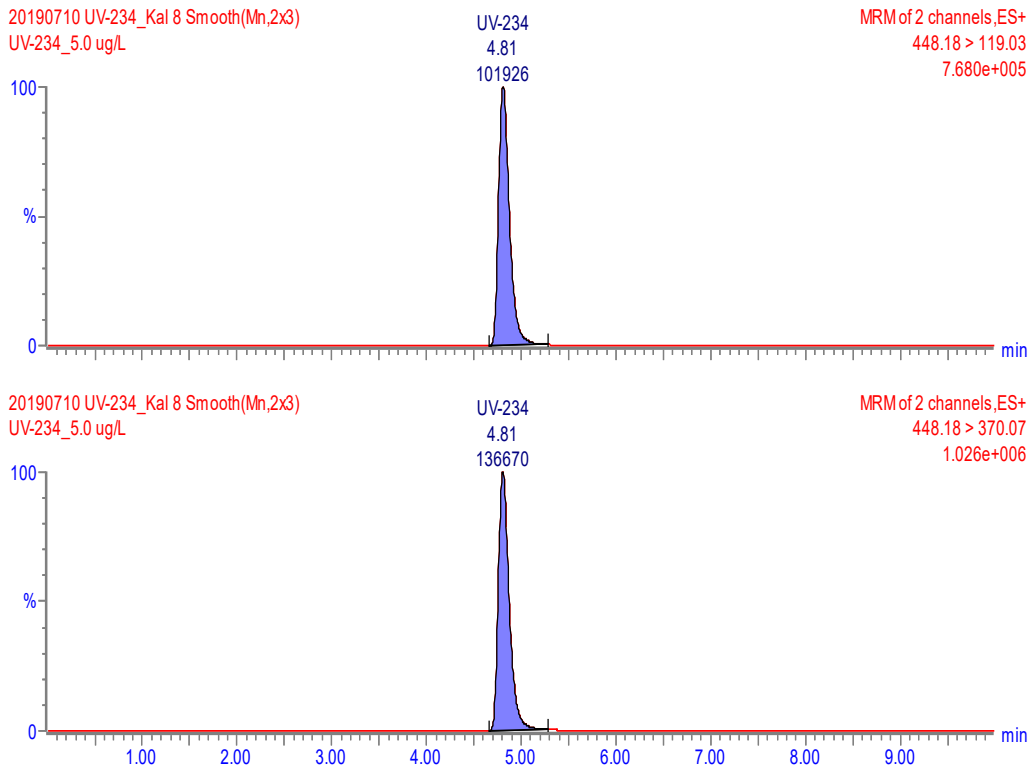


Figure 57: Exemplary matrix-matched calibration curve of UV-234 used for quantification of *H. azteca* samples.

Compound name: UV-234
 Correlation coefficient: $r = 0.998232$, $r^2 = 0.996467$
 Calibration curve: $207706 \cdot x + 153098$
 Response type: External Std, Area
 Curve type: Linear, Origin: Exclude, Weighting: 1/x, Axis trans: None

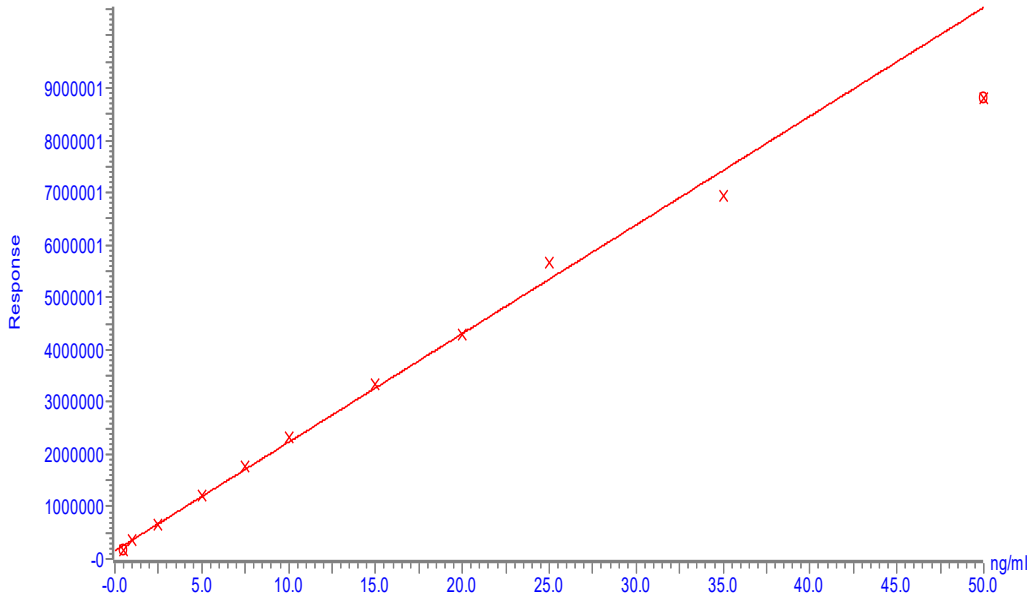


Figure 58: Exemplary chromatogram of matrix-matched UV-234 standard (5 µg/L).

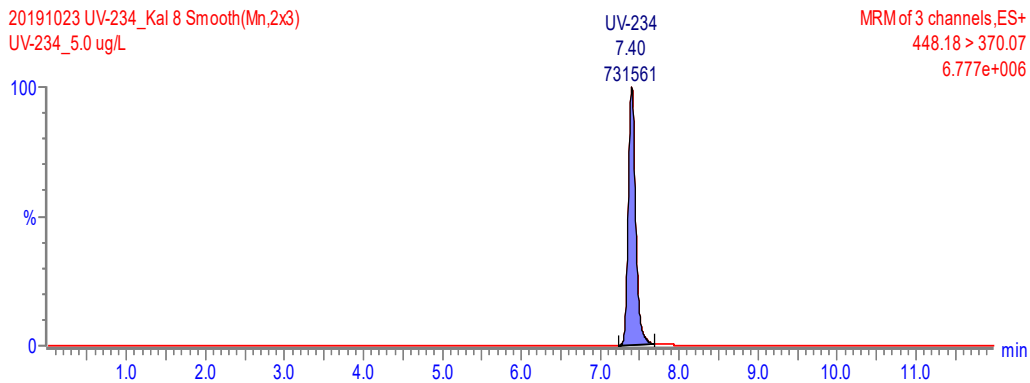
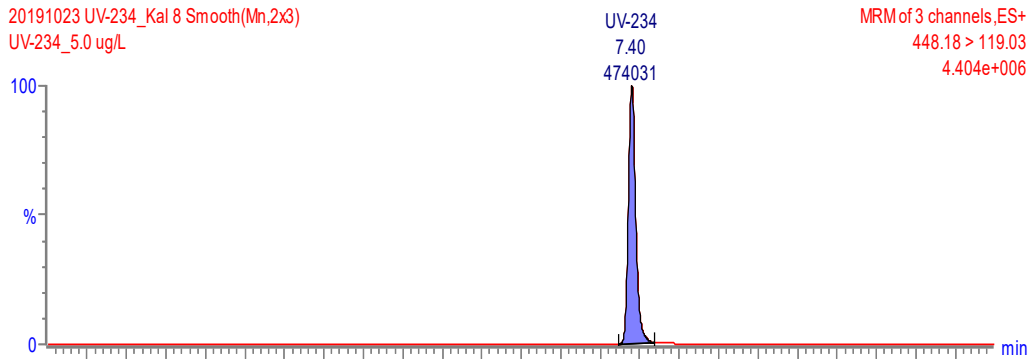


Figure 59: Exemplary calibration curve of UV-329 used for quantification of medium samples.

Compound name: UV-329
Correlation coefficient: $r = 0.999218$, $r^2 = 0.998436$
Calibration curve: $9851.8 * x + 947.037$
Response type: External Std, Area
Curve type: Linear, Origin: Exclude, Weighting: 1/x, Axis trans: None

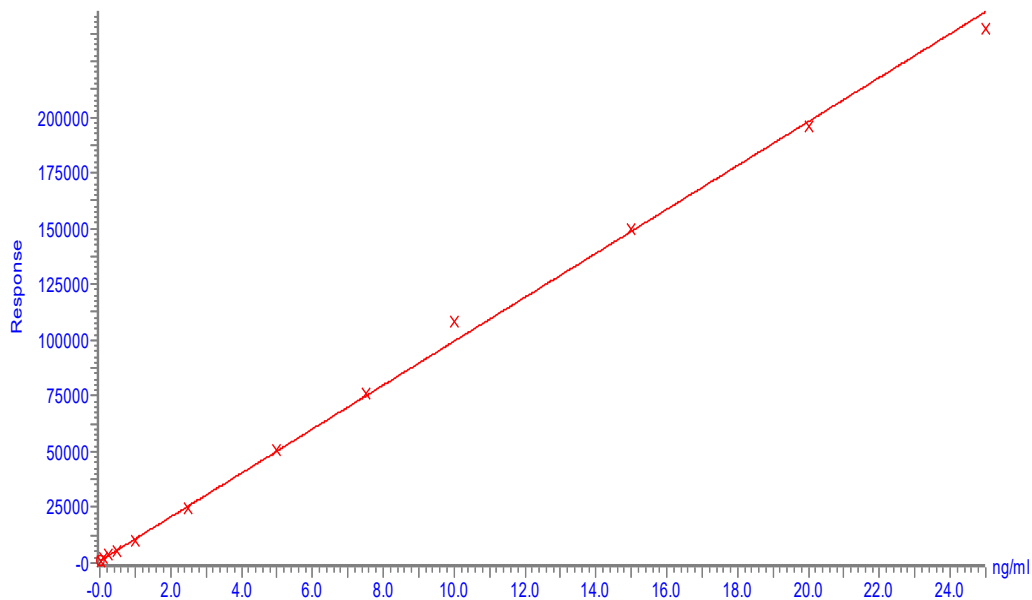


Figure 60: Exemplary chromatogram of matrix-matched UV-329 standard (medium) (5 µg/L).

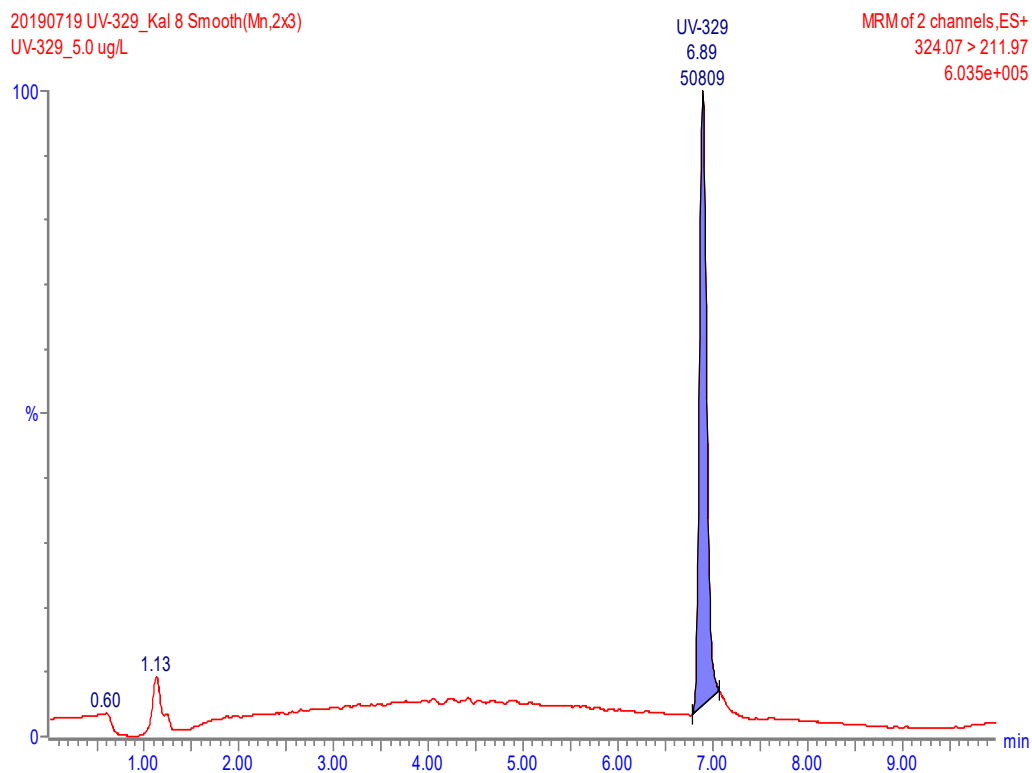


Figure 61: Exemplary matrix-matched calibration curve of UV-329 used for quantification of *H. azteca* samples.

Compound name: UV-329
 Correlation coefficient: $r = 0.999905$, $r^2 = 0.999811$
 Calibration curve: $33963.2 * x + 1722.77$
 Response type: External Std, Area
 Curve type: Linear, Origin: Exclude, Weighting: 1/x, Axis trans: None

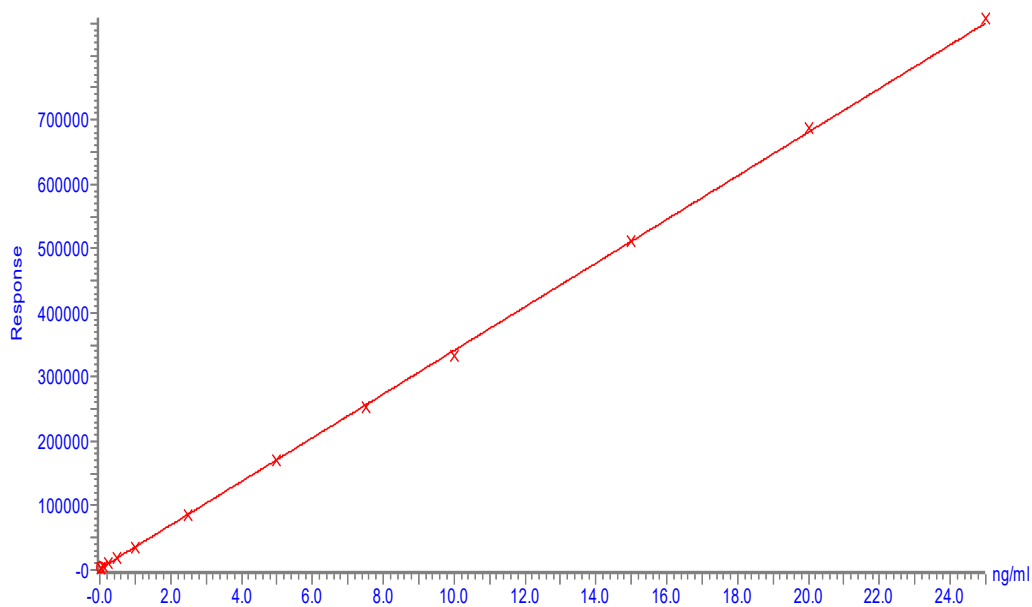
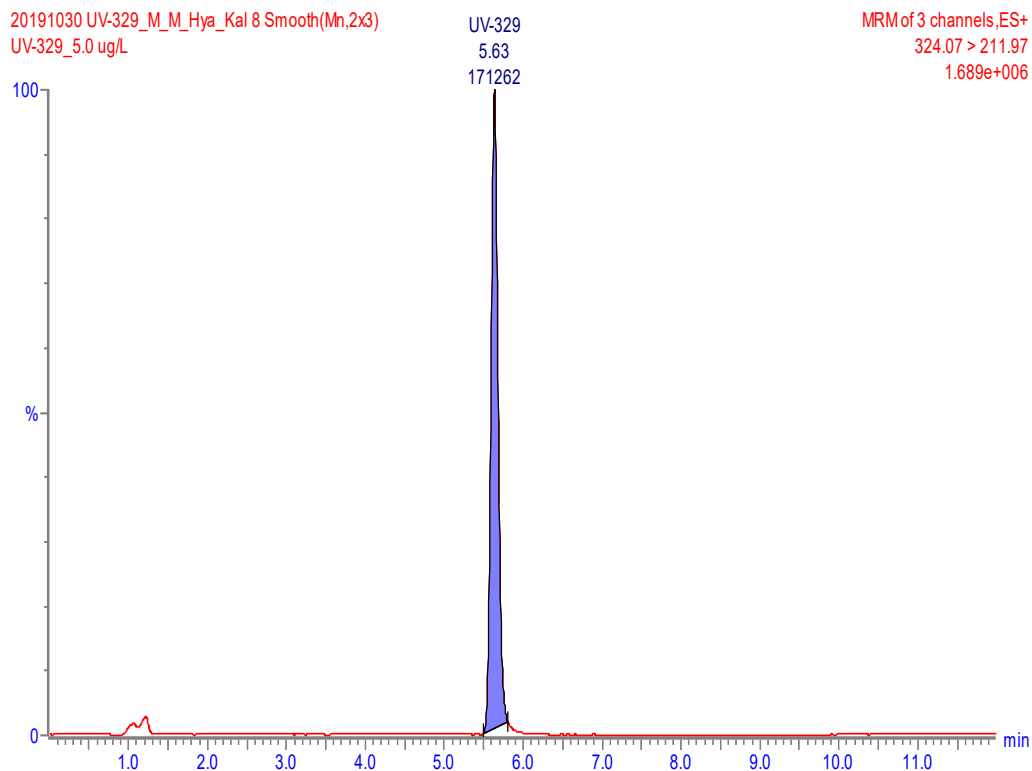


Figure 62: Exemplary chromatogram of matrix-matched UV-329 standard (*H. azteca*) (5 µg/L).



A.2 Nanomaterials

A.2.1 Bioconcentration tests

Table 28: Bioconcentration test AgNO_{3-ML}, TWA 0.67 µg Ag/L, males: total Ag concentration in *H. azteca* tissue and standard deviation.

Time [h]	Tissue conc. [mg Ag/kg]	SD
0	0.04	0.00
2	0.20	0.01
6	0.21	0.01
12	0.30	0.03
24	0.49	0.01
48	0.89	0.06
72	1.24	0.05
96	1.50	0.12
120	1.81	0.07
144	1.91	0.10
168	2.38	0.34
240	3.09	0.16
288	3.87	0.65
336	3.25	0.32

Table 29: Bioconcentration test AgNO_{3-FL}, TWA 0.64 µg Ag/L, females: total Ag concentration in *H. azteca* tissue and standard deviation, * end of uptake.

Time [h]	Tissue conc. [mg Ag/kg]	SD
0	0.04	0.00
2	0.29	0.03
6	0.31	0.04
12	0.38	0.07
24	0.50	0.03
48	0.60	0.03
72	0.81	0.00
96	0.91	0.04
120	1.38	0.17
144	1.90	0.13
168	1.94	0.21
240	2.74	0.00
288	3.22	0.13
336*	3.06	0.10
338	3.82	0.12
342	3.26	0.53
348	3.07	0.33
360	3.13	0.23
384	3.16	0.18
408	2.99	0.31
432	2.79	0.39
480	2.37	0.06
504	2.38	0.17
576	1.85	0.23
624	1.44	0.12
672	1.32	0.12

Table 30: Bioconcentration test AgNO_{3-FH}, TWA 1.64 µg Ag/L, females: total Ag concentration in *H. azteca* tissue and standard deviation.

Time [h]	Tissue conc. [mg Ag/kg]	SD
0	0.04	0.00
2	0.26	0.01
6	0.41	0.02
12	0.55	0.07
24	1.11	0.01
48	2.23	0.00
72	2.57	0.44
96	3.56	0.06
120	4.89	0.04
144	4.13	0.79
168	5.54	0.45
240	7.02	0.56
288	8.45	0.02
336	7.61	0.36

Table 31: Preliminary bioconcentration test NM 300K, TWA 3.734 µg Ag/L: total Ag concentration in *H. azteca* tissue and standard deviation.

Time [h]	Tissue conc. [mg Ag/kg]	SD
0	0.04	0.00
2	0.17	0.00
6	0.24	0.05
12	0.24	0.02
24	0.48	0.05
48	0.76	0.05
72	1.06	0.08
120	1.35	0.09
168*	1.73	0.15
170	1.65	0.03
174	1.60	0.24
180	1.39	0.11
192	1.41	0.14
216	1.32	0.09
240	1.13	0.06
288	1.03	0.18
336	0.88	0.14

* end of uptake.

Table 32: Bioconcentration test NM 300K, TWA 3.00 µg Ag/L, conducted by UBA with classic aquarium set-up: total Ag concentration in *H. azteca* tissue and standard deviation.

Time [h]	Tissue conc. [mg Ag/kg]	SD
0	0.06	0.01
24	0.24	0.01
72	0.44	0.03
144	0.82	0.06
216	1.23	0.12
288	1.74	0.08
312	1.70	0.08
336*	1.98	0.40
360	1.79	0.09
408	1.45	0.11
480	1.47	0.10
552	1.46	0.23
624	1.44	0.04
648	1.13	0.31
672	1.33	0.06

* end of uptake

Table 33: Bioconcentration test NM 300K, TWA 6.729 µg Ag/L, aquarium: total Ag concentration in *H. azteca* tissue and standard deviation.

Time [h]	Tissue conc. [mg Ag/kg]	SD
0	0.04	0.00
24	0.76	0.05
72	1.29	0.13
144	1.60	0.09
216	2.19	0.18
288	3.21	0.15
312	3.32	0.22
336*	3.15	0.08
360	3.21	0.11
408	2.46	0.14
480	2.09	0.12
552	1.86	0.21
624	1.51	0.07
648	1.67	0.02
672	1.41	0.13

* end of uptake

Table 34: Bioconcentration test NM 300K, TWA 6.827 µg Ag/L, Zuger glass: total Ag concentration in *H. azteca* tissue and standard deviation.

Time [h]	Tissue conc. [mg Ag/kg]	SD
0	0.04	0.00
24	1.14	0.43
72	2.22	0.27
144	1.98	0.22
216	2.21	0.26
288	3.12	0.19
312	3.19	0.18
336*	2.97	0.03
360	2.51	0.17
408	2.08	0.17
480	1.81	0.23
552	1.76	0.12
624	1.57	0.24
648	1.57	0.12
672	1.45	0.21

* end of uptake

Table 35: Bioconcentration test NM 105, TWA 3.30 µg TiO₂/L: total TiO₂ concentration in *H. azteca* tissue and standard deviation.

Time [h]	Tissue conc. [mg TiO ₂ /kg]	SD
0	0.33	0.04
2	1.04	0.10
6	0.59	0.08
12	0.52	0.22
24	0.37	0.04
48	0.60	0.09
72	0.48	0.09
120	0.53	0.09
144	0.53	0.10
168*	0.71	0.05
170	0.49	0.03
174	0.33	0.06
182	0.51	0.00
192	0.33	0.03
216	0.13	0.09
240	0.43	0.28
288	0.74	0.21
336	0.33	0.04

* end of uptake

Table 36: Bioconcentration test AuNPs, TWA 0.085 µg Au/L: total Au concentration in *H. azteca* tissue and standard deviation.

Time [h]	Tissue conc. [mg Au/kg]	SD
0	0.000	0.000
2	0.032	0.009
6	0.013	0.006
12	0.017	0.005
24	0.020	0.004
48	0.043	0.004
72	0.041	0.009
120	0.034	0.007
144	0.031	0.010
168	0.046	0.002

Table 37: Bioconcentration test AuNPs, TWA 0.704 µg Au/L: total Au concentration in *H. azteca* tissue and standard deviation.

Time [h]	Tissue conc. [mg Au/kg]	SD
0	0.000	0.000
2	0.021	0.006
6	0.030	0.006
12	0.054	0.023
24	0.062	0.007
48	0.164	0.010
72	0.141	0.009
120	0.105	0.010
144	0.138	0.028
168*	0.108	0.009
170	0.075	0.016
174	0.045	0.008
182	0.042	0.006
192	0.036	0.005
216	0.012	0.003
240	0.006	0.002
288	0.000	0.000
336	0.000	0.000

* end of uptake

A.2.2 Biomagnification tests

Table 38: Biomagnification test NM 300K, food conc. 0.07 mg Ag/kg: total Ag concentration in *H. azteca* tissue and standard deviation.

Time [h]	Tissue conc. [mg Ag/kg]	SD
0	0.04	0.00
72	0.06	0.00
120	0.08	0.00
144	0.07	0.01
168	0.06	0.01

Table 39: Biomagnification test NM 300K, food conc. 0.751 mg Ag/kg: total Ag concentration in *H. azteca* tissue and standard deviation.

Time [h]	Tissue conc. [mg Ag/kg]	SD
0	0.04	0.00
72	0.18	0.01
120	0.20	0.01
144	0.18	0.01
168*	0.18	0.01
192	0.19	0.02
216	0.20	0.02
240	0.19	0.01
264	0.18	0.00
312	0.16	0.00
360	0.14	0.01

* end of uptake

Table 40: Biomagnification test NM 105, food conc. 3.667 mg TiO₂/kg: total TiO₂ concentration in *H. azteca* tissue and standard deviation.

Time [h]	Tissue conc. [mg TiO ₂ /kg]	SD
0	0.59	0.07
72	0.76	0.17
120	0.70	0.02
168	1.05	0.12
192	0.89	0.08
216	0.99	0.06
240	1.19	0.24

Table 41: Biomagnification test NM 105, food conc. 19.4 mg TiO₂/kg: total TiO₂ concentration in *H. azteca* tissue and standard deviation.

Time [h]	Tissue conc. [mg TiO ₂ /kg]	SD
0	0.59	0.07
72	1.18	0.20
120	0.95	0.10
168	1.24	0.15
192	1.05	0.08
216	1.01	0.07
240*	0.97	0.18
264	0.76	0.05
288	0.61	0.02
312	0.77	0.06
336	0.75	0.11
384	0.79	0.03
452	0.79	0.03
480	0.99	0.11

* end of uptake

Table 42: Biomagnification test AuNM, food conc. 0.889 mg Au/kg: total Au concentration in *H. azteca* tissue and standard deviation.

Time [h]	Tissue conc. [mg Au/kg]	SD
0	0.00000	0.00015
72	0.02246	0.00034
120	0.01660	0.00107
168	0.01625	0.00597
192	0.00524	0.00464
216	0.01037	0.00318
240*	0.01525	0.00263
264	0.00046	0.00006
288	0.00028	0.00004
312	0.00022	0.00007
336	0.00022	0.00009
384	0.00018	0.00003
432	0.00035	0.00009
480	0.00035	0.00002

* end of uptake